THE MINERALOGICAL MAGAZINE

AND

JOURNAL OF

THE MINERALOGICAL SOCIETY

No. 233 June, 1956 Vol. XXXI

The characterization of serpentine minerals by X-ray diffraction.

By E. J. W. Whittaker, M.A., B.Sc., A.Inst.P.

Ferodo Ltd., Chapel-en-le-Frith, Stockport,

and

J. Zussman, M.A., Ph.D., A.Inst.P.

Geology Department, University of Manchester.

[Read 3 November 1955.]

Summary.—X-ray diffraction data on serpentine minerals are discussed. There are three structural varieties of chrysotile: ortho-chrysotile, clino-chrysotile, and para-chrysotile. Methods are described for the estimation of the proportions of the first two of these in mixed specimens, and their distribution in nature is reviewed. The variations observed in powder photographs of serpentine minerals are interpreted in accordance with this classification. The criteria proposed by Selfridge for distinguishing between chrysotile and antigorite are shown to be unreliable, but valid criteria are presented. The powder photographs also reveal the existence of a third serpentine mineral, distinct from chrysotile and antigorite, for which the name lizardite is proposed. Four samples of bastite are shown to consist of chrysotile or lizardite rather than antigorite. All the serpentine minerals examined consist either of antigorite or of one or more of the group comprising lizardite and the chrysotile varieties.

THIS paper presents a general discussion of the X-ray diffraction data from serpentine minerals from the point of view of classification, identification, and analysis. In Part I the grounds are presented for classifying normal fibrous chrysotile into two varieties, ortho-chrysotile ($a = 5{\cdot}34$ Å., $b = 9{\cdot}2$ Å., $c = 14{\cdot}63$ Å.) and clino-chrysotile ($a = 5{\cdot}34$ Å., $b = 9{\cdot}2$ Å., $c = 14{\cdot}65$ Å., $\beta = 93° 16'$), rather than into four varieties with $c = 7{\cdot}3$ Å. as proposed by Jagodzinski and Kunze (1954). Methods are described for quantitative determination of the

proportions of these varieties in a fibre specimen from X-ray fibre photographs, and the effects to be expected in powder photographs are calculated. The distribution in nature of ortho- and clino-chrysotile is discussed, and the name para-chrysotile is proposed for the further constituent of many chrysotile specimens which has a 9·2-Å. fibre axis. In Part II the variations observed in powder photographs of serpentine minerals are discussed in the light of the results presented in Part I, and the existence of a third distinct variety of serpentine mineral (approximate cell dimensions 5·3 Å., 9·2 Å., 7·3 Å., $\beta = 90°$) is established. The name lizardite is proposed for this mineral. It is shown that the previously proposed X-ray method (Selfridge, 1936) for distinguishing between chrysotile and antigorite is unreliable, but that more accurate work permits the adoption of valid criteria for this distinction. Data from four samples of bastite are presented from which it is concluded that they are forms of chrysotile or lizardite rather than of antigorite. It is apparent from the powder data that all the serpentine minerals which have been examined consist of either antigorite, or of ortho- or clino-chrysotile, or lizardite, or of mixtures of two or all of the last three, but mixtures of antigorite with either chrysotile or lizardite have not been observed.

Part I (E. J. W. W.).

Description and Recognition of Chrysotile Varieties.

A complete interpretation of the diffraction pattern of chrysotile is complicated and can only be made in terms of the theory of diffraction by cylindrical lattices (Whittaker, 1954; 1955 *a*, *b*, *c*, *d*). The appearance of a fibre photograph of chrysotile is, however, unusually simple owing to the small number of reflections and their division into two easily distinguishable types, sharp and diffuse. The sharp reflections are confined to the even-order layer-lines. On the zero layer-line they form an invariable series which may be indexed as $00l$ reflections from a structure with $c \sin\beta = 7{\cdot}31$ Å. or a multiple thereof.[1] On the other even-order layer-lines they form two series with constant relative intensities within each series, but the intensities of the two series relative to one another are infinitely variable, so that either one or the other may be entirely absent. These two series lie at the positions to be expected for $h0l$ reflections from an orthorhombic structure (i) with $c = 14{\cdot}63$ Å. (orthochrysotile), and in pairs centred on these positions and separated by the

[1] In this paper the axial convention is that with *a* as the fibre axis and *c* as the inter-layer axis, in order to facilitate comparison with antigorite in Part II.

distance appropriate to $h0l$ and $h0\bar{l}$ reflections from a monoclinic structure (ii) with $c \sin\beta = 14{\cdot}63$ Å. and $c \cos\beta = -0{\cdot}835$ Å. (clino-chrysotile). On the 2nd layer-line the pattern is particularly simple because the reflections from structure (ii) with l odd are very weak, and very few of them can be detected even on a well-exposed photograph. Also, the spacing between the $h0l$ and $h0\bar{l}$ spots of a pair is small compared with the distance between such pairs. It is therefore easy to index the reflections and assign them to the appropriate lattice type by inspection.

Basing their argument on the appearance of the 2nd layer-line, Jagodzinski and Kunze (1954) have sought to interpret the pattern in terms of four structures each with a single-layer cell, i.e. $c \sin\beta \simeq 7{\cdot}3$ Å. On this interpretation the reflections from the structures (i) and (ii) above, which have even values of l, are assigned to structures differing from those proposed here only by a halving of the c-axis. Those of series (i) with l odd are assigned to a monoclinic structure (iii) with $c \cos\beta = a/4$ so that the reflection $2.0.l-1$ coincides with $20l$; and those of series (ii) with l odd are assigned to another monoclinic structure (iv) with $c \cos\beta = a/6$. However, these assignments are found to be impossible as soon as even layer-lines of order higher than the 2nd are examined. For example, on the 4th layer-line the reflections from structure (iii) would coincide with those from the single-layer structure of type (i) and those from structure (iv) would coincide with those from the single-layer structure of type (ii). In fact this does not occur, and the 4th and all the even layer-lines up to the 10th can be indexed on the basis of the two two-layer structures (i) and (ii).

Determination of the ratio of ortho-chrysotile to clino-chrysotile.

Specimens of substantially pure clino-chrysotile are of frequent occurrence, but only one specimen of substantially pure ortho-chrysotile fibre has so far been observed. This is a very small specimen of badly crimped fibre (1) from Silesia[1] (Bristol Museum specimen 324, locality unknown) and is not suitable for producing good fibre photographs. It is therefore impossible to prepare a calibrated series of fibre photographs of synthetic mixtures of the two varieties, apart from the experimental difficulty of preparing such mixtures in a well-oriented form. It is possible, however, to determine the ratio of the two varieties present in a specimen by using the intensities of the zero layer-line reflections as an internal standard. It is an empirical fact that the relative intensities of these reflections are

[1] The numerals in parentheses refer to the list of specimens studied, p. 125.

identical for both varieties, and it follows from their structures (Whittaker, 1953) that their absolute values must also be the same.

The method is as follows. The intensities of the zero and 2nd layer-line reflections from (2), a substantially pure specimen of clino-chrysotile (Bell Mine, Thetford, Quebec), were determined by micro-densitometry of fibre photographs taken by the semi-integrating method (Whittaker, 1952) with the multiple-film technique. Similar measurements were made of the reflections from (3), a specimen rich in ortho-chrysotile from Cuddapah, India. The intensities of the zero layer-line reflections from the two photographs were then put on to the same arbitrary scale. The ratio of the intensities of the 2nd layer-line clino-chrysotile reflections on the two photographs then gave the proportion of this variety in the Cuddapah specimen, and also permitted the intensities of the ortho-chrysotile reflections to be put on to the same scale.

The above method, which involves putting the intensities of reflections on at least two photographs on to the same scale, is necessary for the primary determination of the proportions of ortho- and clino-chrysotile. But because it permits the determination of the relative intensities of the reflections from the two varieties once and for all, it is possible subsequently to use these data in a much more convenient method for determining the proportions in other specimens, as the intensities of the reflections from each variety provide an internally calibrated scale against which those from the other may be determined. For suppose that on the photograph of a mixed specimen of clino- and ortho-chrysotile it is observed that some particular clino-chrysotile reflection is equal in intensity to some particular ortho-chrysotile reflection. Let the intensities of these reflections from specimens of the pure varieties (on the same arbitrary scale as discussed above) be I_{cl} and I_{or} respectively. Then the proportion of ortho-chrysotile in the mixed specimen is given by $I_{\mathrm{cl}}/(I_{\mathrm{or}}+I_{\mathrm{cl}})$.

In practice there may not be two such reflections with equal intensities, but several inequalities may be established in the same way to give the proportion to within reasonably narrow limits. The method is particularly convenient in that the determination may be made by mere inspection of the photograph provided that the same radiation and orientation conditions are used each time so that the Lorentz and polarization factors are constant for each particular reflection. If the specimen is of small diameter and either cylindrical or rotated, the absorption factor varies so little among the reflections used that the specimen diameter is unimportant. Table I gives the appropriate values of I_{or} and I_{cl} for the

principal reflections on the 2nd layer-line of a normal beam fibre photograph taken with filtered Cu-$K\alpha$ radiation. Appropriate pairs of these reflections provide equalities for all proportions of ortho-chrysotile to within the nearest 3 % from 0 to 95 %. This accuracy is better than is justified by the data except at the extreme upper and lower ends of the range, where equalities corresponding to 1, 2, 3, 7, 10, 90, 91, 95, 96, and 97 % ortho-chrysotile can be found.

TABLE I. Uncorrected observed intensities of 20*l* reflections as observed on normal beam fibre photographs with Cu-$K\alpha$ radiation.

Ortho-chrysotile.		Clino-chrysotile.	
Reflection.	Intensity.	Reflection.	Intensity.
202	1910	202	1420
203	275	$20\bar{4}$	53
204	70	204	250
205	132	$20\bar{6}$	22
206	61	206	208
207	159	$20\bar{8}$	101
208	41	208	36
209	56		

Since it has been shown (Whittaker, 1953) that the difference between the two varieties lies in the different stacking arrangement of otherwise similar layers, it might be expected that stacking faults would occur leading to disordered intergrowths of the two varieties. This has been observed in three specimens from Kranskop, Natal (4, 5, and 6), and in a specimen from the Premier Mine, Transvaal (7), where it is evidenced by *h*0*l* reflections that are very much more diffuse than the 00*l* reflections. In extreme cases the *h*0*l* reflections may almost disappear by merging together into a continuous layer-line. Under these circumstances the determination of the proportions of the two varieties present becomes very inaccurate. However, the specimens used for the primary determination, and the vast majority of other specimens examined, do not show this intergrowth phenomenon to an appreciable extent. In specimen (2) there is not more than 2 % ortho-chrysotile so that any considerable degree of intergrowth is obviously unlikely and the uncorrected integral breadths of the 00*l* and *h*0*l* reflections are 0·011 and 0·020. In (3) the corresponding values are 0·013 and 0·019, so that the phenomenon is certainly no more extensive in this material. The difference between the breadths of the 00*l* and *h*0*l* reflections is presumed to be due partly to instrumental factors, though it would be very sensitive to the presence of even a small number of layers in the 'wrong' stacking arrangement.

Calculated powder patterns.

The determination of the proportions of clino- and ortho-chrysotile in a powder specimen is more difficult than in an oriented fibre specimen owing to the overlapping of reflections of the various types $00l$, $h0l$, and $hk0$. It would be possible to produce a series of calibration photographs from mixtures of powdered material prepared from specimens previously examined in the oriented state, but a microtome is necessary to produce satisfactory chrysotile 'powder' from long fibres, and the scarcity of good specimens of high ortho-content is a further difficulty. Theoretical microdensitometer curves for powder photographs taken with filtered Cu-$K\alpha$ radiation have therefore been constructed from the data obtained from fibre photographs and are shown in fig. 1.

In this figure and throughout the remainder of the paper it is convenient to adopt a notation to distinguish between the indices of three types of reflections. Those which occur only if $\beta = 90°$ are followed by †, those which occur only if $\beta \approx 93° 16'$ are followed by *, and those which are unaffected (or nearly so) by the value of β are unqualified.

In the construction of the curves of fig. 1 the values of $|F|^2$ have been multiplied by the various factors involved in such a photograph, and the breadths of the reflections have been made to conform approximately to those commonly obtained. The curves are drawn for the range from $\theta = 16°$ to $\theta = 36°$ only. At lower angles the only reflections which occur are 002, 020+110, and 004, which are identical for the two varieties, and at higher angles the lines become very weak.

This region of the photograph is dominated by the 130 reflection with its intense tail, on which a number of the sharp reflections are superimposed. When such a photograph is examined visually, however, this feature is largely subtracted, subconsciously, as background. The resolution of the 130 peak from the following $20\bar{2}$* reflection is critically dependent on the reflection breadths and on the detailed profile of the 130 tail immediately following the peak. As this differs appreciably from one specimen to another (probably as a function of fibril diameter distribution) another variable is introduced in addition to the variations in ortho-chrysotile content. This may result in the $20\bar{2}$* reflection being resolved from 130, merged with it into an unresolved intensity plateau, or even disappearing altogether, leaving the 130 reflection alone. These phenomena have all been observed in actual powder photographs.

As the region of the powder photograph involved in the method proposed by Selfridge (1936) for distinguishing between chrysotile and anti-

gorite is the same as the region that is sensitive to the proportion of ortho-chrysotile present, Selfridge's method is vitiated. A mixed ortho- and clino-chrysotile specimen can easily simulate an antigorite specimen according to this method, although the distinction can be made satisfactorily by the method described in Part II of this paper.

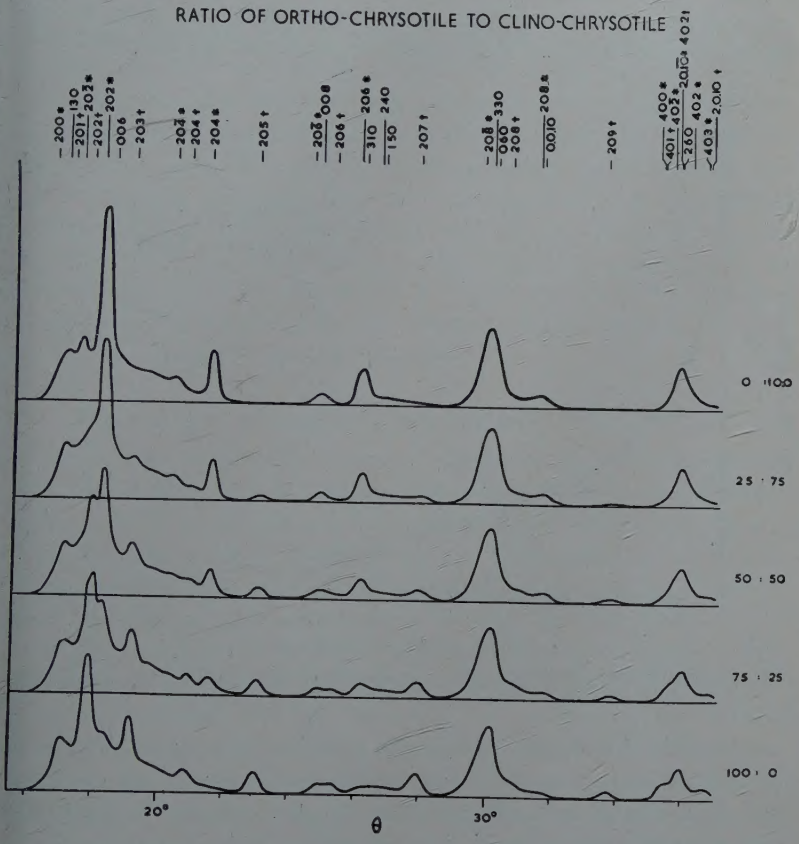

FIG. 1. Theoretical microdensitometer curves for powder photographs of mixtures of ortho- and clino-chrysotile taken with Cu-$K\alpha$ radiation.

The distribution of ortho-chrysotile.

Oriented fibre specimens containing a mixture of ortho- and clino-chrysotile have been shown to contain the same proportions of the two varieties at different points along their length and also in different parts of their cross-section. The latter result was obtained by taking a series of

fibre photographs after successively halving the cross-section of a specimen down to a diameter of 0·05 mm. This shows that if the fibrils of the two varieties have any tendency to segregate into homogeneous bundles, these bundles must be less than about 10^{-3} cm. in diameter.

In an attempt to find some correlation between the proportion of orthochrysotile and the local geological or mineralogical conditions this proportion was determined in a series of specimens taken from known positions in the Shabani Mine, Southern Rhodesia, but no correlation

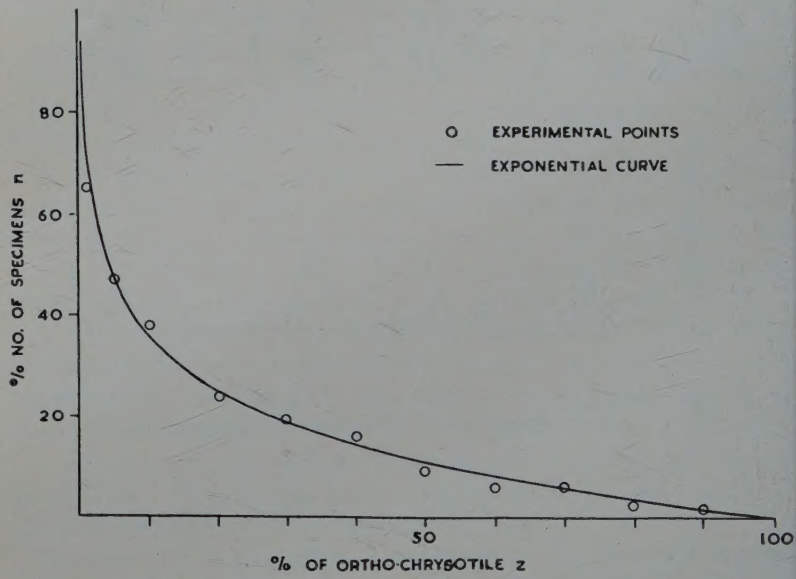

FIG. 2. Cumulative frequency curve for the occurrence of different percentages of ortho-chrysotile in admixture with clino-chrysotile.

with position was found. It was also observed that abrupt changes in proportion may occur. In one particular hand-specimen from Shabani the proportion of ortho-chrysotile was found to change abruptly from approximately zero to about 15% across an invisible boundary parallel to the fibres.

Rather more than a hundred oriented fibre specimens from many localities have been analysed for ortho-chrysotile content. From many localities only one specimen has been examined, but appreciable numbers have been examined from Thetford (Bell Mine), Shabani (170 Section), and Cuddapah. Substantially pure clino-chrysotile occurs in each of these localities, but the range of ortho-chrysotile contents varies markedly

from one locality to another. Thus the maximum values observed are Thetford 7 %, Shabani 35 %, and Cuddapah 81 %. It is also found that if all the specimens investigated are grouped together without distinction of locality, then the percentage number of specimens (n) containing more than z % ortho-chrysotile is given by

$$z = 100e^{-0{\cdot}065n}.$$

This is demonstrated in fig. 2. This procedure is certainly not beyond reproach, since there are very significant differences between the distributions from the different sources, and no attempt has been made to obtain a distribution representative of the world as a whole. However, as the relationship is so striking, and there is a tendency for the ortho-chrysotile contents of specimens from the individual sources to show similar distributions (albeit less perfectly and with different constants), it seems worth while to draw attention to it. No satisfactory explanation of the relationship has so far been found. It might presumably be related to energy differences between the two varieties during nucleation or during growth, or possibly to interconversion.

The occurrence of a variety of chrysotile with a 9·2-Å. *fibre axis.*

It has been reported by various workers (Aruja, 1943; Hargreaves and Taylor, 1946) that X-ray fibre photographs of chrysotile show weak extra layer-lines indicating a fibre axis of about 9·2 Å. Aruja showed that the reflections on the first three of these layer-lines correspond approximately to the stronger diffuse reflections of chrysotile if they are assumed to arise from material oriented with either the [010] or [310] axis parallel to the fibre direction. He also estimated the amount of such material in a specimen of Thetford chrysotile as about 3 %. Hargreaves and Taylor showed that this material is not present in all specimens of chrysotile, and may be removed by prolonged extraction with water.

These results have now been extended. The amount of the material has not been found to vary in the various Thetford specimens studied, but specimens from some Rhodesian and South African localities have been found to vary widely in this respect from zero to about 10 %. Specimens from Cuddapah on the other hand are found to be uniformly free from the material.

The availability of specimens giving stronger extra layer-lines has permitted the recording of a greater number of reflections, and the range of the reflections has been extended by obtaining photographs of the 2nd, 3rd, and 6th of these layer-lines in the equi-inclination position. It is

confirmed that the diffuse reflections may be indexed in accordance with Aruja's proposals, and it is shown that sharp reflections also occur, but only on the 6th layer-line. These sharp reflections characterize the material as having an orthorhombic cylindrical lattice structure (Whittaker, 1955*c*) with a cell dimension perpendicular to the layers of 14·6 Å., and disprove the suggestion of Hargreaves and Taylor that it might consist of layers stacked in a less orderly manner than in chrysotile. The detailed considerations leading to this structure assignment will be presented elsewhere, but it may be remarked here that the structure is very closely analogous to that of ortho-chrysotile apart from the orientation of the 9·2-Å. axis, instead of the 5·3-Å. axis, along the cylinder axis. This material must therefore clearly be regarded as chrysotile, not antigorite, notwithstanding the fact that Zussman (1953) has shown previously that fibrous serpentines commonly show an association between the 9·2-Å. fibre axis and antigoritic character. The classification of the serpentine minerals which is presented in Part II of this paper makes allowance for this exception to the general rule.

It is proposed that the variety of chrysotile with a 9·2-Å. fibre axis be described as para-chrysotile (para = alongside of; amiss).

Part II (J. Z.).

In this part powder data obtained from serpentine minerals are presented. Detail of the photographs is interpreted, as far as possible, in the light of the data given in Part I, and analogies and distinctions between different structural types are noted. All patterns were recorded with a 19-cm. camera using Ni-filtered radiation from a Cu target, and intensities were estimated by eye. The powder was in each case loaded into a thin-walled glass capillary of diameter 0·2 mm.

Since all except the antigorites (section 3 of the list of specimens, p. 125) possess closely related unit cells, their interplanar spacings may be listed conveniently in one table (table II). A few weak lines obtained from some specimens have been omitted since they were identified as deriving from an impurity (calcite, talc, magnesite, or magnetite). Specimens are referred to by number, and a key is provided which gives locality of origin and, where relevant, a collection number for each.

Ortho- and clino-chrysotile.

The powder photographs of the specimens in section 1 of the list of specimens (p. 125) show them to be most like those already dealt with in Part I, for they may be indexed on the basis of a cell with $a = 5{\cdot}32$,

TABLE II. Chrysotile and lizardite. Here are listed the d values in Å. and the intensities for individual, or average values for groups of similar, specimens. Column 1 gives the indices of the reflections, and the last column gives calculated spacings using the cell dimensions listed on page 119. The meanings of symbols following indices are explained on page 112.

Specn. *hkl.*	8 & 9.	10.	11.	14.	15 & 16.	17, 18, 19, and 20.	22.	23.	$d_{calc.}$
002	7·36 vs	7·37 vs	7·36 vs	7·36 vs	7·35 vs	7·35 vs	7·36 vs	7·37 vs	7·32
020	4·58 m	4·58 m	4·56 m	4·62 ms	4·61 m	4·60 m	4·58 m	4·59 m	4·60
022	—	—	—	3·89 w	3·90 mw	—	—	—	3·89
004	3·66 vs	3·66 vs	3·66 s.	3·64 vs	3·66 vs	3·66 vs	3·66 vs	3·66 vs	3·66
024	—	—	—	—	2·85 w	—	—	—	2·86
200	2·66 mw	2·66 mw	2·66 w	2·65 mw	2·66 mw	2·66 w	—	2·66 mw	2·66
201†	—	2·604 mw	2·604 mw	—	—	—	2·617 w	2·614 vw	2·614
201*	2·594 mw	—	—	—	—	—	—	—	2·590
202*	2·549 m	2·548 mw	2·547 vw	—	—	—	—	—	2·548
202†	—	2·500 ms	2·500 m	2·495 s	2·499 s	2·500 s	2·498 s	2·500 s	2·497
202*	2·456 s	2·455 s	2·451 ms	—	2·446 m	—	—	2·450 m	2·454
006	—	—	—	—	—	2·437 mw	—	—	2·438
203†	—	2·338 vw	—	—	—	—	2·340 mw	2·340 vw	2·332
200	—	2·289 vw	2·285 vw	2·299 w	—	2·290 vvw	—	—	2·301
203*	2·282 w	—	—	—	—	—	—	—	2·280
241*	2·215 w	2·211 vw	2·212 vw	—	—	—	—	—	2·214
241†	—	2·152 mw	—	2·148 m	2·150 ms	2·151 ms	2·150 mw	2·147 m	2·148
241*	2·096 m	2·094 m	2·093 mw	—	2·092 w	—	—	2·096 vvw	2·094
205†	—	—	1·972 vw	—	—	—	1·968 w	—	1·966
208	1·829 w	1·830 vw	1·828 w	1·830 w	1·826 w	1·830 w	1·830 w	1·826 w	1·829
206†	—	1·798 w	—	1·794 mw	1·795 m	1·796 m	1·797 w	1·795 mw	1·796
206*	1·748 m	1·747 mw	1·746 mw	—	—	—	—	—	1·748
060	—	—	—	1·737 mw	1·740 w	1·740 w	1·739 mw	1·739 mw	1·739
208	—	—	—	1·695 vw	1·699 w	1·696 vw	—	—	1·698
207†	—	—	—	—	—	—	1·640 w	—	1·643
060	1·536 s	1·534 s	1·531 ms	1·534 ms	1·535 s	1·535 s	1·534 s	1·537s	1·534
208†	—	—	—	1·503 m	1·503 ms	1·504 ms	1·504 m	1·504 m	1·506
060.10	1·465 w	1·465 vw	1·464 w	1·460 vw	1·462 w	1·463 w	1·464 w	1·462 vw	1·463
244	—	—	—	1·415 w	1·415 w	1·416 w	—	—	1·414
060	—	—	—	1·328 w	1·328 w	—	1·326 w	—	1·328
262*	1·317 mw	1·321 mw	1·319 mw	—	1·319 vw	—	—	—	1·322
262†	—	1·309 mw	1·310 mw	1·307 m	1·308 m	1·308 m	1·308 m	1·310 m	1·307
060.10†	—	—	—	1·279 w	1·282 mw	1·281 vw	—	—	1·281
264†	—	—	—	1·252 vw	1·250 vw	1·247 vw	—	—	1·248
060.12	—	—	—	1·218 vw	1·217 vvw	1·218 vvw	—	—	1·218
268†	—	—	—	1·167 vw	1·168 vw	—	—	—	1·167
268†	—	—	—	1·073 vvw	1·074 vvw	—	—	—	1·074
060	—	—	—	1·056 vvw	1·058 vvw	—	—	—	1·056
264†	—	—	—	0·994 w	0·995 w	—	—	—	0·998

$b = 9{\cdot}2$, $c = 14{\cdot}64$ Å., and $\beta = 93° 20'$ or $\beta = 90°$, and are seen to be clino-chrysotile or mixtures of clino- and ortho-chrysotile.

Specimens (8) and (9) give the pattern of pure clino-chrysotile, while (11) is evidently a mixture of clino- and ortho-chrysotile. It is a very well-oriented silky asbestos similar to those examined by Whittaker and its fibre photograph shows approximately 16% of ortho-chrysotile to be present. (10) shows prominently the pattern of clino-chrysotile, but some

additional weak lines indicate the presence of another species (see next section). (12) gives rather diffuse and weaker lines on a slightly higher background but is recognizable as mainly clino-chrysotile. Specimen (13) has not been examined by the writer, but a diffractometer chart recording of its powder lines, made available by Dr. G. H. Francis, showed it to be a mixture of clino- and ortho-chrysotile.

For all specimens in this group reflections of the type 0*kl* and *hkl* are absent (in (12) the *h*0*l* reflections are very weak). They may be presumed, therefore, to be structurally similar to chrysotile asbestos although their texture is generally splintery rather than silky. Many of them show at least a moderate degree of fibre orientation with *a* as fibre axis. 201* is the only clino-chrysotile line having *l* odd that is resolved from other lines. It may be seen in the pure clino- varieties but may be obscured by 201† when there is some ortho-chrysotile present. A notable feature on all photographs is the long 'tail' of the 130 reflection which often appears to end in a sharp edge coinciding with the reflections 202* and 006. The shape of this tail and its effects on the pattern's appearance have been discussed in Part I. Furthermore, if the position of 060 is taken to define the *b* parameter it is seen that the 040 and 020 reflections are displaced to higher angles (Aruja, 1943; Whittaker, 1955*a*).

Lizardite.

The powder patterns of specimens in section 2 of the list of specimens (p. 125) may be indexed on the basis of a cell with $a = 5{\cdot}31$, $b = 9{\cdot}2$, $c = 7{\cdot}31$Å., $\beta = 90°$, but for ease of comparison with data from section 1, the indices given refer to a cell with $c = 14{\cdot}62$ Å., so that reflections with *l* odd do not appear.

Specimens (14) and (15) show some reflections of the type 0*kl*, and from (15) a few weak lines of clino-chrysotile are observed. (16) is similar to (15) but has a greater proportion of clino-chrysotile, while (17), (18), (19), and (20) show no 'clino-' lines and their 0*kl* reflections are considerably weaker, in some cases being barely visible. These observations suggest that we are dealing with a new structural species of serpentine mineral composed of the $H_4Mg_3Si_2O_9$ sheets stacked orthogonally over one another with varying degrees of three-dimensional order. It must be recorded, however, that the observed relative intensities are not consistent with those calculated for a simple model. In the case of ortho-chrysotile the two possible sets of coordinates for Mg and (OH) ions in the octahedral section are occupied alternately in successive layers (Whittaker, 1953), whereas a single-layer cell would require that the

same set of coordinates be occupied in every layer. The observed intensities from specimens of section 2 correspond more closely to those calculated from the former model, and it is probable that in these cases the two alternative sets of positions are occupied randomly in successive layers.

For specimens (22) and (23) the lines may all be indexed only if an ortho-cell with $c = 14{\cdot}6$ Å. is assumed. They might appear, therefore, to be mainly ortho-chrysotile, but this is refuted by the relative intensities of the $20l$† lines. Table I shows that for ortho-chrysotile those with $l = 3$, 5, and 7 are stronger than those with $l = 4$, 6, and 8, whereas here the even index lines are the stronger. This seems to indicate the presence of the single-layer serpentine mixed with a smaller amount of ortho-chrysotile. (22) would appear to have a greater proportion of ortho-chrysotile since its reflections with l odd are relatively stronger than corresponding ones from (23). From neither of these specimens are $0kl$ reflections observed. The intensities of 'ortho'-cell reflections with l odd as compared with those having l even were also significant for specimens (10) and (11). Both are predominantly clino-chrysotile, but for specimen (11) 203† and 205† are visible while 204†, 206†, and 208† are not. For specimen (10) 204†, 206†, and 208† are visible while 203† and 205† are not. Thus (10) is a mixture of clino-chrysotile with the single-layer serpentine and not with ortho-chrysotile.

It is of interest to note the consistency of d values shown in all photographs dealt with so far, particularly when specimens which have a cell with $\beta = 90°$ are considered separately from those which do not. This is so in spite of widely different sources of material, and suggests that at least some of the variation in corresponding spacings hitherto reported may be due to differences in experimental conditions. In the present work all specimens were examined under identical conditions and the variations in observed d values are generally within the limits of the estimated probable error ($\pm 0{\cdot}1$ % for lines at $\theta \approx 30°$).

The average of uncorrected d values for specimens in each of the above categories correspond to cell dimensions as follows:

$\beta = 90°$	$a = 5{\cdot}31$	$b = 9{\cdot}20$	$c = 7{\cdot}31$ (or $14{\cdot}62$) Å.
$\beta = 93° 20'$	$a \sin\beta = 5{\cdot}32$	$b = 9{\cdot}20$	$c \sin\beta = 14{\cdot}64$ Å.,

and these parameters were used to derive the 'd_{calc}' list shown in table II.

Specimens (15), (17), (18), and (22) can be described as 'massive' serpentine and indeed are so fine-grained and unoriented that a stationary

specimen gives powder lines with no trace of spottiness. (16) and (23) show some orientation with fibre axis 5·3 Å. Specimen (14), however, is completely different in being white, not green, and separable into small platey crystals. It is the variety examined by Midgley (1951), who concluded that it was most like antigorite. This does not appear to be the case, and a more detailed investigation of the mineral is in progress.

Antigorite.

This section relates to those specimens whose lines cannot be indexed on the basis of the above cells or mixtures of them but which possess the large unit cell described below. Specimens (24) to (28) inclusive are practically monomineralic rock specimens from which small, platey single crystals may be obtained. Optical properties have been measured for three of these specimens (Hess, Smith, and Dengo, 1952; Zussman, 1954; Francis, 1956) and are seen to be closely similar. The data used for specimen (25) were presented by Hess *et al.*, while (26) (antigorite from Mikonui, New Zealand) has already been studied in some detail and was seen to have cell dimensions: $a = 43{\cdot}5$, $b = 9{\cdot}26$, $c = 7{\cdot}28$ Å., $\beta = 91° 24'$ (Aruja, 1944). Since the powder patterns of all five specimens are almost identical, it is safe to assume that this large cell is characteristic of all antigorites and not merely an exceptional variant, as may have been supposed. Table III contains average spacings, although some lines were not observed in all five patterns. The numerical intensity estimates are those measured by diffractometer for (25) by Hess, Smith, and Dengo, and these are approximately paralleled by the photographic visual estimates, with a few notable exceptions that may arise through orientation effects in the powder specimens.

Specimens (29) and (30) are best described as splintery with fibre axis 9·25 Å. Their powder photographs show fewer lines, which tend to be broader, but they correspond in each case with lines from the previous antigorite specimens, as can be seen in table III. It is assumed, therefore, that they possess the same basic cell and structure but are of smaller grain size and are less well ordered. (31) gives a photograph intermediate in quality between those from (28) and (30).

Indexing of the antigorite patterns was carried out with the aid of single-crystal Weissenberg and oscillation photographs, and the cell parameters corresponding to average uncorrected d values are as follows: $a = 43{\cdot}5$, $b = 9{\cdot}25$, $c = 7{\cdot}26$ Å., $\beta = 91° 23'$ (cf. those by Aruja). Eight reflections of the type $h0l$ and $h0\bar{l}$ were used to determine β.

TABLE III. Antigorite. Column 1 gives intensities recorded by Hess *et al.* (1952, p. 70). Column 2 gives d values in Å. obtained by combining data from photographs of specimens (24), (26), (27), and (28) with those given by Hess *et al.* for (25). The average d value is recorded for each reflection, although some were not observed in all five cases. Those without a visually estimated intensity were observed only from (25). Column 3 lists d values calculated for a cell with dimensions shown on page 120, and column 4 the indices of the reflections. Where indices are given for more than one reflection 'd_{calc}' corresponds to the first mentioned. Columns 5 and 6 give observed d values and intensities for specimens (29) and (30).

I.	$d_{obs.}$	$d_{calc.}$	*hkl.*	d_{obs}(29).	d_{obs}(30).
400	7·30 vs	7·26	001	7·28 vs	7·30 vs
24	6·95 —	6·93	$20\bar{1}$	—	—
16	6·52 w	6·56	$30\bar{1}$	6·40 w	—
8	5·80 w	5·96	401	—	—
3	5·11 vvw	5·15	710	—	—
6	4·67 mw	4·68	810	—	—
7	4·64 mw	4·63	020	4·64 mw	4·66 m
4	4·27 w	4·28	910	4·24 w	4·25 w
6	3·95 mw	3·95	$81\bar{1}$	—	—
300	3·63 s+	3·63	102, $10\bar{2}$	3·61 vs	—
24	3·52 vvw	3·50	302, $20\bar{2}$	—	—
2	2·88 —	2·88	$14.0.\bar{1}$	—	—
3	2·66 vvw	2·66	15.0.1	—	2·67 vvw
4	2·60 vw	2·60	930	2·60 w	—
8	2·57 mw	2·55	17.0.0, $16.0.\bar{1}$	—	—
70	2·53 vs	2·52	16.0.1	2·53 vs	2·53 ms
9	2·46 m	2·46	$93\bar{1}$	2·45 w	—
38	2·42 mw	2·42	003, 18.0.0	2·42 w	2·42 w
9	2·39 w	2·39	17.0.1, $30\bar{3}$, $10.3.\bar{1}$	2·38 vw	—
5	2·35 mw	2·35	403 ?	—	—
6	2·24 mw	2·24	15.0.2	2.25 vw	—
7	2·21 mw	2·20	$16.0.\bar{2}$	2·21 w	—
22	2·169 ms	2·169	$83\bar{2}$	2·163 m	—
20	2·153 m	2·150	16.0.2	—	—
4	2·127 w	2·126	$93\bar{2}$	—	—
4	2·113 w	2·113	$17.0.\bar{2}$	—	—
4	2·035 vw	2·033	$11.3.\bar{2}$	—	2·03 mw
3	1·879 w	1·879	$15.0.\bar{3}$	—	—
12	1·832 m	1·836	15.0.3	1.835 w	—
23	1·813 w	1·815	004, $10\bar{4}$, 833	1·813 w	1·819 mw
14	1·782 m	1·782	$93\bar{3}$	1·779 m	—
4	1·755 w	1·756	$10.3.\bar{3}$	—	—
10	1.738 mw	1·737	17.0.3	1.732 mw	—
2	1·680 vw	1·680	21.3.1	—	—
2	1·638 vw	1·636	$22.3.\bar{1}$	—	—
3	1·587 w	1·583	$14.0.\bar{4}$	—	—
12	1·563 m+	1·561	24.3.0	1·566 ms	1·561 m
9	1·541 m	1·541	060	1·541 ms	1·541 m
9	1·534 m	1·531	$24.3.\bar{1}$	—	—
13	1·523 m	1·522	15.0.4, $16.0.\bar{4}$, $22.3.\bar{2}$	1·525 w	1·528 w
8	1·509 mw	1·508	061	1·509 w	1·508 mw
10	1·497 m—	1·495	$17.0.\bar{4}$, $93\bar{4}$	1·494 w	—
7	1·480 w	1·479	934	1·477 vw	—
6	1·468 w	1·467	$18.0.\bar{4}$	—	—
6	1·462 —	1·462	10.3.4	—	—
10	1·452 w	1·451	$20\bar{5}$	1·449 vw	1·453 w
9	1·448 mw	1·446	205	—	—

Nomenclature.

In view of X-ray studies in recent years it would be desirable to reconsider the nomenclature of the serpentine minerals. It is clear firstly that only those should be called antigorite that possess the large cell and give the specific pattern described above. If any other name is to be used, perhaps picrolite could be retained to describe those antigorites that are distinctly fibrous or splintery. Among other serpentine minerals the names ortho-, clino-, and para-chrysotile can be applied as defined by Whittaker. These have structures based upon cylindrical layers; they have $c = 14{\cdot}6$ Å. and do not show three-dimensional order. There remains the orthogonal variety with $c = 7{\cdot}3$ Å., which can possess varying degrees of three-dimensional order. Unfortunately none of the previously used names (e.g. marmolite, metaxite, schweizerite) has been applied consistently to specimens of the latter type, but very many of them have been called 'serpentine'. Selfridge (1936) proposed that a third sub-group of the serpentine minerals should be referred to as 'serpentine', but use of this name for the whole and also for a particular part of the group has obvious disadvantages. It appears, therefore, that a new name is desirable by means of which specimens possessing the single-layer ortho-cell can be distinguished from chrysotile and from antigorite.[1] Since a well-known locality for serpentine minerals is the Lizard area of Cornwall, England, and since specimens of the sub-group in question are known to occur there (e.g. (14) and (22)), the name lizardite would seem appropriate.

Thus we have:

- serpentine
  - chrysotile
    - ortho-chrysotile
    - clino-chrysotile
    - para-chrysotile
  - lizardite
  - antigorite

Most of the light green or yellowish-green massive rock specimens examined, which would commonly be called serpentine, have in fact turned out to belong to the lizardite sub-group according to the above classification. Most of the splintery specimens that have any degree of ordering about the *a*-axis belong to the chrysotile sub-group, a few to lizardite, and none to antigorite. All of the splintery ones with *b* as fibre axis are seen to be antigorite, with the exception of para-chrysotile,

[1] It does not seem wise to add to the already large number of 'modified chrysotile' names ortho-, clino-, para-, α-, β-, γ-.

which has only been observed as intergrowths with ortho- and clino-chrysotile. Generally, the non-fibrous antigorites are more coarsely grained than other varieties and are blue-green in colour.

Bastite.

'Bastite' is the name commonly applied to serpentine pseudomorphs after orthopyroxene in basic and ultra-basic rocks, and it has been used as a synonym of antigorite (e.g. Winchell, 1951 ; Hess, Smith, and Dengo, 1952), presumably because the relict structures exhibited resemble the platey character of antigorite rather than the fibrous nature of chrysotile.

In the present study three bastite specimens were examined, two of which are of material from the type locality. They are seen, however, to give patterns of chrysotile (12) or of lizardite ((19) and (20)) and not of antigorite. Another bastite (21), for which a diffractometer record was made available by G. H. Francis, gave broad peaks spread across the chrysotile and lizardite positions and did not give those characteristic of antigorite. It seems likely, therefore, that other specimens described as bastite are similarly not antigorite, if the latter mineral is defined in the strict sense suggested in this paper.

Comparison between powder patterns of antigorite and other serpentine minerals.

In much published work recognition of a serpentine mineral as either antigorite or chrysotile has been made on the basis of the powder data given by Selfridge (1936) and Gruner (1937). In the former case molybdenum radiation was used giving rather poor resolution, relatively few lines were recorded, and indexing was not attempted. In the latter work iron radiation was used, but with a camera of small radius, and so, in both, no clear indication of the various chrysotile and lizardite cells can be discerned. Distinction between antigorite and chrysotile is, however, possible, although deductions using the region of the pattern near 202† may be misleading when resolution is poor, since, as can be seen from fig. 1, it is just here that the most marked variations within non-antigorites occur. Indexing of both antigorite and chrysotile using one set of cell dimensions has been attempted (Gruner, 1937) and led to some false correspondences'.

With the better resolution of a 19-cm. camera and the improved understanding of the atomic structure of serpentine minerals in the years since 1941,[1] the distinction between antigorite and the remainder

[1] Warren and Hering (1941) suggested a 'sheet' structure for chrysotile.

becomes possible in various parts of the powder diagram, but most reliably from the pattern of lines as a whole. Some antigorite lines do occur in positions close to those from chrysotile, but if the complete pattern is observed and accurately measured then the intensity relationships, the presence of many extra lines, and the small but significant differences between apparently corresponding spacings make correct identification certain. When the specimen is less well ordered (e.g. (29)) many weak lines are hardly, if at all, visible and the pattern may look very similar to one of lizardite, but distinction is still quite definite. The strong line from antigorite at $d = 2{\cdot}52$ Å. may be confused with 202† of lizardite but it should be noted that in the latter varieties $d_{202\dagger}$ has not been observed greater than 2·50 Å. The strong line at $d = 1{\cdot}563$ Å. in antigorite is important in that it is not 060 and has no counterpart in chrysotile or lizardite patterns. With the moderately strong 060 ($d = 1{\cdot}541$ Å.) it forms a prominent pair of lines which are not strictly 'equivalent' to the strong pair at $d = 1{\cdot}535$ Å. and 1·503 Å. given by lizardite. Lines on antigorite photographs, even for the more poorly crystalline varieties, are generally sharper than those from other serpentine minerals.

Among other antigorites for which data are available are those from Antigorio, Hokitika, and Griffin Range (Aruja, 1943), and one referred to as bowenite (Francis, 1956). These all have patterns similar to those discussed above. One other from Unst, Shetlands, described by Brindley and von Knorring (1954) as ortho-antigorite, appears in the light of the present work to be predominantly ortho-chrysotile. Although it shows many closely spaced weak lines which suggest a large cell parameter of 43·8 Å. it is certainly different from antigorite (see criteria above). The lines, moreover, are not the same as those given by the specimens here examined. Some discussion of the note by Brindley and von Knorring occurs elsewhere (Zussman, 1956).

While it is believed that the scheme of classification proposed here should form a sound basis for further work, it is not claimed to be exhaustive. A complete classification of the serpentine minerals may well involve further distinctions between structural varieties which have not so far been recognized.

Acknowledgements.—J. Z. wishes to acknowledge the co-operation of the many people involved in making available the specimens used in this investigation, and to thank Dr. G. H. Francis for helpful discussions. E. J. W. W. wishes to thank the Directors of Ferodo Ltd. for permission to publish the work described in Part I.

List of specimens studied.

No.	*Ref.*[1]	
		1. *Mainly chrysotile.*
1	B. 324	Chrysotile. Silesia.
2	—	„ Bell's Mine, Thetford, Quebec.
3	—	„ Cuddapah, Madras, India.
4	—	„ Kranskop, Natal.
5	—	„ „ „
6	—	„ „ „
7	—	„ Premier Mine, Transvaal.
8	O. 3930	'Schweizerite.' Findelen Glacier, Zermatt, Switzerland.
9	B.M. 27612	'Metaxite.' Reichenstein, Silesia.
10	B.M. 93645	'Marmolite.' Hoboken, New Jersey, U.S.A.
11	M. 14676	Chrysotile asbestos. Cross fibre vein in (17).
12	—	'Bastite.' Port Macquarie, New South Wales.
13	C. (H.) 76140	Chrysotile asbestos. Milton, Glen Urquhart, Scotland (Francis, 1956).
		2. *Mainly lizardite.*
14	—	'Serpentine mineral.' Kennack Cove, Lizard, Cornwall (Midgley, 1951).
15	O. 17788	'Serpentine mineral.' Snarum, Norway.
16	B.M. 47963	'Marmolite.' Hoboken, New Jersey, U.S.A.
17	M. 14676	Serpentine rock in dolomite. Transvaal.
18	—	'Serpentine mineral.' Hindubagh, Baluchistan.
19	B.M. 170 Ap.	Bastite. Baste, Harz, Germany.
20	B.M. 67807	„ „ „ „
21	C. (H.) 76113	„ Polmaily, Glen Urquhart, Scotland (Francis, 1956).
22	—	Serpentine. I.C.I. Quarry, Kennack, Lizard, Cornwall.
23	O. 1899	„ New York.
		3. *Antigorite.*
24	O. 16328[2]	Serpentine. New York.
25	—	Antigorite. Caracas, Venezuela (Hess, Smith, and Dengo, 1952).
26	C. 11566	Antigorite. Cross River, Mikonui, New Zealand (Aruja, 1954; Zussman, 1954).
27	C. (H.) 76095	Antigorite. Milton, Glen Urquhart, Scotland (Francis, 1956).
28	O. 16327	Serpentine mineral. Val Antigorio, Switzerland.
29	O. 16336	Picrosmine, Tyrol.
30	C. TW. 2915	Picrolite. Taberg, Sweden.
31	C. 7236	Serpentine. Asbestos Creek, Mikonui, New Zealand.

[1] B. Bristol Museum; O. Oxford University Museum; B.M. British Museum (Nat. Hist.); M. Manchester University, Dept. of Geology; C. Cambridge University, Dept. of Mineralogy and Petrology; (H.) Harker Collection.

[2] In the paper by Zussman (1954) two errors occur in table II. O. 16328 should not have been [illegible] all, and O. 1899 should refer to the specimen labelled 'Serpentine (N[illegible]

References.

Aruja (E.), 1943. Ph.D. Thesis, Cambridge.
—— 1944. Min. Mag., vol. 27, p. 65.
Brindley (G. W.) and Knorring (O. von), 1954. Amer. Min., vol. 39, p. 794 [M.A. **12**–463].
Francis (G. H.), 1956. Amer. Journ. Sci., vol. 254, p. 201.
Gruner (J. W.), 1937. Amer. Min., vol. 22, p. 97 [M.A. **7**–93].
Hargreaves (A.) and Taylor (W. H.), 1946. Min. Mag., vol. 27, p. 204.
Hess (H. H.), Smith (R. J.), and Dengo (G.), 1952. Amer. Min. vol. 37, p. 68 [M.A. **12**–31].
Jagodzinski (H.) and Kunze (G.), 1954. Neues Jahrb. Min., Abt. A, Monatshefte, p. 113 [M.A. **12**–436].
Midgley (H. G.), 1951. Min. Mag., vol. 29, p. 526.
Selfridge (G. C.), 1936. Amer. Min., vol. 21, p. 463.
Warren (B. E.) and Hering (K. W.), 1941. Phys. Rev., vol. 59, p. 925.
Whittaker (E. J. W.), 1952. Acta Cryst., vol. 5, p. 143 [M.A. **11**–539].
—— 1953. Ibid., vol. 6, p. 747 [M.A. **12**–337].
—— 1954. Ibid., vol. 7, p. 827.
—— 1955 *a*, *b*, *c*, *d*. Ibid., vol. 8, pp. 261, 265, 571, and 726.
Winchell (A. N.), 1951. Elements of Optical Mineralogy, Part II (New York and London), p. 386 [M.A. **11**–463].
Zussman (J.), 1953. Nature, vol. 172, p. 126 [M.A. **12**–212].
—— 1954. Min. Mag., vol. 30, p. 498.
—— 1956. Amer. Min., vol. 41, p. 148.

Replacements involving early carnallite in the potassium-bearing evaporites of Yorkshire.

By F. H. Stewart, B.Sc., Ph.D., F.G.S.

Department of Geology, Science Laboratories, South Road, Durham.

[Read 26 January 1956.]

Summary.—Evidence from four recent boreholes in the Yorkshire potash field suggests that carnallite was an important original constituent of the Middle Evaporite Bed, and that much of the sylvine of the potash zone is of secondary origin.

The carnallitic rocks have been affected by complex replacements, an earlier series involving sylvine, halite, and anhydrite, and a later series involving rinneite, halite, sylvine, and carnallite.

THE experimental work of van't Hoff and other workers has shown that in the evaporation of sea-water the principal potassium-bearing chloride deposited should be carnallite. Sylvine does not appear in the experimental salt succession at reasonable temperatures. In most natural deposits, however, sylvine is one of the most abundant potassium salts, and carnallite is generally subordinate in quantity. These facts have led to suggestions that sylvine is, at least partly, formed by secondary replacement of earlier carnallite, due to contemporaneous or post-consolidation reaction or solution and redeposition, involving brines originating in various ways (e.g. contemporaneous influx of sea-water, later ground water, residual trapped brines, brines formed by rise in temperature during burial, &c.).

Although in many cases direct evidence of these processes is not available, in most salt deposits there is evidence of redistribution of salts, especially in the potash zones, where the minerals are highly susceptible to solution or reaction. In the Permian potash deposits of Yorkshire evidence of widespread replacement and recrystallization has been described (Stewart, 1949, 1951; Armstrong, Dunham, and others, 1951; Raymond, 1953), but hitherto there has been no evidence of the former presence of primary carnallite in large quantity in the potash zones, where sylvine is abundant and carnallite relatively scarce. The home of carnallite is in the Carnallitic Marl, which separates the Upper and Middle Evaporite Beds, and most of this carnallite is secondary, occurring as veinlets in the clay.

Fisons Limited have recently sunk four boreholes in the Yorkshire potash field, sited at Robin Hood's Bay (F.1 borehole), Staintondale (F.2), Little Beck (F.3), and Hawsker (F.4) (see map in Stewart, 1954, p. 212). In these boreholes the evaporite succession is similar to that found in previous boreholes in the Whitby district. All four holes show a potash zone with abundant sylvine in the Middle Evaporite Bed, and two holes (F.2 and F.4) show a sylvine-rich zone in the Upper Evaporite Bed. In all these boreholes the writer has found structures in the potash zone of the Middle Evaporite Bed which he interprets as pseudomorphs, mainly of halite, after carnallite. These are so abundant as to indicate that carnallite was an important original constituent of this zone. The potash zone of the Upper Evaporite Bed shows no evidence of this type.

Nature of the pseudomorphs.

The pseudomorphs are normally composed of halite, which in some cases has been replaced by later minerals, as described below. Typical examples are shown in figs. 3 and 4. When enclosed in clay they are often well formed, but where clay is subordinate they tend to show poorly developed outlines. They are generally fairly small in comparison with the average grain size of chlorides in these evaporites, the well-shaped pseudomorphs reaching a diameter of a few millimetres. Many have hexagonal outlines and others are diamond shaped, while some have more than six sides. Sections of cubic halite would provide a variety of shapes, and hexagonal sections would not be uncommon, but in all such sections the cleavage traces should be parallel to the edges. In the pseudomorphs the halite cleavages are variably orientated with respect to the edges. Rectangular and trigonal sections are relatively rare where the pseudomorphs are abundant.

It seems clear that these grains are pseudomorphs. That they represent early carnallite is suggested by the fact that corroded relics of carnallite are occasionally found within them, in the form of very small ragged grains in common optical orientation. Sometimes the residual carnallite has apparently recrystallized as pseudo-hexagonal crystals, and sometimes it fills negative cubic cavities in the halite.

The shapes of the pseudomorphs are similar to those of small crystals of carnallite found, enclosed in halite, through a considerable depth range in this evaporite bed. The interfacial angles of the sharpest hexagonal sections of the pseudomorphs agree with the angles $110 \wedge 010$ and $110 \wedge 1\bar{1}0$ of carnallite, although precise measurement is impossible

because of irregularities in outline. Some of the diamond-shaped sections give angles corresponding to $110 \wedge 1\bar{1}0$ of carnallite, and zoning of impurities within such crystals shows that the form 010 was present at an earlier stage of growth. Some rounded pseudomorphs may represent sections of complex carnallite crystals like those figured in mineralogical textbooks (e.g. *Dana's System of Mineralogy*, 7th edition, vol. 2, p. 93).

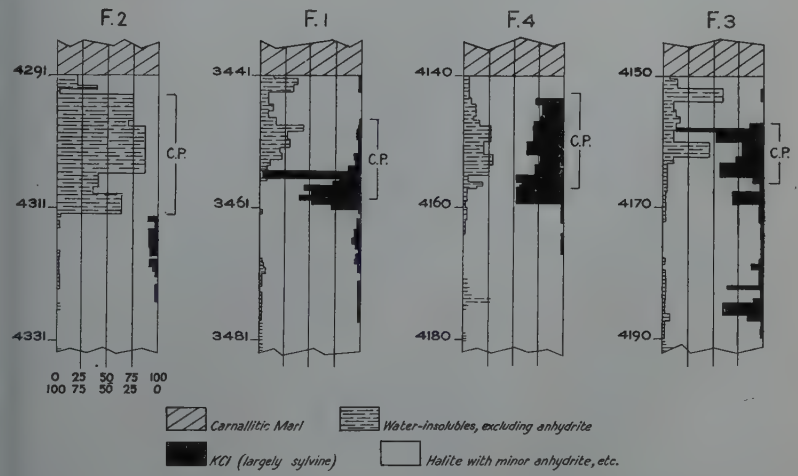

FIG. 1. Partial logs of Fisons's boreholes in north Yorkshire, showing the upper halite and potash zones, and part of the lower halite zone, of the Middle Evaporite Bed. The analytical values for KCl and water-insoluble material were determined by Fisons Limited for the following depth ranges: F. 1 borehole, 3441–78 feet; F. 2 borehole, 4291–4325 feet; F. 3 borehole, 4150–90 feet; F. 4 borehole, 4140–67 feet below surface. CP = pseudomorphs after carnallite.

Distribution.

Fig. 1 shows the range through which the pseudomorphs are found in the potash zone of the Middle Evaporite Bed of the four F. boreholes. The KCl content of the potash zone (largely contained in sylvine) and the content of water-insoluble material (largely magnesitic clay) is also shown. Within the depth ranges indicated, the pseudomorphs are extremely abundant. In the F.1 borehole, for example, it is estimated that carnallite originally formed more than 50 % of the soluble salts in the upper part of the potash zone.

It can be seen that the distribution of early carnallite does not coincide with the present distribution of sylvine, although their ranges overlap. It is believed that much of the sylvine has formed during secondary

redistribution of salts. The zone rich in early carnallite is succeeded upwards by a thin zone consisting largely of halite with clay (the upper halite zone); carnallite occurs here in the form of veinlets cutting clay, and pseudomorphs after early carnallite are absent.

Pseudomorphs after carnallite occur in thin clay-rich layers within the lower halite zone of this evaporite bed, indicating periods of almost complete desiccation followed by influx of more brine.

Petrography.

The rocks have been affected by complex replacements which can be divided into two main series. The earlier series involves the replacement of original carnallite and perhaps rinneite by sylvine, halite, and anhydrite, and the later involves the introduction of new rinneite, sylvine, and carnallite. These replacements are depicted graphically in fig. 2.

First replacement series. Where least modified by the later replacements, the rocks are medium grained and consist of variable proportions of dark grey to black clay and halite, with subordinate anhydrite, magnesite, and quartz, and scarce sylvine and carnallite. Tiny hematite plates are abundant inclusions in some of the halite. Pyrite is an occasional accessory. The original bedding, approximately horizontal, is shown by variations in the quantity of clay, and the distribution of the pseudomorphs indicates an original roughly layered series of carnallite-rich and halite-rich layers.

In some of these rocks irregular patches of blood-red halite, interstitial to pseudomorphs of brown halite after carnallite, suggest the former presence of an iron-bearing mineral. The red halite is crowded with minute hematite inclusions, which are often arranged in zones which do not appear to bear any definite relation to crystallographic directions in their host. The patches closely resemble patches of rinneite of the later replacement series which are partly replaced by sylvine or halite with hematite inclusions. It is therefore suggested that the red halite of the first replacement series has replaced early rinneite which may itself be a secondary mineral.

The original rocks, then, apparently consisted of carnallite, halite, magnesitic clay, and subordinate anhydrite. Rinneite may have been introduced at an early stage. The replacement of carnallite and the mineral believed to be rinneite is almost complete. Corroded relics of sylvine in pseudomorphs of halite after both the early minerals show that sylvine appeared at an intermediate stage and was then converted to halite. Secondary anhydrite sometimes accompanies the halite in

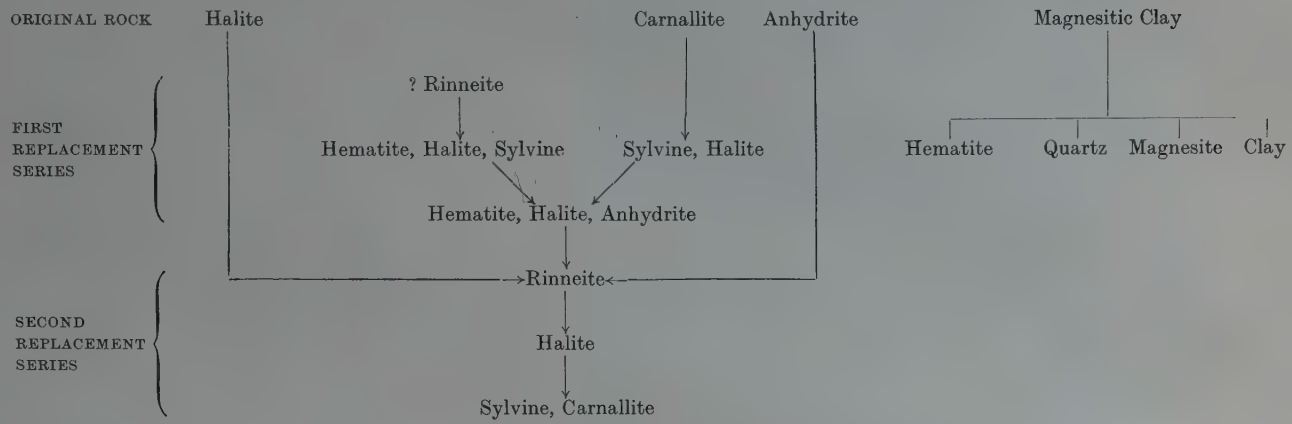

FIG. 2. Replacements in the potash zone of the Middle Evaporite Bed.

pseudomorphs after carnallite and is occasionally the dominant secondary mineral.

In addition to the hematite derived from early rinneite (?), hematite is present in extremely small particles in most of the halite, colouring it pink or brown. The colour is most pronounced near the contact of halite

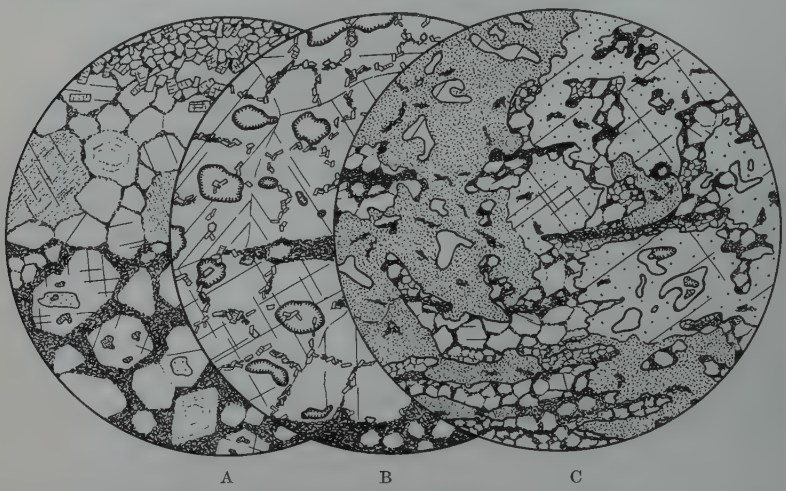

Fig. 3. A. Halite pseudomorphs after early carnallite, enclosing relics of carnallite (heavily stippled), and sylvine (lightly stippled), are partly enclosed in clay. Two large halite grains, with lines of hematite inclusions (right and left centre) may have replaced earlier rinneite. Anhydrite projects into halite at top of diagram. Magnesite and quartz, present in small quantity, are omitted. F. 1 borehole, 3452 feet below surface. ×23. B. Large colourless halite grains of the second replacement series enclose corroded, optically continuous, relics of rinneite. The rinneite has replaced earlier halite pseudomorphs after carnallite, whose boundaries are indicated by strings of anhydrite and magnesite. Some unaltered pseudomorphs are enclosed in clay layers. F. 1 borehole, 3450 feet below surface. ×23. C. Halite-clay rocks of the first replacement series (the halite is red-brown in colour) are invaded by large grains of sylvine (lightly stippled) and carnallite (heavily stippled) of the second replacement series. The latter contain corroded relics of colourless halite and rinneite, introduced at earlier stages of the second replacement series. The rinneite relics (SE. quadrant) are optically continuous, and several halite relics (NW. quadrant) have parallel cleavages. Small quantities of anhydrite, magnesite, and quartz are omitted. F. 1 borehole, 3454 feet below surface. ×8·6.

with clay, and it is believed that the iron oxide has been derived by leaching of the clay. This hematite is present in sylvine relics but not in relics of early carnallite and not in minerals of the second replacement series, which suggests that the modification of the clay took place during the early replacements.

Euhedral quartz is mainly associated with clay, and was probably formed at the same time as the hematite, the silica being derived from the clay. Some quartz crystals contain zones of hematite inclusions. Magnesite plates, often fringing clay, may have been formed by

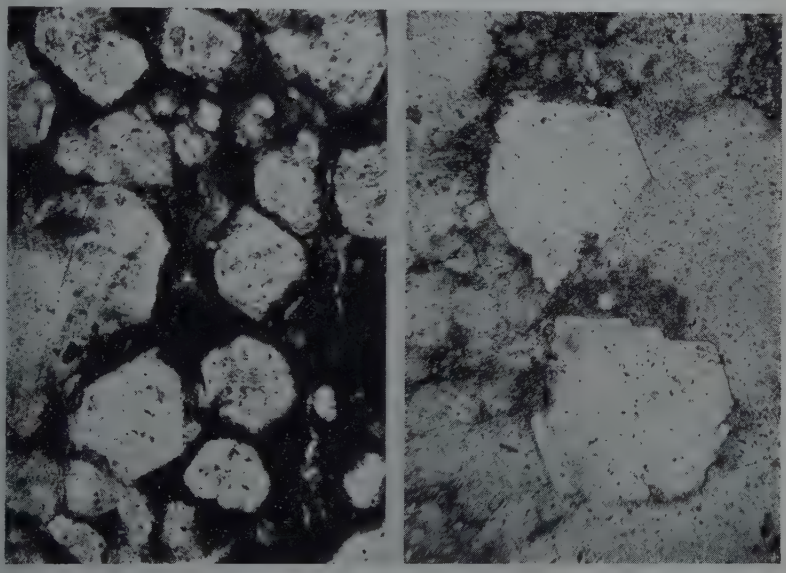

A B

FIG. 4. A. Halite pseudomorphs after carnallite, enclosed in clay. F. 1 borehole, 3452 feet below surface. ×32. B. Halite pseudomorphs after carnallite, enclosed in sylvine of the second replacement series. One of the pseudomorphs has been partly replaced by sylvine, but retains some sharp boundaries. The dark material is clay, which encloses a quartz crystal near the centre of the figure. F. 3 borehole, 4060 feet below surface. ×23.

recrystallization of fine-grained magnesite. This mineral also occurs as small grains in thin anhydrite layers which are considered to be primary.

In the first replacement series the original textures of the rocks have been preserved, and there has been no appreciable mechanical displacement of material.

Second replacement series. These replacements involve the introduction of rinneite, halite, carnallite, and sylvine in irregular patches and vein-like masses. The original structures are sometimes largely obliterated, the older material being partly displaced and broken up, including the clay. In other cases a network of anhydrite, quartz, magnesite, and clay indicates the original structure.

The first change is the introduction of rinneite, and this is well seen in material from the F.1 borehole, near the top of the potash zone. The mineral forms large irregular grains, which have replaced halite. It is normally colourless, and it is possible that the pre-existing hematite in the halite has contributed iron to the secondary rinneite. Plentiful relics of brown halite are found in the rinneite. The secondary mineral forms fairly large grains, up to about a centimetre in length, but these are often represented by optically continuous relics in later minerals. Anhydrite has been partly attacked at this stage.

The second change is the replacement of rinneite by colourless halite, and most of the rinneite now seen has been partly replaced and occurs as small relics enclosed in the halite.

The third change is the replacement of the early red halite, the rinneite, and the late colourless halite by sylvine and carnallite, which enclose optically continuous relics of these minerals, and occur as irregular veins penetrating them. The sylvine and carnallite form irregular grains, of variable size and occasionally very large (up to 2 inches across in the veins). They may have formed simultaneously, as there is no evidence of the one replacing the other. The carnallite is honey-yellow in hand specimen, and the sylvine white or red, or white with red edges, the red colour being due to inclusions of hematite.

Rinneite and carnallite of this replacement series are abundant only in the upper part of the potash zone of the F. 1 borehole. Sylvine is the main late replacing mineral in the F. 3 and F. 4 boreholes, and is also abundant in the lower part of the range of pseudomorphs after carnallite in the F. 1 borehole. In the F. 2 borehole the upper part of the potash zone is extremely rich in clay, and the late potassium-bearing salts are present only in very small quantity.

In all these rocks veinlets of halite and carnallite, sometimes with slickensided walls, penetrate clay and all the minerals so far described.

Conclusions

It is suggested that carnallite was an important original mineral of the potash zone of the Middle Evaporite Bed, occurring in a layered series of carnallite-rich and halite-rich rocks. This accords with the experimental evidence. Pseudomorphs after carnallite have been seen in all the F. borings and in one of the few specimens recovered from the potash zone in the E. 2 boring.

In the first replacement series this primary carnallite has been almost completely replaced; $MgCl_2$ and then KCl have been removed, and

NaCl and $CaSO_4$ introduced, the end-products being halite and anhydrite. In the thin pseudomorphous layers within the lower halite zone these replacements have probably been effected by influx of less saline marine brine after periods of almost complete desiccation. A similar origin may be invoked for the main pseudomorphous range, in the potash zone, the new brines being responsible for deposition of the upper halite zone. The absence of pseudomorphs after carnallite in the upper halite zone supports this origin, rather than that of post-consolidation leaching.

The second replacement series involves local introduction of $MgCl_2$ and $FeCl_2$, and general introduction of KCl, at the expense of NaCl and some $CaSO_4$. The fact that sylvine is the main secondary mineral suggests either that the replacements were effected at a relatively high temperature (perhaps resulting from burial under a considerable thickness of later rock), or that the brines responsible had compositions lying off the liquid line of descent from sea-water. After removal of $MgCl_2$ the second stage of the first replacement series involves the removal of sylvine, and this would result in brines rich in KCl. The migration of these brines might lead to re-deposition of sylvine at different levels of the potash zone. Potash-rich brines might, however, arise in various other ways (e.g. from connate waters, geothermal metamorphism, post-consolidation leaching). Whatever may be the cause or date of the later replacements, it is apparent that the present distribution of potash salts does not coincide with their original distribution in a vertical sense, although it approximates to it. This also appears to be true in a horizontal sense; for example, pseudomorphs after carnallite are widely distributed but sylvine is scarce in the F. 2 borehole. This horizontal redistribution of salts is an important factor to be taken into account in exploration of the potash field for economic purposes.

In conclusion I wish to record my sincere thanks to Fisons Limited for permission to publish data on their material and to use the results of analyses carried out in their laboratories.

References.

Armstrong (G.), Dunham (K. C.), Harvey (C. O.), Sabine (P. A.), and Waters (W. F.), 1951. Min. Mag., vol. 29, p. 667.

Raymond (L. R.), 1953. Quart. Journ. Geol. Soc., vol. 108, p. 283.

Stewart (F. H.), 1949. Min. Mag., vol. 28, p. 621.

—— 1951. Ibid., vol. 29, p. 445.

—— 1951. Ibid., vol. 29, p. 557.

—— 1954. Proc. Yorks. Geol. Soc., vol. 29, p. 185.

A phase-contrast microscopic study of the surface structure of blende crystals.

(With Plates III and IV.)

By Ajit Ram Verma, M.Sc., Ph.D.
Royal Holloway College, University of London.[1]

[Communicated by Dr. G. F. Claringbull; taken as read 26 January 1956.]

Summary.—The surface structure of blende crystals from Joplin, Jasper County, Missouri, U.S.A., has been explored by the application of phase-contrast microscopy and light-profile microscopy. Attention has been specially directed to the small-scale features with thicknesses (or depths) of molecular dimensions.

Some growth features of special interest were observed. A large number of beautifully developed growth spirals were observed on the tetrahedral face of a blende crystal. These are in accord with the dislocation theory of Burton, Cabrera, and Frank. The high visibility of these growth spirals is possibly due to the preferential deposition of some impurity, or etching, which also gives a mottled appearance to the entire surface. In addition, an extensive microscopic structure has been observed on some crystal faces. Triangular growth terraces and markings are seen, both orientated parallel to the edges of the crystal. Some triangles, inverted with respect to the latter, have been explained on similar lines to the well-known 'growth trigons' on the octahedral faces of diamond as arising from imperfect dislocations.

An attempt has been made to explain the growth features in the light of known theories of crystal growth.

THE surface structure of mineral and other crystals has been studied from time to time by several workers, and these observations have helped us to understand the mode of growth of crystals. Most of the work has been done microscopically, using bright field illumination or polarized light. Recently Seager (1953) examined the surfaces of a large number of mineral crystals for the study of growth structures but utilized only a metallurgical type of microscope using low powers (usually 1 inch objective). Improved optical and interferometric techniques are now available. Tolansky (1948) and his co-workers have used multiple-beam interference fringes extensively for the study of the surface topography of crystals such as quartz, mica, diamond, silicon carbide, &c. Until recently phase-contrast microscopy has received only slight attention for the study of minerals, but some uses have been described by Bennett, Jupnik, Osterberg, and Richards (1946), and by Smithson (1946, 1948), the latter confining himself mainly to thin sections of rocks. But lately, mainly

[1] Now at the University of Delhi, India.

because of the interest stimulated by the dislocation theory of crystal growth (Frank 1949*a*; Burton, Cabrera, and Frank, 1951), a closer examination of surface structure has been carried out for a large number of crystals and minerals by several workers. Over the past few years the author has also been carrying on a study of the topography of crystals, including minerals, utilizing a combination of multiple-beam interferometry and phase-contrast microscopy, with high magnifications. The different minerals that have been studied have been chosen mainly from the collection at the British Museum (Natural History). The choice of crystals has often been dictated by the demands of interferometry which requires crystals with almost perfectly plane faces. Attention has particularly been directed to the study of small-scale features with thicknesses of only molecular dimensions. A phase-contrast microscopic study of zinc-blende crystals is now presented. The multiple-beam interferometric study of some minerals will be described in a later communication.

Experimental methods.

Phase-contrast microscopy is a well-established technique and it is not proposed to give any detailed account here. Its principles were enunciated by Zernicke (1934), and recently an account of this branch of microscopy, including its applications and an extensive bibliography, has been given by Bennett, Jupnik, Osterberg, and Richards (1951). We give below some of the special features pertaining to the present investigation.

The microscopic study of the crystal surfaces has been carried out on phase-contrast equipment which can be fitted on to a Vickers projection microscope manufactured by Cooke, Troughton, and Simms. Since the crystals studied were opaque, only the reflection type of equipment has been used, which has an additional advantage that for two features differing in level by t the path difference becomes $2t$ in reflection and hence has a greater sensitivity as compared with transmission. A diagrammatic scheme of the general arrangement is shown in fig. 11. An annular diaphragm D serves as the entrance pupil of the optical system consisting of the field lens, the microscope objective, and the reflecting surface of the specimen. The field lens and the objective form an image D_1 of the field diaphragm just below the surface of the specimen The reflected light passes through the objective and forms a real image D_2 (shown by solid lines) of the diaphragm D. Image D_2 is the exit pupil and the place where the phase plate is placed. In the present equipment the optical assembly, consisting of the microscope objective lenses, 45° inclined beam splitter, and the phase plate, is all mounted on the objective. Objectives of focal

length 25 mm., 16 mm., 8 mm., 4 mm., and 2 mm. (oil immersion) were available. The equipment used was a positive phase contrast with the phase retardation of $\pi/2$, the absorption of the phase plate being equal to 80 %. Whenever permission could be obtained for silvering the surface of the specimen this was always done, since silver truly contours the

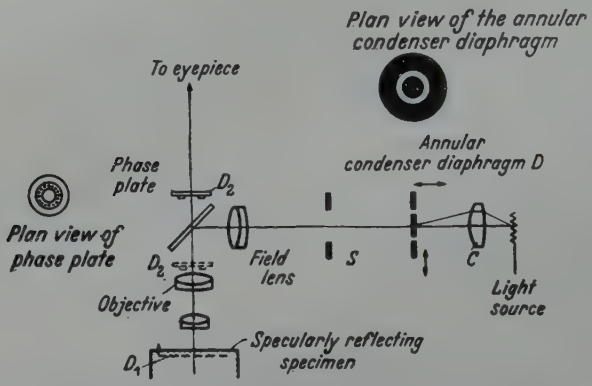

FIG. 11. Diagrammatic sketch of the arrangement for phase-contrast microscopy by reflected light.

surface and does not impose any topography of its own, but cuts down the exposure time and thus reduces the background fogging of the photographic plate. The same silvered crystal can then also be used for multiple-beam interferometric studies or light-profile microscopy. The thin layer of silver deposited on the crystal is usually 400–500 Å. thick, giving a reflectivity of 80–90 %. The silvering is done *in vacuo* in a commercial evaporating unit manufactured by Edwards & Co.

When dealing with rough surfaces, as in the present case of blende crystals, the interferometric techniques cannot be adequately applied. For such specimens having surface features of heights (or depths) ranging from a fraction of a micron to a few microns and requiring the use of high-power or even oil-immersion objectives, the technique of light-profile microscopy is specially suitable (Tolansky, 1952).

Results of observation (pls. III and IV).

Of a large number of blende crystals examined, one group was found to show several interesting surface features, and all the following illustrations refer to them. They all come from Joplin, Jasper County, Missouri, U.S.A., and form a part of the Trechmann collection of the British

Museum. The Pb–Zn ores of Joplin are of low-temperature metasomatic origin. On the matrix of some of the specimens small crystals of pyrite were observed. The first crystal (crystal no. 1) has one fairly well-developed face of a tetrahedron of which the sign was not determined, together with a face of the form {100}. The appearance of this tetrahedral face is shown in pl. III, fig. 1, which is a low-power photomicrograph taken with bright field illumination using the green line, $\lambda 5461$, of a mercury arc. To the naked eye the face shows somewhat dark metallic lustre, the surface appearing quite polished and smooth but showing some interference colours; some interference fringes can be seen in fig. 1. On examining this tetrahedral face by the phase-contrast microscope without silvering it, the whole surface appeared mottled, though according to Miers (1929) this mineral is exceptionally free from tarnish. However, on this messy background several surface features could be observed and are discussed below. Crystal no. 2, which also showed some interference tints, has one prominently developed cube face nearly 7 mm. $\times$ 8 mm., together with faces of {111} and {$\bar{1}$11}. Pl. III, figs. 4 and 5, refer to crystal no. 2, all others to crystal no. 1.

The observed surface structures may be summarized as follows:

The commonly observed triangular growth terraces and lines may be seen in pl. III, figs. 3, 4, and 6; the triangular shape of these hills on tetrahedral faces is in conformity with the general observation that growth layers show the same degree of symmetry as the face on which they grow.

Growth spirals on the tetrahedral face of crystal no. 1 are observable on the mottled background in pl. IV, figs. 7, 8, and 10.

Small triangular markings can be seen at the bottom of fig. 7, and are shown enlarged, using high power, in fig. 9; these triangular markings are, throughout the surface of the crystal, orientated in the same direction as the edges of the tetrahedral face of fig. 1.

A hexagonal area (see fig. 2, which shows a part of fig. 1 under high power) is completely free from the messy background. This hexagonal area does not appear to be orientated in any simple crystallographic direction with respect to the edges of the growth terraces, which continue into or right across the figure. To decide whether this smooth hexagonal area is an elevation above or a depression below the general level of the crystal surface around it, a light-profile photomicrograph was taken; the shift of the profile line showed it to be a depression. Thus the possibility that it is an overgrowth can be ruled out. Perhaps a small adherent crystallite protected the surface underneath during the last

phase of growth and was dislodged afterwards; it may have been an inclusion of calcite or galena.

An extensive system of substructure was seen on the tetrahedral faces of crystals 1 and 2 (figs. 6 and 4). It appears as if these figures were produced as a result of solution, but it is not possible to verify this since permission could not be obtained to etch these crystals. However, according to Gebhardt (1933), etching experiments give sharply defined triangular or hexagonal pits on (111) and no figures on ($\bar{1}11$).

Fig. 5 shows several deep triangular pits on a tetrahedral face on crystal number 2.

Perfect screw dislocations and growth spirals.

The formation of a perfect screw dislocation in a crystal creates on the surface a terminated step with a height equal to (or an integral multiple of) the X-ray unit cell. When growth proceeds on this step it winds itself into a spiral shape, giving rise to growth spirals with molecular step heights (Burton, Cabrera, and Frank, 1951). These predicted growth spirals have been observed on several crystals (for a detailed list of references see Verma, 1953). A growth spiral originating from a unit dislocation in a blende crystal would not be easy to observe because of the small size of the unit cell ($a = 5{\cdot}42$ Å.). However, it has been observed that a deposit of a suitable impurity along the growth edges can often lead to a remarkably high visibility (Verma, 1951; Vand, 1951; Forty and Frank, 1953). The growth spirals of figs. 7 and 10, which have possibly unimolecular step heights, may have been revealed by this 'decoration effect' of the impurities. However, it is not possible to measure the step heights of these growth spirals by multiple-beam interferometry because of the extensive background on the surface of the crystal. Applebe and Kaye (1953) attributed the exceptional visibility of small steps on beryl crystals to etching, since they found a high concentration of pits along the step edges.

To discover the nature of the surface layer of the crystal it was examined by electron diffraction methods;[1] it was found to be amorphous. It is possible that this amorphous impurity layer was formed on the surface of the crystal in the last phase of growth, or it could be due to chemical alteration after growth, either by natural processes underground or by atmospheric attack after it was mined. Indeed, the surface of the crystal, though highly reflecting, shows interference colours, and these interference fringes with monochromatic light can be seen in fig. 1;

[1] The author is indebted to Dr. H. Wilman for this examination.

they are proof of the presence of a thin layer on the crystal surface. But it is at once clear that the growth spirals are not built of the impurity atoms since a regular arrangement of the impurity atoms over the extension of the growth spirals would give them a crystalline arrangement. Moreover, the growth spirals take crystallographic shape, the spiral edges tending to become straight lines that are orientated at simple crystallographic angles (e.g. 90°) with respect to the edges of the triangular growth hills. The structure of the underlying ZnS and the growth spirals thus appears to be alike.

The behaviour of the spiral growth steps originating from different dislocations is similar to that observed on other crystals. A compound growth pattern, from two dislocations of the same hand close to each other, is illustrated at the bottom right of fig. 7 (pl. IV). Another noteworthy observation, which is in striking similarity to an observation on silicon carbide crystals (Verma, 1951), is that in any one region of the crystal the dislocations are usually of the same sign. Thus in fig. 7 there are some twenty growth spirals, all of which appear to be right-handed. Different parts of the crystal were therefore searched and, as seen in fig. 10, the top left corner contains several left-handed growth spirals: this region being separated from the rest of the crystal by a boundary marking a region containing triangular markings of the type shown in fig. 9. Examples of two dislocations of opposite hand close together can also be seen in fig. 10. The predominant occurrence of dislocations of the same sign in any one region of the crystal has been explained by Frank (1951) on an hypothesis about the mechanism of the creation of the dislocations. According to this the initial crystal plate formed by the nucleation process gets self-stressed, through inhomogeneous distribution of impurities. When this stress reaches the yield stress, the plate will buckle and shear, raising terminated steps that will not be of constant height all along, and macroscopically speaking will taper away. Every time the step height is reduced by one unit cell a dislocation will be left behind, and these will obviously be all of the same hand. During growth these dislocations will repel each other and spread over the surface of the crystal. The above observation on zinc-blende crystals thus lends support to Frank's hypothesis about the creation of dislocations. Few other crystals have shown a large density of individual dislocations on the same crystal plate.

Imperfect dislocations and growth trigons.

The triangular growth terraces of fig. 3 represent a triangular growth hill, as is easily seen from the positive phase-contrast image showing a

white border on the edge of the step towards the higher level side. In addition to this, a closer examination of the step edge shows some 'trigons' in different stages of formation. These trigons are pits, oppositely orientated to the triangular growth hills. A small completed trigon can be seen nearly in the right middle of the bottom growth layer (it is indicated by arrows). Several incomplete trigons, which were still in the process of formation when growth ceased, can be seen at the top right-hand end of the figure. The formation of several oppositely orientated trigons can be seen in fig. 4 also. These trigons closely resemble similar features on diamond. Indeed, this is to be expected since the structure of blende and diamond are very similar: the Zn and S atoms are each arranged on a face-centred cubic lattice, and by replacing both Zn and S by C we get a structure like that of diamond. As was shown by Tolansky and Wilcock (1946, 1947), these oppositely orientated triangular pits on the octahedral faces of diamond are not the result of an etching but are 'growth trigons' arising from the meeting of the three systems of growth layers advancing at 60° to each other. Halperin (1954) has put forward a theory about the formation of trigons and has explained them on the basis of the presence of imperfect dislocations, which arise by the transfer of atoms from lattice positions to twin lattice positions (Frank, 1949*b*). The strength of these dislocations, i.e. the displacement of the atoms, is only a fraction of the lattice unit, and imperfect steps result. These steps are thought by Halperin (loc. cit.) to be formed as a result of accumulations of interstitial faults in the lattice. It is therefore possible to explain the formation of oppositely orientated trigons in zinc-blende arising from imperfect dislocations, since stacking faults can be easily created in the *ABC* sequence of the hexagonal close-packed layers which form the face-centred cubic blende crystal. It should be noted that the triangular growth hills are not of this origin. If growth takes place on imperfect dislocations zinc-blende may also be thought to exhibit 'polytypism' of the type shown by silicon carbide crystals (Thibault, 1944). This has recently been reported by X-ray diffraction studies (Strock and Brophy, 1955; Buck and Strock, 1955). The step lines originating from two imperfect dislocations cannot fuse with one another crystallographically, and a surface of lattice discontinuity marking out a fault surface should be formed; some of the markings separating growth spirals in figs. 7 and 10 may be of this origin.

The creation of dislocations by buckling and slip mechanism may also create some slip steps on the surface of the crystal. Votava, Amelinckx, and Dekeyser (1953) have carried out microscopic studies of (111) faces

of deformed blende crystals from Trepča (Yugoslavia) to which they assign a pegmatitic-pneumatolytic origin with growth at elevated temperature and pressure. They reported the observation of some slip-step lines in addition to poorly developed growth spirals. In the extensive substructure on some crystal faces one can occasionally see step lines running along certain crystallographic directions and cutting across the growth steps. Two such lines parallel to a crystallographic direction can be seen in fig. 5, running from the pit at the left edge of the figure to the edge of the crystal on the bottom right of the figure. Several other such faint lines can be seen in other photographs, e.g. fig. 6. Votava *et al.* have in addition observed some faint lines, which are rows of etch pits, and which they have interpreted as polygonization lines (rows of Taylor dislocations).

Acknowledgements.—I have great pleasure in expressing my thanks to Prof. S. Tolansky, F.R.S., for his interest and the facilities of the laboratory of the Royal Holloway College, where this work was done. I am indebted to the authorities of the British Museum (Natural History), especially to Dr. G. F. Claringbull, for the loan of the minerals. This work has been done during the tenure of an I.C.I. fellowship of the University of London, while on study leave from the University of Delhi.

References.

Applebe (B. J.) and Kaye (H. F.), 1953. Phil. Mag., ser. 7, vol. 44, p. 105.
Bennett (A. H.), Jupnik (H.), Osterberg (H.), and Richards (O. W.), 1946. Trans. Amer. Microsc. Soc., vol. 55, p. 99; Phase Microscopy, New York, 1951.
Buck (Daniel C.) and Strock (Lester W.), 1955. Amer. Min., vol. 40, p. 192.
Burton (W. K.), Cabrera (N.), and Frank (F. C.), 1951. Phil. Trans. Roy. Soc., ser. A, vol. 243, p. 299 [M.A. **12**–312].
Forty (A. J.) and Frank (F. C.), 1953. Proc. Roy. Soc., ser. A, vol. 217, p. 262.
Frank (F. C.), 1949*a*. Discussions Faraday Soc., no. 5, p. 48.
—— 1949*b*. Proc. Phys. Soc., ser. A, vol. 62, p. 202.
Gebhardt (Tim), 1933. Neues Jahrb. Min., Abt. A, Beil.-Bd. 67, p. 1.
Halperin (A.), 1954. Proc. Phys. Soc., ser. B, vol. 67, p. 538.
Miers (H. A.), 1929. Mineralogy, 2nd edn, New York and London, p. 368.
Seager (A. F.), 1953. Min. Mag., vol. 30, p. 1.
Smithson (F.), 1946. Nature, vol. 158, p. 621.
—— 1948. Min. Mag., vol. 28, p. 384.
Strock (Lester W.) and Brophy (Vincent A.), 1955. Amer. Min., vol. 40, p. 94.
Thibault (N. W.), 1944. Ibid., vol. 29, pp. 249 and 327 [M.A. **9**–96].
Tolansky (S.), 1948. Multiple-beam Interferometry of Surfaces and Films. London.
—— 1952. Nature, vol. 169, p. 445.
—— and Wilcock (W. L.), 1946. Nature, vol. 157, p. 583 [M.A. **10**–135].
—— —— 1947. Proc. Roy. Soc., ser. A, vol. 191, p. 182 [M.A. **10**–325].
Vand (V.), 1951. Phil. Mag., ser. 7, vol. 42, p. 1384.

Verma (A. R.), 1951. Phil. Mag., ser. 7, vol. 42, p. 1005.
—— 1953. Crystal Growth and Dislocations. London [M.A. **12**–234].
Votava (S.), Amelinckx (S.), and Dekeyser (W.), 1953. Physica, vol. 19, p. 1163.
Zernicke (F.), 1934. Ibid., vol. 1, p. 689; Month. Notices Roy. Astron. Soc., vol. 94, p. 377.

Explanation of Plates III and IV.

Plate III.

Fig. 1. The entire tetrahedral face of a zinc blende crystal under low power using bright field illumination and mercury green light λ5461, showing a series of growth edges on which some broad and diffuse interference fringes due to a layer on the surface can be seen. ×10.

Fig. 2. A phase-contrast picture of a part of fig. 1, showing an hexagonal area which is remarkably smooth compared with the mottled crystal surface around it. ×75.

Fig. 3. The triangular growth terraces on the tetrahedral face of blende, using the phase-contrast microscope. Some inverted triangles in different stages of formation can be seen, e.g. one completed 'trigon' in the right middle of the bottom growth layer. ×75.

Fig. 4. A phase-contrast picture of another blende crystal, showing an extensive system of substructure which is quite shallow in depth (or height). ×45.

Fig. 5. A phase-contrast picture of another tetrahedral face of the same crystal as fig. 4, showing triangular pits in addition to the growth edges. ×30.

Fig. 6. A phase-contrast picture of the extensive substructure on a tetrahedral face of a blende crystal. ×60.

Plate IV.

Fig. 7. A phase-contrast picture of a part of fig. 1, showing on the tetrahedral face of the blende crystal a number of growth spirals on the mottled background. Note that the spirals are all of the right-handed type. At the bottom of the figure small triangular markings can also be seen. ×140.

Fig. 8. A phase-contrast picture of a part of fig. 7 under higher power, showing a growth spiral. ×270.

Fig. 9. A phase-contrast picture of a portion of the bottom of fig. 7, showing the triangular markings under higher power. ×440.

Fig. 10. A phase-contrast picture of another part of the tetrahedral face of fig. 1, showing a system of both left- and right-handed growth spirals together with the triangular markings on the mottled background. ×100.

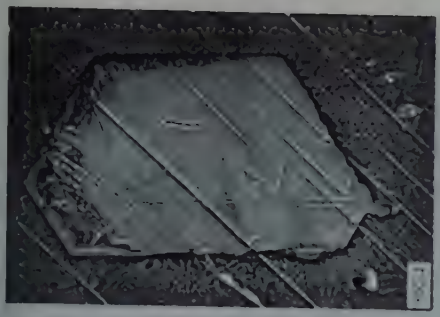

A. R. Verma on Phase-Contrast Microscopy of Blende

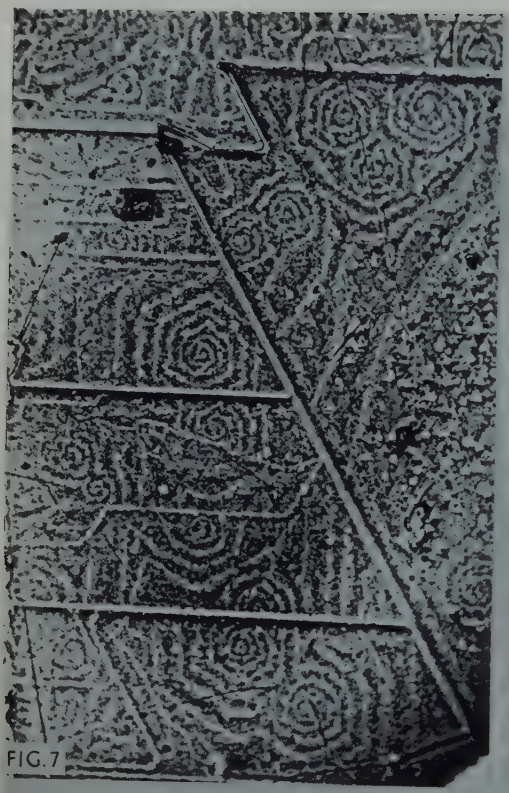
FIG. 7

FIG. 8

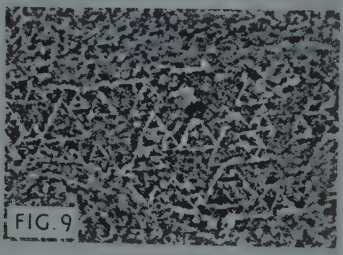
FIG. 9

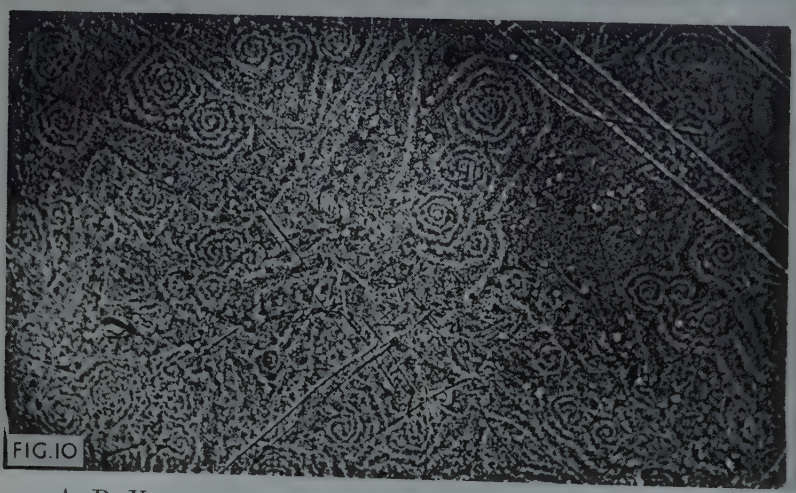
FIG. 10

A. R. VERMA ON PHASE-CONTRAST MICROSCOPY OF BLENDE

Staurolite twinning.

(With Plates V–VI.)

By Vernon J. Hurst,[1] B.S., M.S., Ph.D., and
J. D. H. Donnay, E.M., Ph.D.
The Johns Hopkins University, Baltimore 18, Maryland, U.S.A.

and Gabrielle Donnay, B.A., Ph.D.
Geophysical Laboratory, Carnegie Institution of Washington,
Washington, D.C., U.S.A.

[Taken as read 26 January 1956.]

Summary.—The space group *Ccmm* of the accepted staurolite structure (7·82:16·52:5·63 kX = 0·473:1:0·341, Náray-Szabó, 1929) is a pseudo-space group; the true one has no *c* glide plane. Staurolite is monoclinic pseudo-orthorhombic, as shown optically by horizontal dispersion and morphologically by unequal developments of forms $r(201)$ and $r'(\bar{2}01)$. It has variable cell dimensions, 7·83–7·95:16·50–16·82:5·62–5·71 Å., constant $\beta = 90° \pm 3'$, aspect C^*, and probable space group $C2/m$ (negative pyroelectric test). This leads to the prediction of a new type of twin, 'by high order merohedry', a penetration twin that simulates an orthorhombic single crystal. It is known (Friedel, 1922) that the 90°-cross can be accounted for by two different twin laws and the 60°-cross by five. The twin operations are respectively the pseudo-symmetry operations of a pseudo-tetragonal cell, obtained by transformation 010/003/100, and those of Mallard's pseudo-cube, resulting from transformation $013/0\bar{1}3/300$. By precession methods more than one twin law is established for each type of cross: both laws $[100]_{90°}$ and $[013]_{180°}$ are found for 90°-crosses; $[313]_{180°}$ and $[102]_{120°}$, for 60°-crosses.

THE question of the staurolite twin laws has never been answered satisfactorily because of the poor quality of the morphological measurements. The assumption has been that the 90°-cross and the 60°-cross should each be defined by a single twin law. We set out to check this assumption by means of Buerger's precession X-ray camera (1944), which can be used to yield accurate goniometric data. When the morphological analysis gave a space group different from that in the literature, we had to re-examine the symmetry of staurolite. We noted the variations of cell dimensions with composition, for these could be expected to affect twinning.

[1] Present address: Department of Mines, Mining, and Geology, 425 State Capitol, Atlanta, Georgia, U.S.A.

The material studied consists mainly of about 2100 specimens from Hackney's Farm, near Blue Ridge, Fannin County, Georgia, 1800 of which were provided by the Georgia Department of Mines, Mining, and Geology and 300 by Mr. Gilbert Withers, of Atlanta, Georgia. Also examined were: (1) other specimens from Fannin County; (2) a single crystal from Barrow County, Georgia; (3) material from Ducktown, Tennessee; (4) one specimen from Namib, Africa, U.S. Nat. Museum No. 8642; (5) one specimen from Alpe Sponda, Pizzo Forno, given to us by Dr. Hans Eugster of the Geophysical Laboratory (according to whom this locality is often referred to erroneously as Monte Campione or as St. Gotthard).

In this paper all symbols refer to the structural cell, with axial ratios $a:b:c = 0{\cdot}473:1:0{\cdot}341$, and β equal to 90° within limits of error.

The symmetry of staurolite.

In the past staurolite has been considered orthorhombic and holohedral. The forms reported in Goldschmidt's *Atlas* (vol. 8, 1922) can be listed as follows, in order of decreasing frequency: (1) Most common: $m(110)$, $b(010)$, $c(001)$; (2) Common: $r(201)$; (3) Uncommon: $q(021)$, $s(111)$, $a(100)$, $f(101)$, $l(041)$, $\gamma(401)$, $\beta(103)$, $\alpha(105)$. Biswas (1928) reported q—as a new form—on three specimens from India. Forms γ, β, and α were reported only by Weiss (1901, in Goldschmidt). Our material shows only m, b, c, and r. Fifteen crystals from Hackney's Farm, measured on the Terpstra two-circle goniometer, yield the angles $bm = 64°\ 40'$ (average of 45 measurements, ranging from 64° 21′ to 65° 1′) and $cr = 55°\ 14'$ (average of 28 measurements, ranging from 54° 42′ to 55° 38′). They give the axial ratios $a:b:c = 0{\cdot}473:1:0{\cdot}341$, in agreement with previous values.

These meagre morphological data (fig. 1) can be used to determine the space group that best expresses the Generalized Law of Bravais (Donnay and Harker, 1937; Donnay, 1947). According to the morphological analysis (fig. 2), s must be taken as unit form (111) and the morphological aspect is C*** with possible space groups *Cmmm*, *C*222, *C*2*mm*, *Cm*2*m*, and *Cmm*2 (see Appendix). This result conflicts with the space group *Ccmm* previously determined by X-rays (Cardoso, 1928; Náray-Szabó, 1929). It is compatible with monoclinic as well as orthorhombic symmetry, and as we found no evidence against the presence of a centre of symmetry—staurolite gave us a negative pyroelectric test—the space group indicated by the relative frequencies of forms is either *Cmmm* or *C*2/*m*.

Morphological evidence, however, points towards monoclinic symmetry, since the four r faces are commonly unequal in size, apparently forming two pinacoids. This observation is not on record in the literature, yet in many instances only one pinacoid is to be seen. The angular

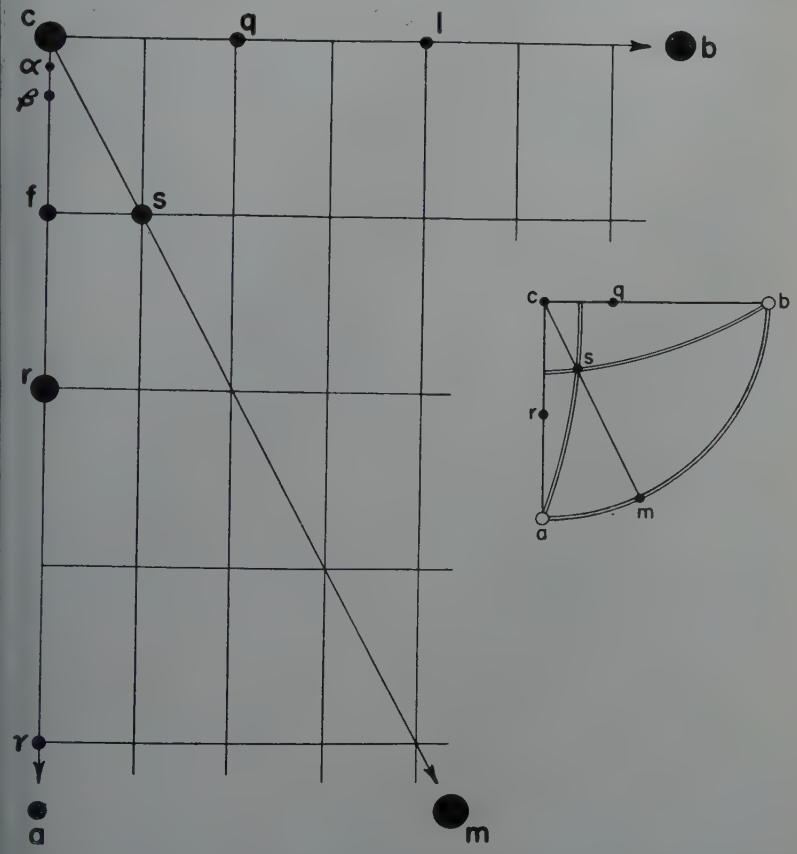

FIG. 1. Gnomonic projection of staurolite, radius of projection 3·3 cm. Only one octant is shown. The relative sizes of the poles roughly indicate the relative frequencies of the corresponding forms. The small stereographic projection summarizes the morphological development of aspect C^{***}.

measurements are too crude to tell the two pinacoids apart. Let the larger pinacoid be $r(201)$ and the smaller $r'(\bar{2}01)$. We found $cr = 55° 8'$ (average of 6 values, 54° 54′ to 55° 14′) and $cr' = 55° 4'$ (average of 4 values, 54° 40′ to 55° 38′).

The evidence provided by X-ray diffraction is completely in favour of orthorhombic symmetry. No deviation from it can be detected on precession photographs taken at room temperature, either as to the positions or the intensities of the spots.

Optical measurements were made on plates cut from the Alpe Sponda

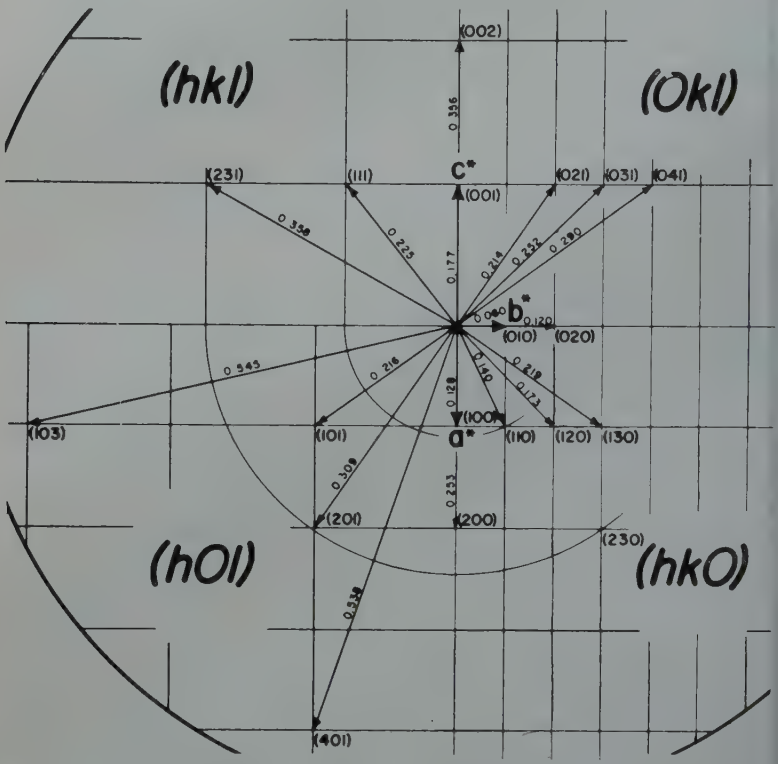

FIG. 2. Graphical determination of the lengths of reciprocal lattice vectors. The primitive translations **a***, **b***, **c*** correspond to the choice of s as (111). All vector lengths are shown in Å.$^{-1}$ for future reference, but this can be thought of as an arbitrary scale. For the purpose of morphological analysis, relative lengths obtained by goniometry can be used: $a^*:b^*:c^* = 1/a:1/b:1/c$.

specimen, as the Georgia specimens contain too many mineral inclusions. A plate cut parallel to c(001) gave α 1·739 and β 1·744; another plate, cut parallel to b(010), gave γ 1·749 (all values $\pm$0·003; in yellow light, $\lambda = 5890$ Å.). Dispersion was observed on two plates, about 0·4 mm. thick, perpendicular to the c-axis. The measurements were made on the

universal stage, with glass hemispheres of index 1·649 (checked to be free from strain), first in red light (λ 6907 Å.) then in blue light (λ 4667 Å.) obtained from a monochromator. For each wavelength each optic axis in turn was centred by means of the interference figure, and the settings of the universal stage were adjusted to bring both optic axes into a vertical N.-S. plane. (This manner of orienting the plane of the optic axes simplifies the corrections required by the difference in refractive index of the glass hemispheres and the crystal plate.) The results, plotted on a stereographic net, show that the known dispersion of the optic axes, $r > v$, is accompanied by a dispersion of the acute bisectrix. The first plate, cut parallel to c(001), gave 2V 88·6° in red light and 2V 83·8° in blue light; the second plate gave concordant values, 88·5° and 84·0° respectively. As to the difference in orientation of the two optical indicatrices, it is small but unmistakable (V. J. Hurst, observer).

In order to check the above results, plates cut parallel to b(010) were used to obtain the extinction angle, and three observers made independent measurements. In white light the extinction angle,[1] determined on the universal stage, is −3·1° (Wm. S. MacKenzie, observer) and −3·2° (J. R. Smith, observer). In monochromatic light the measurements were made on the stage of the microscope; as the plane of the plate was not rigorously parallel to b(010), the extinction angles found were bound to be low: −2·0° for blue light (Wratten filter 50, λ 4500 Å.), −2·2° for green (Wratten 74, λ 5250 Å.), and −2·7° for red (Wratten 70, λ7000 Å.) were obtained at one and the same point on the plate (J. D. H. Donnay, observer). Finally, in order to rule out the possibility that the crystal was triclinic, a plate cut normal to the c-axis was examined, to check that the b(010) face is a plane of optical symmetry. The plate showed traces of the m(110) and $m(1\bar{1}0)$ faces; it was easy to check that the extinction direction bisects the angle between the m faces. In green light (λ 5250 Å.) the readings for the extinction position and for the bisector of the angle mm differed by less than 0·1°; for red light (λ 7000 Å.) and blue light (λ 4500 Å.) the differences were larger, 0·4° and 0·3° respectively, but the extinction position was much more difficult to ascertain (three observers, J. D. H. D., W. S. MacK., J. R. S.).

These results prove that staurolite is monoclinic, strongly pseudo-orthorhombic. They enable us to predict the existence of a new type of twin, 'by high order merohedry'.

[1] The negative sign given to the extinction angle means that the vibration direction lies between the $+c$-axis and the $-a$-axis. The crystal is oriented by making the larger r face (201).

Twinning 'by high-order merohedry'.

With β equal to 90° within the limits of error, staurolite comes close to being an example of the legendary 'high-order merohedry' (Friedel, 1926, p. 56), in which a monoclinic crystal would have an orthorhombic lattice. Twinning by pseudo-merohedry, with a vanishingly small obliquity (equal to zero within limits of error), can be called 'twinning by high-order merohedry'. Like twinning by merohedry it should give rise to penetration twins.

The following twin operations can be predicted: (*a*) reflection in (100), which, because of the monoclinic mirror, is equivalent to a 180° rotation about [001]; this twin law brings crystal I into coincidence, say, with crystal II; (*b*) reflection in (001), equivalent to a 180° rotation about [100]; this twin law brings crystal I into coincidence with crystal II′. If $\beta \neq 90°$, X-ray photographs will show doubling of spots along the c^* row in case (*a*) and along the a^* row in case (*b*). In each of the two cases, the symmetry of the twin is $2/m\ 2/m\ 2/m$. If $\beta = 90°$ the two cases are indistinguishable, and the neighbouring twinned orientations II and II′ merge into one. The twin law can then be expressed by any one of the four above operations, which function simultaneously as twin operations. The twin symmetry is again $2/m\ 2/m\ 2/m$, but neither the c^* row nor the a^* row should show any doubling of spots. The twin by high-order merohedry thus simulates an orthorhombic holohedral single crystal to perfection. Such twinning can conceivably occur on a very fine scale, which would further enhance the pseudo-symmetry shown by our precession photographs of 'single crystals'. Although such effects in X-ray diffraction may have vitiated the intensities,[1] so that the crystal structure of staurolite may have to be re-examined, they have little bearing on the interpretation of the previously known twins. The latter are simply superimposed on the new twin described in this section.

Previously observed twins.

Two types of twin are well known. The more common one consists of two interpenetrating crystals of simple prismatic habit (fig. 3) crossing each other at an angle of about 60° (fig. 4). The absence of r and r' faces on this twin is unusual. In the less common type of twin the two crystals have their c-axes at an angle of 90°; one of the crystals is often larger than

[1] X-ray pictures taken at different temperatures would presumably show doubling of spots revealing the presence of twinning.

the other (fig. 9). We shall call these two types the 60°-cross (St. Andrew's cross) and the 90°-cross (Greek cross), respectively.

Diversity in the appearance of staurolite twins is attributable to five factors: (1) unequal development of forms (figs. 5, 6, and 8); (2) multiple

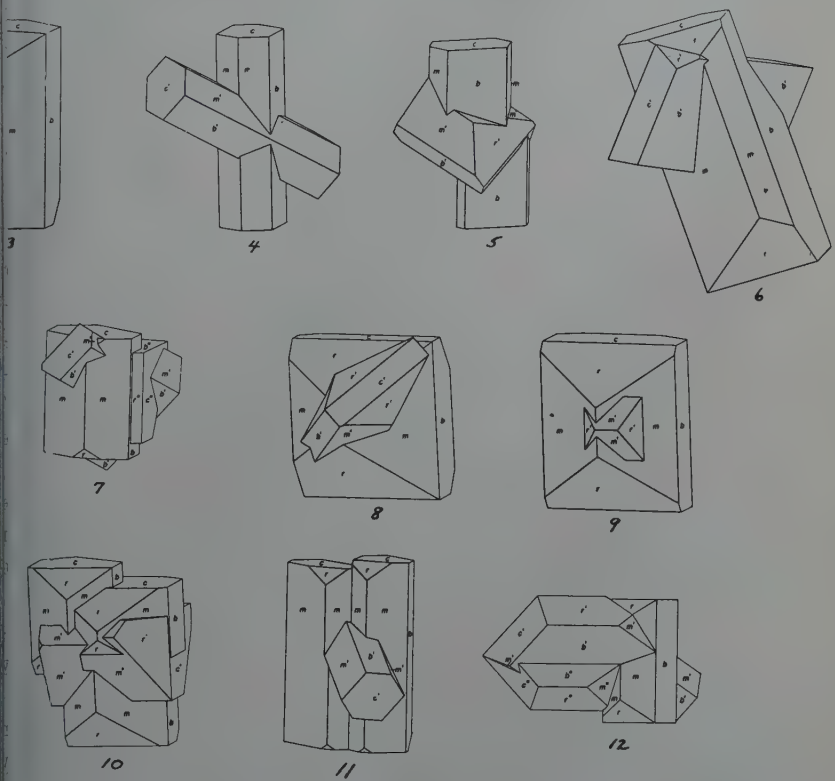

FIGS. 3–12. Portrait-drawings of staurolite specimens from Fannin County, Georgia: 3, Typical habit of staurolite crystal; 4, Typical 60°-cross; 5, 6, Malformed twins (60°-crosses); 7, Combined 60°-cross and 90°-cross; 8, Malformed 60°-cross; 9, Typical 90°-cross; 10, Parallel intergrowth and 90°-cross; 11, Parallel intergrowth and 60°-cross; 12, Trilling (repeated 60°-twin).

twinning (fig. 7); (3) repeated twinning (fig. 12); (4) combination of twinning with parallel intergrowth (figs. 10 and 11); (5) differences in the relative sizes of the twinned crystals.

The frequency of twinning and the ratio of the number of 60°-crosses to that of 90°-crosses vary greatly from place to place. In the various localities of Fannin County, Georgia, the proportion of twinned crystals

ranges from 10 to 75 %. The 60°-crosses greatly predominate, outnumbering the 90°-crosses nine to one.[1]

Prediction of twin laws.

Friedel (1904; 1926, p. 461) has shown how twin laws can be predicted —the possible twin operations being the operations of pseudo-symmetry of a multiple cell (or super-cell). He used one and the same cell to predict all the possible twin laws for both the 90°-cross and the 60°-cross. The

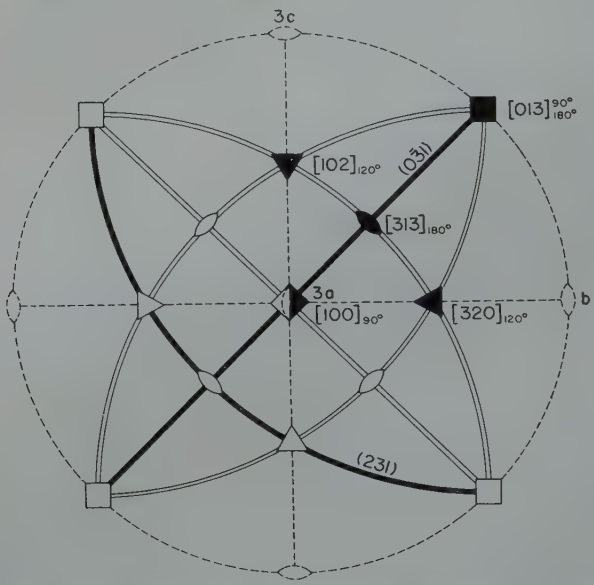

FIG. 13. Direct stereographic (cyclographic) projection of staurolite. Dashed lines: crystal pseudo-symmetry $2/m\ 2/m\ 2/m$. Solid lines: twin-lattice pseudo-symmetry $4/m\ \bar{3}\ 2/m$. Solid symbols: possible twin elements.

multiple cell is Mallard's pseudo-cube (Friedel, 1904, p. 293), which can be obtained from the structural cell by transformation $013/0\bar{1}3/300$. Friedel's treatment stands, with minor modifications to take the monoclinic symmetry into account (fig. 13). The pseudo-axes of fourfold symmetry

[1] Statistical data on staurolite specimens from Hackney's Farm, near Blue Ridge, Fannin County, Georgia; observations by Furcron (1949) in parentheses: Untwinned crystals 32·7 % (63·3 %); 60°-crosses 57·1 % (32·8 %); 90°-crosses 4·7 % (3·7 %); trillings of 60° twins 4·3 % (multiple twins 0·2 %); twin combinations and parallel growths 1·0 %; random intergrowths 0·2 %. Total number of crystals examined 1804 (1226).

are [013], [0$\bar{1}$3], [100]. The corresponding pseudo-mirrors are (031), (0$\bar{3}$1), (100), respectively. The pseudo-axes of threefold symmetry are [102], [$\bar{1}$02], [320], [3$\bar{2}$0]. The pseudo-axes of twofold symmetry are: [313], [3$\bar{1}$3], [$\bar{3}$13], [$\bar{3}\bar{1}$3], [001]. The corresponding pseudo-mirrors are (231), (2$\bar{3}$1), ($\bar{2}$31), ($\bar{2}\bar{3}$1), (001). We see that reflections in (100) and (001), and rotations of 180° about [001] and [100] must now be added to the operations of pseudo-symmetry of the multiple cell. They define the twin by high-order merohedry described above. Among the other operations of pseudo-symmetry, the possible twin laws for the 90°-cross are: (1) rotation of $\pm$90° about [100]; (2) rotation of 180° about [013] or [0$\bar{1}$3]; (3) reflection in (031) or (0$\bar{3}$1). The remaining operations of pseudo-symmetry are possible twin laws for the 60°-cross: (1) rotation of $\pm$120° about [102] or [$\bar{1}$02]; (2) rotation of $\pm$120° about [320] or [3$\bar{2}$0]; (3) rotation of 180° about [313], [3$\bar{1}$3], [$\bar{3}$13], or [$\bar{3}\bar{1}$3]; (4) reflection in (231), (2$\bar{3}$1), ($\bar{2}$31), or ($\bar{2}\bar{3}$1); (5) rotation of $\pm$90° about [013]. In order to visualize the elements of pseudo-symmetry, it may be helpful to use multiple indices; for instance, [306] instead of [102]. The pseudo-cubic cell has multiplicity 18. Three nodes out of every 18 are restored by twinning; the twin index is 6.

It may be remarked that it is not necessary to call on the pseudo-cube in order to account for the 90°-cross. A pseudo-tetragonal multiple cell would suffice, either the triple cell obtained by transformation 010/003/100 or the sextuple cell given by 013/0$\bar{1}$3/100. In either case the twin index is 3.

Graphical determination of possible twin laws: the 60°-cross.

Consider the polar stereographic projection (fig. 14) of a 60°-cross plotted from measurements. The coordinate axes of crystal I are xyz, those of crystal II are $x'y'z'$. Both systems are right-handed. Only four rotations are possible whereby crystal II can be brought to coincidence with crystal I (Friedel, 1920, p. 258; 1926, p. 246): (1) $x'x$, $y'y$, $z'z$; (2) $x'x$, $y'\bar{y}$, $z'\bar{z}$; (3) $x'\bar{x}$, $y'y$, $z'\bar{z}$; (4) $x'\bar{x}$, $y'\bar{y}$, $z'z$. (In this notation $x'x$ means that the x'-axis is brought on the positive x-axis, whereas $x'\bar{x}$ means that the x'-axis is brought on the negative x-axis.)

1. The axis of the first rotation is the common line of intersection of the three planes ('perpendicular bisectors') which bisect the arcs xx', yy', zz'. This line, whose pole is **1**, nearly coincides with the zone axis [102] or with the normal to (101). The angle of rotation is $x'\mathbf{1}x = y'\mathbf{1}y = z'\mathbf{1}z \approx 120°$.

2. The planes bisecting the arcs $x'x$, $y'\bar{y}$, z' intersect in a line whose

pole **2** lies near the pole of (130) and also near the pole of the zone axis [320]. The angle of rotation is $x'\mathbf{2}x = y'\mathbf{2}\bar{y} = z'\mathbf{2}\bar{z} \approx 120°$.

3. The planes bisecting the arcs $x'\bar{x}$, $y'y$, z'^{-} intersect in a line whose pole **3** lies near the pole of $(\bar{2}31)$ and also near the pole of the zone axis $[\bar{3}13]$. The angle of rotation is $x'\mathbf{3}\bar{x} = y'\mathbf{3}y = z'\mathbf{3}\bar{z} \approx 180°$. Note that a

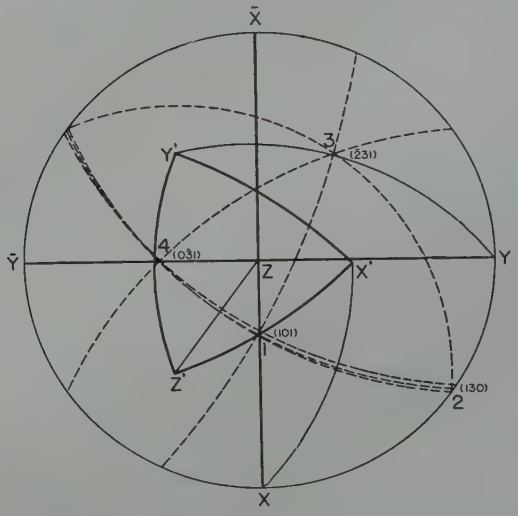

FIG. 14. Polar stereographic projection of staurolite, showing graphical determination of possible twin laws.

180°-rotation about the normal to $(\bar{2}31)$ is equivalent to a reflection in $(\bar{2}31)$ because the crystals are centrosymmetric.

4. The fourth rotation must be performed about the common line of intersection of the three planes that bisect the arcs $x'\bar{x}$, $y'\bar{y}$, $z'z$. This line, whose pole is **4**, nearly coincides with the zone axis $[0\bar{1}3]$ or with the normal to $(0\bar{3}1)$. The angle of rotation is $\bar{x}\mathbf{4}x' = \bar{y}\mathbf{4}y' = z\mathbf{4}z' \approx 90°$.

According to Mallard's law, a row line can always be chosen as a twin axis and a net plane as a twin plane. The possible twin operations whereby one crystal may be brought to coincidence with the other are thus reduced to four rotations about row lines and one reflection in a net plane. They are, in self-explanatory notation: $[102]_{120°}$, $[320]_{120°}$, $[313]_{180°}$, $[013]_{90°}$, and (231).

The 90°-cross.

By using the same procedure as for the 60°-cross, one could show that the 90°-cross can be defined by only three twin operations, namely:

$[100]_{90°}$, $[013]_{180°}$, and (031). Note that $[100]_{+90°}$ and $[100]_{-90°}$ lead to two neighbouring orientations, twinned with respect to each other by $[100]_{180°}$ if $\beta \neq 90°$, but merging into one if $\beta = 90°$. Note also that the two orientations obtained by $[013]_{180°}$ and $[0\bar{1}3]_{180°}$ are symmetrical to each other by reflection in (010) and so are the orientations obtained by reflections in (031) and $(0\bar{3}1)$.

The twin laws $[013]_{180°}$ and $(0\bar{3}1)$ would be strictly equivalent if staurolite were orthorhombic. Indeed, the product of a twin reflection in $(0\bar{3}1)$ by a crystal reflection in the orthorhombic mirror (100) is equivalent to a 180° rotation about [013], the line of intersection of two reflection planes perpendicular to each other. Now that staurolite is known to be monoclinic, the two operations will lead to two neighbouring twinned orientations that, rigorously speaking, are distinct. Practically, however, it will not be possible to tell them apart. Either one, combined with twinning in (100), will become equivalent to the other.

The possible twin operations determined graphically from the stereographic projections of measured staurolite twins are seen to be the same as the twin operations predicted on the basis of pseudo-symmetry.

Twin laws indicated by morphology.

Previous workers have always assumed that there can be only one twin law for each type of cross, and they have endeavoured to ascertain it. For the 60°-cross, for instance, reflection in (231) had long—and uncritically—been accepted as the twin law. Friedel (1922) tried to refine the goniometric data in an effort to distinguish between the five possible definitions. He measured the angle $b_{\mathrm{I}}b_{\mathrm{II}}$ between b(010) of crystal I and b(010) of crystal II. The average of 46 measurements gave him the value of 120° 2′, with maximum deviations of +52′ (in one case +71′) and −50′. By comparison with the predicted values for $b_{\mathrm{I}}b_{\mathrm{II}}$ (recalculated by us),[1] he concluded that rotation of 120° about [102] afforded the best definition of the twin. The spread of his measurements (102′) exceeded the largest difference (72′) between the predicted values. We can only confirm Friedel if we adopt his line of approach. Eight of the best 60°-crosses, selected from the 1804 specimens from

[1] Predicted angle $b_{\mathrm{I}}b_{\mathrm{II}}$ for each of the twin laws, based on $a:b:c = 0{\cdot}473_4:1:0{\cdot}341_0$

60°-cross	twin law	$[102]_{120°}$	$[320]_{120°}$	$[313]_{180°}$	(231)	$[013]_{90°}$
	predicted $b_{\mathrm{I}}b_{\mathrm{II}}$	120° 0′	119° 49′	120° 30′	119° 30′	119° 18′
90°-cross	twin law	$[100]_{90°}$	$[013]_{180°}$ or (031)			
	predicted $b_{\mathrm{I}}b_{\mathrm{II}}$	90° 0′	91° 14′			

Fannin County, gave us $b_I b_{II} = 119° 59'$, with maximum deviations of $+55'$ and $-50'$. Five measurements of $b_I b_{II}$ in 90°-crosses gave us an average value of 89° 55′ (range 89° 40′ to 90° 6′), which, compared with predicted values, tends to confirm Friedel's suspicion that $[100]_{90°}$ would be the best twin law.

Averaging the values of $b_I b_{II}$, however, can have significance only if, as Friedel supposed, the large range of measurements is wholly due to macroscopic crystal deformation. Our X-ray results will show that this is not the case. The occurrence of several twin laws can also account for the spread of the measurements of $b_I b_{II}$.

Space group and cell dimensions.

Because the space group indicated by the morphology differed from *Ccmm*, previously reported in the literature,[1] the study of systematic extinctions was repeated with Buerger's precession method (1944). All the observed reflections obey the criterion '$(h+k)$ even'. No other presence criterion is found for any set of reflections. The $(0kl)$ reflections with l odd are very weak, but definitely visible on several photographs; for instance: 021, 041, 061, 081, 0.10.1, 0.12.1, 023, 043, 065, 0.12.5. The diffraction aspect is thus *C****, while *Cc*** is a pronounced pseudo-aspect. The crystal structure proposed by Náray-Szabó (1929) will have to be revised: the *c* glide plane parallel to (100) must be eliminated and the space group must become $C2/m$, to agree with the results of the optical study; the intensities must be checked to guard against possible misleading effects due to twinning, on which Buerger (1954) has recently commented. The fact that the β angle, if different from 90°, is close to it, supports the known structural result that (100) of kyanite is parallel to (010) of staurolite in the epitaxic overgrowth of one mineral on the other; indeed, the α angle of kyanite, which would correspond to the β angle of staurolite, is reported as 90° 5′ in the literature.

We determined the cell dimensions of seven different specimens, in the hope of finding some relationship (through the obliquity) between twin law and axial ratios. (As we shall see presently, this hope did not materialize.) The results are listed in table I, together with data of previous workers. They show appreciable ranges of variation (for all

[1] Space group *Pmab* given by Gottfried (1927) was due to erroneous indexing (Strukturbericht, 1931, vol. 1, p. 453).

Lusakite was described (Skerl, Bannister, and Groves, 1934) as a cobalt-bearing staurolite, with space group *Ccmm*. These authors point out that the staurolite structure is not as simple as that proposed by Náray-Szabó (1929).

TABLE I. Variations of cell dimensions and axial ratios in staurolite specimens. Cell dimensions of first seven specimens given to ±0·3 %. Angle β equal to 90° within limits of error, ±3′.

Locality.	a (Å.).	b (Å.).	c (Å.).	$a:b:c$.	Remarks.
Hackney's Farm, Fannin Co., Georgía	$7{\cdot}86$	$16{\cdot}56$	$5{\cdot}67$	$0{\cdot}471_3:1:0{\cdot}338_5$	Typical specimen from Hackney's Farm.
	$7{\cdot}94_9$	$16{\cdot}64_4$	$5{\cdot}68_2$	$0{\cdot}477_6:1:0{\cdot}341_4$	60°-cross, twin law $[\bar{3}\bar{1}3]_{180°}$, plate No. 1.
	$7{\cdot}86_8$	$16{\cdot}61_0$	$5{\cdot}67_9$	$0{\cdot}473_7:1:0{\cdot}341_9$	,, ,, ,, plate No. 2.
	?	$16{\cdot}81_5$	$5{\cdot}71_0$	? :1:$0{\cdot}339_6$	90°-cross, twin law $[100]_{90°}$.
	?	$16{\cdot}50$	$5{\cdot}61_7$	? :1:$0{\cdot}340_4$	,, twin law $[013]_{180°}$.
Ducktown, Tennessee	$7{\cdot}88$	$16{\cdot}64$	$5{\cdot}67$	$0{\cdot}473_6:1:0{\cdot}340_7$	From powder pattern taken on Philips diffractometer.
Namib, Africa	$7{\cdot}87$	$16{\cdot}72$	$5{\cdot}68$	$0{\cdot}470_7:1:0{\cdot}339_7$	U.S. National Museum No. 8642.
?	$7{\cdot}86$	$16{\cdot}55$	$5{\cdot}62$	$0{\cdot}474_6:1:0{\cdot}339_6$	Gottfried,* 1927. (Å. from kX.)
Monte Campione	$7{\cdot}83$	$16{\cdot}62$	$5{\cdot}65$	$0{\cdot}470_8:1:0{\cdot}340_0$	Cardoso,* 1927. (Å. from kX.)
St. Gotthard	$7{\cdot}84$	$16{\cdot}55$	$5{\cdot}64$	$0{\cdot}473_4:1:0{\cdot}340_8$	Náray-Szabó, 1929. (Å. from kX.)
N. Rhodesia	$7{\cdot}88$	$16{\cdot}65$	$5{\cdot}66$	$0{\cdot}473:1:0{\cdot}340$	Lusakite. Skerl *et al.*, 1934. (Å. from kX.)
Hackney's Farm	—	—	—	$0{\cdot}473_4:1:0{\cdot}341_0$	Average ratios based on 15 crystals.
?	—	—	—	$0{\cdot}472_3:1:0{\cdot}340_2$	Des Cloizeaux's values ($c/2$).
?	—	—	—	$0{\cdot}473_4:1:0{\cdot}341_0$	Hörner's values ($c/2$).

* Note misprint in Strukturbericht, vol. 1, p. 453: instead of $c = 6{\cdot}61$, read $c = 5{\cdot}61$(kX). Also on p. 487: 0·4726 and 0·4708 are interchanged.

localities): 1·5 % for a and c; 1·9 % for b. The single locality of Hackney's Farm shows a larger range of values than all other localities put together: for a, 1·1 % as compared with 0·6 %; for b, 1·9 % against 1·0 %; and for c, 1·5 % against 1·0 %. Each of the axial ratios has a range of variation of about 1 %. Such variations are to be expected in view of the variable chemical composition of staurolite.

Actual twin laws found by X-rays.

As was pointed out by Buerger (1944), the precession instrument is particularly well suited to the study of twinning. A plane-parallel plate, about 0·5 mm. thick, is cut from the twin, by the standard techniques for grinding oriented sections of crystals. The plane of grinding is chosen, by visual inspection, normal to the suspected twin element, either (*a*) twin plane, or (*b*) twin axis.

(*a*) In the case of a suspected twin plane (*hkl*), the plate is mounted and adjusted on the precession instrument in such a way that (*hkl*) contains (is parallel with) the X-ray beam. Both individuals of the twin may be diffracting simultaneously, or each one can be made to diffract in turn by translating the plate and taking a double exposure. If (*hkl*) is a twin plane, whether or not the beam is normal to a reciprocal-lattice *net*, the reciprocal-lattice rows $[hkl]^*_{\mathrm{I}}$ and $[hkl]^*_{\mathrm{II}}$ of crystals I and II coincide along the dial axis of the instrument and will appear as a single row of diffraction spots on the photograph.

(*b*) In the case of a suspected twin axis [*uvw*], the plate is mounted and adjusted with [*uvw*] along (parallel with) the X-ray beam. If [*uvw*] is a twin axis the reciprocal-lattice nets $(uvw)^*_{\mathrm{I}}$ and $(uvw)^*_{\mathrm{II}}$ of crystals I and II lie in a common plane parallel to the film. The photograph will show the two nets rotated with respect to each other, about the trace of the twin axis, through the angle of the twin rotation (90°, 120°, 180°, as the case may be).

Another method of identifying a twin axis, developed during the present study, has been described elsewhere (Donnay, Donnay, and Hurst, 1955). Even if the twin axis [*uvw*] is only roughly adjusted along the direct beam, the nets $(uvw)^*_{\mathrm{I}}$ and $(uvw)^*_{\mathrm{II}}$ will lie in the same plane and will produce, on an orientation photograph, a *single* 'limiting circle'—the 'circle' due to the sharp cut-offs of white-radiation streaks, which is used in the adjustment procedure. If $(uvw)^*_{\mathrm{I}}$ and $(uvw)^*_{\mathrm{II}}$ produce two limiting circles, one of them, say $(uvw)^*_{\mathrm{I}}$, can be centred by proper adjustment, which brings $[uvw]^*_{\mathrm{I}}$ along the X-ray beam. The

eccentricity of the other circle gives the angle $[uvw]_I^* : [uvw]_{II}^*$, whence the proposed name of 'precession goniometry'.

Three 90°-crosses from Hackney's Farm were studied. Plates were ground normal to [100]. In two cases the twin law was established as $[100]_{90°}$. On a zero level photograph of such a twin (shown in pls. V and VI A), the b_I^*- and c_{II}^*-axes coincide. In the third case, the appearance of two limiting circles indicated that the twin law could not be $[100]_{90°}$; it could only be $[013]_{180°}$. This was confirmed by adjusting the plate with [013] along the beam and taking another picture, on which only one limiting circle was visible (pls. V and VI B).

The 60°-crosses are more complicated, as five possible twin laws must be distinguished. Plates were cut normal to [102], the suspected twin axis. In one case the twin law $[102]_{120°}$ was, indeed, established (pls. V and VI C). In two other cases two limiting circles appeared, from which the angle between the two corresponding direct rows could be determined by precession goniometry. If the cell dimensions have been determined for the particular specimen under investigation, such an angle can be calculated for every possible twin law. A comparison between measured and calculated angles will then disclose the actual twin law, provided the calculated angles are known with sufficient accuracy to make the comparison a significant one. Our cell dimensions are known to $\pm 0{\cdot}3$ %; as a result our calculated angles may vary by as much as $\pm 33'$, but the ranges of the various angles need not necessarily overlap and the method may still be applicable (for table of calculated angles of staurolite twins, see Donnay, Donnay, and Hurst, 1955). If the cell dimensions have not been determined for the specimen in question, the method cannot be trusted because of the variability of the axial ratios. For instance, the calculated angle $[10\bar{2}]_I : [\bar{1}02]_{II}$ is found to be 1° 55′ (range 1° 22′ to 2° 29′) or 0° 59′ (range 0° 26′ to 1° 32′), according as the cell dimensions (table I) of plate No. 1 or of plate No. 2 are used. We have checked each of the possible twin laws by taking an orientation picture with the X-ray beam along the twin axis or contained in the twin plane. The two twins mentioned above turned out to obey the twin law $[313]_{180°}$ (pls. V and VI D).

The reorientations necessary for testing the different twin laws on the same plate are done on a two-circle goniometer. All available reflections are used, including those of the cleavage planes *b* and *m*, which can still be observed on the plate after grinding. The desired positions of the faces in the new orientation are first plotted on a stereographic projection of the twin. The plate, mounted in wax, can then be pushed into

the position where each face reflects at the correct ϕ and ρ settings read off the projection.

A plate ground normal to a certain direct-lattice row, suspected to be a twin axis, will not be normal to the beam any more after it has been reoriented to test another twin possibility. Even in the worst case of a horizontal plate, nearly parallel to the X-ray beam, a usable picture was obtained. If, however, the specimen is large, it is better to saw it into halves and to grind two plates: one plate normal to [102] for a first photograph, from which a prediction can be made as to the probable twin element, and a second plate normal to this expected twin element.

The obliquity of the twin (Friedel, 1926, p. 249) is a function of the axial ratios. For example, the obliquity of the twin $[102]_{120°}$ varies from 0° 41′ to 1° 8′ when a/b ranges from $0{\cdot}474_6$ to $0{\cdot}470_8$ and c/b from $0{\cdot}341_4$ to $0{\cdot}338_5$. For the same ranges of the axial ratios, we calculated the following obliquities: for $[320]_{120°}$, 0° 10′ to 0° 24′; and for $[013]_{90°}$, $[013]_{180°}$, or (031), 0° 54′ to 1° 22′. For plate No. 1 and plate No. 2 (table I), the obliquities are 0° 58′ and 1° 7′, respectively (ranges not calculated), for both twin laws $[313]_{180°}$ and (231). For $[100]_{90°}$ the obliquity, defined as the angle between [100] and the normal to (100), is equal to zero if $\beta = 90°$.

We can observe that the obliquities are all small (about 1° or less), on which ground all seven twin laws could be expected to occur; but we have not been able to prove that the obliquity determines the twin law. Note that all the twin laws actually observed are twin axes, which explains why the twins are penetrations. It is known (Friedel, 1904) that if the twin law were reflection in (231), the composition surface would be expected to be planar and parallel to (231); such is not the case.

The unproved twin law of Dana.

A staurolite twin with (230) or $(\bar{1}30)$ as twin plane has been reported by E. S. Dana (1876). It is represented by a single specimen collected in Fannin County, Georgia. The measured angle between the twinned b faces was reported as 70° 30′. Twinning in (230) would require this angle to be 70° 45½′; twinning in $(\bar{1}30)$ would make it 70° 18′ (Dana, 1892, p. 560). Friedel (1926, p. 462) has pointed out that the proposed twin planes, (230) and $(\bar{1}30)$, are respectively octahedral and leucitohedral faces of the pseudo-cube and that the twin might be described by a 180° rotation about [320] or $[3\bar{2}0]$, which are two of the threefold axes of the pseudo-cube. However, the existence of a new twin can be established only by the accuracy of the measurements or by the frequency of

occurrence. We have not encountered any example of this twin, although we examined several thousand specimens from Fannin County. It is therefore yet to be demonstrated that what Dana reported as a twin is not a random intergrowth.

Conclusions.

The old assumption that each type of staurolite cross obeys one twin law only is unjustified. We have observed four of the predicted seven laws. Should these be the only ones to be expected? There is no obvious reason why they should. The other twin axes may well occur, especially $[320]_{120°}$, which has the smallest obliquity. The small number of twins on which we have determined the twin law permits no generalization.

Having established that for the 90°-cross the two possible twin laws exist and that for the 60°-cross more than one twin law is obeyed, we do not feel that it would be of any particular interest to search for the remaining ones.

Acknowledgements.—We are greatly indebted to Dr. W. S. MacKenzie and Dr. J. R. Smith for discussing and checking our optical results. Thanks are also due to Dr. Elizabeth A. Wood, Dr. H. Eugster, and Mr. D. Appleman for constructive criticism of the manuscript.

Appendix.

Morphological determination of the space group.

Consider the gnomonic projection (fig. 1). The following facts are observed: (1) only one (*hkl*) form, *s*, is known; (2) only one (*hk*0) form, *m*, is known; (3) the zone of the (0*kl*)s is a *simple zone* (Donnay, 1938), with *q* more frequent than *l*; (4) the zone of the (*h*0*l*)s is a *simple zone*, with *r* dominant; (5) the three pinacoids are observed, with *b* about as frequent as *m*, *c* more frequent than *r*, *a* uncommon.

The choice of the unit face rests on the following considerations. Face *s* must be indexed (111), unless the lattice is body-centred, in which case the sum of the indices should be even and *s* must be (112). Neither *s*(121) nor *s*(211) would be compatible with the presence of *q*, *r*, and *m* as dominant forms in the axial zones, for the latter must be indexed (011), (101), and (110), respectively, in order to obey the lattice criterion 'sum even'.

First let *s* be (111). If the lattice were *F*, the dominant faces in the axial zones would be at unit distances from the *c* pinacoid; this is ruled out by *q* and *r*. The *A* and *B* lattices are likewise ruled out by *q* and *r*.

The *C* lattice is possible with the dominant faces *q*(021) and *r*(201) correctly shifted 'away from the centred pinacoid' (Donnay, 1939). In this case *c* must be (001), not (002), as its reciprocal-lattice vector 0·177 must be smaller than that of *q*, which is equal to 0·214 (fig. 2). Because *m* is more frequent than *a*(200) and as frequent as *b*(020), it must be indexed *m*(110), not (220). The reciprocal-lattice vectors are 0·140 for *m*(110), 0·120 for *b*(020), and 0·253 for *a*(200). These two conclusions uniquely determine the morphological aspect as *C****, compatible with five possibilities: *Cmmm*, *C*222, *C*2*mm*, *Cm*2*m*, and C*mm*2. (If the symmetry were

monoclinic, the aspect would be C^*, with the possible space groups $C2/m$, $C2$, and Cm.)

The P lattice is also possible, with aspect $Pban$ or Pba^*. If the zone of the $(hk0)$s were a *simple zone*, one would expect (120) to have been observed, for its reciprocal-lattice vector $L^*(120) = 0{\cdot}173$ is smaller than that of $c(001)$. If the zone is made a *double zone* (Donnay, 1938), the next face would be (130), with $L^*(130) = 0{\cdot}219$; it has not been reported, which is anomalous, in view of the occurrence of r with $L^*(201) = 0\ 309$. The double zone, however, is less anomalous than the simple zone. This interpretation uniquely defines $Pban$, a space group that would require the point-group symmetry to be orthorhombic holohedral.

Now let s be (112), with an I lattice. The reciprocal vector c^* must be halved, as compared with its value on fig. 2. All forms must have their third index doubled. The I lattice requires that in each axial zone the unit face shall be dominant, with indices coprime, and that the zone shall be of the double-zone type. Since the $(0kl)$s and $(h0l)$s both form simple zones, glide planes must be inferred. The zone of the $(hk0)$s is not affected by any glide plane; if it were, m would be (220) and its importance ($m > a$) would not be properly expressed. The only possible aspect, with an I lattice, is Iba^*.

In order to decide between C^{***}, $Pban$, and Iba^*, we must be guided by the general forms (hkl), for all other forms obey the same conditions in all three aspects. The latter can best be compared if the cell of Iba^* (with c doubled) is also used for C^{***} and $Pban$. The conditions then become: for $Pban$, l even; for C^{***}, $(h+k)$ even and l even; for Iba^*, $(h+k+l)$ even, which can be fulfilled in two ways: either $(h+k)$ even with l even, or $(h+k)$ odd with l odd. It is clear that more forms could be expected with $Pban$ or with Iba^* than with C^{***}. The observed fact is that only one (hkl) form is known. It follows that C^{***}, which imposes the most restrictive conditions, is the best choice on morphological evidence.

References.

Biswas (S. L.), 1928. Quart. Journ. Geol., Min. Met. Soc. India, vol. 1, p. 151 [M.A. **5**–37].

Buerger (M. J.), 1944. The photography of the reciprocal lattice. ASXRED Monograph No. 1 [M.A. **10**–10].

—— 1954. Anais Acad. Brasil. Ciências, vol. 26, p. 111.

Cardoso (G. M.), 1928. Zeits. Krist., vol. 66, p. 485 [M.A. **3**–529].

Dana (E. S.), 1876. Amer. Journ. Sci., ser. 3, vol. 11, p. 384.

—— 1892. System of Mineralogy, 6th edn, New York.

Donnay (Gabrielle) and Donnay (J. D. H.), 1954. Acta Cryst., vol. 7, p. 619.

—— —— and Hurst (V. J.), 1955. Ibid., vol. 8, p. 507.

Donnay (J. D. H.), 1938. Ann. (Bull.) Soc. géol. Belg., vol. 61, p. B260 [M.A. **7**–242].

—— 1939. Amer. Min., vol. 24, p. 184.

—— 1947. Bull. Soc. franç. Min., vol. 69, p. 151 (1946) [M.A. **10**–466].

—— and Harker (D.), 1937. Amer. Min., vol. 22, p. 446 [M.A. **7**–241].[1]

Evans (R. C.), 1946. An introduction to crystal chemistry, Cambridge.

Friedel (G.), 1904. Étude sur les groupements cristallins. Bull. Soc. Ind. Min. (4), vols. 3–4. Reprinted in book form, Saint-Étienne, 1904.

[1] Note misprint in M.A. **7**–241, last line: *instead of* hexagonal mode, *read* hexahedral mode.

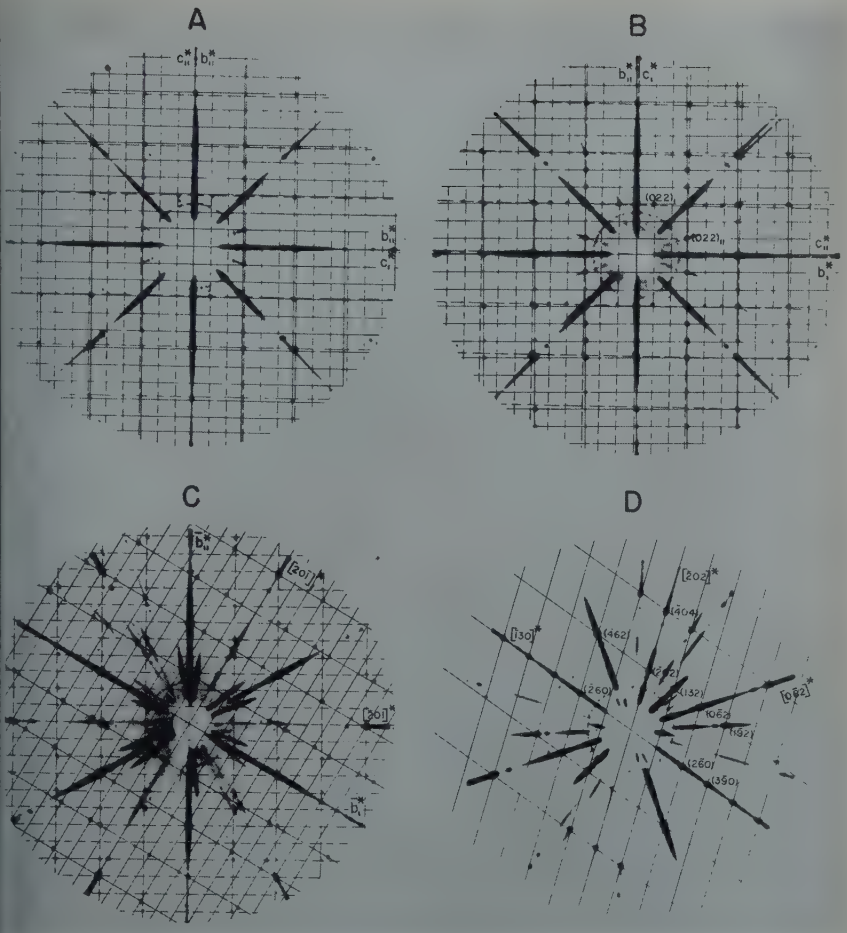

HURST, DONNAY, AND DONNAY: STAUROLITE TWINNING

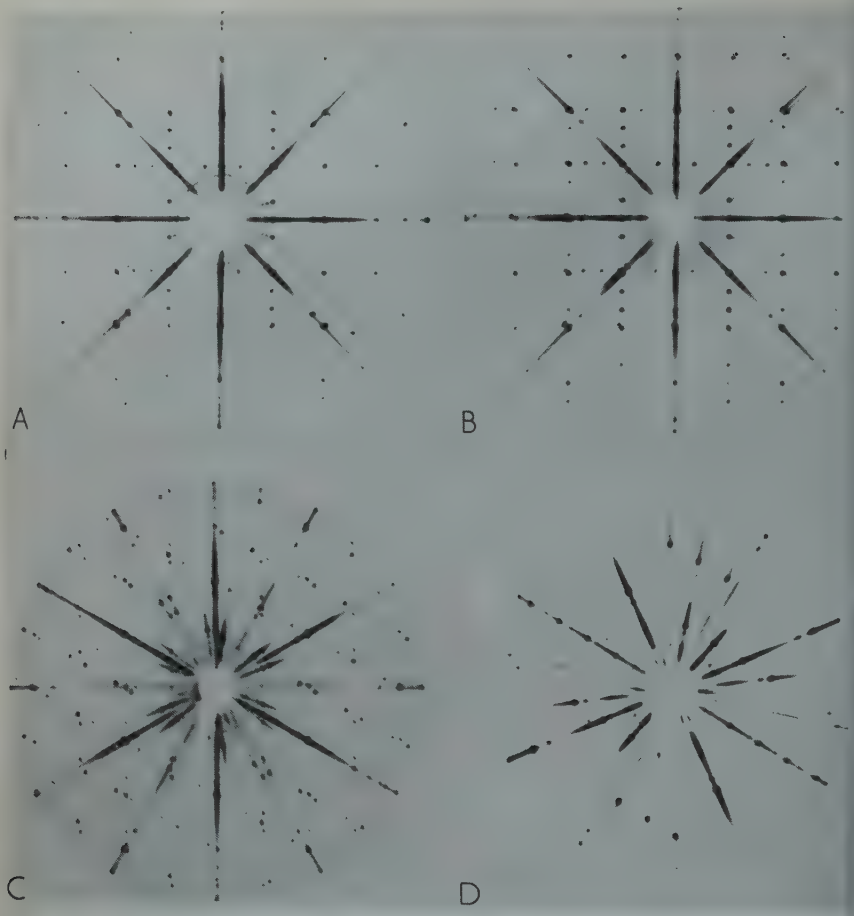

Hurst, Donnay, and Donnay: Staurolite Twinning

Friedel (G.), 1920. Bull. Soc. franç. Min., vol. 43, p. 246 [M.A. 2–368].
—— 1922. Ibid., vol. 45, p. 8 [M.A. 2–144].
—— 1926. Leçons de cristallographie, Paris. (See pp. 245–252 and 421–493.)
Furcron (A. S.), 1949. The Earth Science Digest, vol. 3, No. 7, p. 7.
Goldschmidt (V.), 1922. Atlas der Kristallformen, vol. 8, Heidelberg [M.A. 2–289].
Gottfried (C.), 1927. Zeits. Krist., vol. 66, p. 103 [M.A. 3–434].
Náray-Szabó, 1929. Ibid., vol. 71, p. 103 [M.A. 4–160].
Skerl (A. C.), Bannister (F. A.), and Groves (A. W.), 1934. Min. Mag., vol. 23, pp. 598, 633.
Weiss (K.), 1901. Zeits. Ferdinandeum, Innsbrück, ser. 3, vol. 45, p. 129.

Explanation of Plate V.

Precession photographs of four different staurolite twins, plate ground normal to twin axis, X-ray beam along the twin axis. Mo-$K\alpha$ radiation. Precession angle 30° in A, B, C; 25° in D. Reciprocal-lattice nets shown in solid line for crystal I, in dashed line for crystal II.

A. 90°-cross; twin law $[100]_{90°}$.
B. 90°-cross; twin law $[013]_{180°}$.
C. 60°-cross; twin law $[102]_{120°}$.
D. 60°-cross; twin law $[313]_{180°}$. Reciprocal-lattice nets coincide; only one crystal indexed.

Explanation of Plate VI.

Same photographs as on Plate V before reciprocal-lattice nets were drawn in.

A first attempt at a determination of felspars by activation analysis.

By J. E. S. Bradley, B.Sc., Ph.D.,

and Olive Bradley, B.Sc., Ph.D., F.G.S.

King's College, London, W.C. 2.

[Read 24 March 1955.]

Summary.—Small crystals (2 mg.) of plagioclase and potassium felspar were irradiated for four weeks in an atomic pile. Subsequent analysis of the radiation showed that this is a possible method for the determination of the sodium and potassium content, and it should be possible to develop the method further in this direction. It has not proved a suitable method for the determination of calcium.

THE felspars, like so many silicates, have variable compositions When dealing with such material, it is seldom satisfactory to relate optical measurements, made on single grains or crystals, to chemical analyses which have been made on bulk material. This paper describes an attempt to develop an alternative method of analysis, a so-called activation analysis, which can be carried out on a very small amount of material—2 or 3 milligrams. It has, moreover, the advantage of being a non-destructive method, and the analysis can be repeated on the same material. It should be noted that these results are from the first experiments, and that fully satisfactory methods of mounting, handling, and measuring have yet to be developed. The material selected was not made up of 'ideal' crystals but was a fair cross-section of the sort of material that a geologist might like to have analysed. The results have proved sufficiently encouraging to justify a brief report on progress.

Method.

The crystals used were in section, 100μ thick. Each was mounted individually on aluminium foil with the minimum possible quantity of a dilute solution of Canada balsam; the foil was then folded over, envelope fashion, to prevent damage to the crystal during transit. Reference material packed in the same can comprised small, flat cleavage rhombs of calcite (mounted in the same way as the felspar crystals),

sodium and potassium carbonate (sealed in a silica tube), and blank samples of foil plus Canada balsam. The whole was irradiated for one month in the Harwell atomic pile, at the highest flux available.

When the can was returned, the calcite and felspar crystals were removed from the aluminium foil and remounted. A solution of the carbonate mixture was evaporated on a mounting disk to give a film of comparable thickness: the concentration of the solution was determined by means of a flame photometer.

The sodium and potassium radiations were measured over the first 40 hours. Aluminium filters were used to discriminate between the different types of radiation; the principles on which the measurements were based are as follows:

Sodium has an exceptionally high activation cross-section, rivalled by few common elements other than the rare-earth metals. It yields a radioactive isotope, Na^{24}, which has very hard and abundant γ-rays (2·76 MeV[1] and 1·38 MeV) together with a moderately hard β-ray (1·39 MeV).

Potassium has a moderately high activation cross-section, and gives an isotope having an exceptionally hard β-radiation (3·58 MeV max.), with a few γ-rays. This β-radiation is equalled only by Mn^{56} and Ga^{72}. Consequently, filters capable of discriminating between the very hard (3·58) and medium energy (1·39) β-rays and between β-rays and γ-rays, can give very good discrimination between sodium and potassium. If measurements are made at widely separated intervals an additional check is available from a consideration of the half-life period. The only element capable of seriously interfering here is gallium.

The *calcium* radiation is much weaker (β 0·25 MeV) and longer-lived: the half-life is 150 days. In addition, the activation cross-section is very low. Two tests are available. Firstly, as no γ-rays are emitted, a filter just thick enough to cut off the Ca^{45} β-ray should pass no radiation at all; any radiation getting through must be due to other elements. Some estimate of the hardness of this radiation can be made by inserting the original filters (used in the Na/K determinations), and the residual radiation, not transmitted by the other filter (that opaque to Ca^{45} β-rays), can be calculated. Secondly, the residual radiation, as measured above, can be determined from time to time, and its rate of decay plotted. This should correspond with the 150-day half-life of Ca^{45}.

The results shown are from two separate irradiations, the same methods being employed in both. It was found that the radiation

[1] Mega-electron-volts.

transmitted by a filter opaque to Ca^{45} β-rays often decayed rapidly. In the crystals investigated the decay was complex, and no assignment of element or elements was made. Unfortunately, when dealing with a long half-life element, it is difficult to maintain sufficiently stable counting conditions over an adequately long period to obtain a good half-life determination. It is generally preferable to follow the decay for at least two half-lives, which is clearly impracticable for calcium. The calcium results were divided into two classes. In the first the penetrating component was of relatively small proportions, and the curve after correction for it corresponded reasonably well with the half-life of Ca^{45}. In the second group the penetrating component was the major long-lived activity, and the residual activity, after correcting for it, still showed a rapid decay. Clearly no value for the calcium content could be deduced under these circumstances.

Sodium and potassium determinations.

Plagioclase felspars. In table I results obtained from the activation analyses and from the refractive index measurements are compared. Refractive index readings were made, after irradiation, on the crystal or part of a crystal which showed the greatest birefringence. These readings appear in the table as α' and γ', except in those cases where the optic figure showed that β had in fact been measured. If the crystal is ideally orientated (giving α and γ) the composition values obtained from the two indices will be equal: in less favourable cases a composition range of up to 6 % An is recorded.

Each value is the mean of three determinations (Na light: the probable error is 0·001 or less). The refractive index—composition graph of K. Chudoba[1] has been used to determine composition, but where the values given by the revised graph of F. Chayes[2] are different, these are included too.

Three plagioclases were examined:

The bytownite in a leuco-norite from the Bushveld Complex is clear, without visible inclusions, and with sharp, broad twin boundaries. Single crystals are not large enough for separate irradiation, but since the rock is largely made up of plagioclase, it was possible to select a small unit of 4 or 5 crystals free of other minerals. Earlier[3] universal-stage measurements made on the plagioclase from this rock had shown

[1] The determination of the feldspars in thin section. London, 1933 [M.A. 5–386].
[2] Amer. Journ. Sci., 1952, Bowen vol., p. 85 [M.A. 12–134].
[3] O. Bradley, Min. Mag., 1953, vol. 30, p. 223 [M.A. 12–291].

it to be a homogeneous low-temperature bytownite, with Ab 20–30 %. The present investigation confirmed that this was a homogeneous felspar, and the consistently low potassium value is worth noting. The albite content (12–18 %) given by the activation analysis is always lower than that given by refractive index determinations (17–32 %).

TABLE I. Activation analysis of sodium and potassium in plagioclase felspars.

Material.	Spec. no.	Wt. in mg.	Activation analysis. % K.	% Na.	% Or.	% Ab.	Refr. ind.	% Ab. A.	% Ab. B.
Bytownite in leuconorite. Bushveld complex.	1	1·25	0·075	1·55	0·5	18	α' 1·565	22·5	27·5
							γ' 1·575	22·5	27·5
	2	1·3	0·10	1·41	0·7	16	α' 1·570	12·5	17
							γ' 1·576	19	25
	3	1·2	0·01	1·30	0·1	15	α' 1·568	17	21
							γ' 1·576	19	25
	4	0·9	0·13	1·35	0·9	15	α' 1·566	22	26
							γ' 1·572	28	32
	39	2·2	0·18	1·10	1·3	12	not suitable		
Oligoclase from pegmatite. Locality unknown.	45	1·9	2·4	5·45	17	62	α' 1·537	82	
							γ' 1·543	86	
	46	2·0	0·9	4·73	6	54	α' 1·537	81	
							γ' 1·542	88	93
	47	1·5	1·67	5·08	12	58	not suitable		
	48	1·5	0·5	5·38	3·5	61	α' 1·537	82	
							γ' 1·543	86	87
Andesine in olivine-gabbro. Stonehead, Aberdeen.	63	1·85	1·67	4·25	11	49	β' 1·560	43·5	45
							γ' 1·562	44·9	
	64	1·30	0·96	2·6	9	30	β' 1·560	43·5	45
							β'' 1·562	40	43
	65	0·9	2·2	3·75	16	43	not suitable		

A. Ab values from the refractive index—plagioclase composition graph of Chudoba.
B. Ab values from the revised refractive index—plagioclase composition graph of Chayes.

The pegmatitic oligoclase was unfortunately an unlocalized specimen, but it is included because in other respects it was very suitable for analysis. The fragments examined were parts of large single crystals and contained only a very small amount of sub-microscopic inclusions. The sodium values are fairly consistent, the potassium ones much less so—although this is not unexpected when dealing with pegmatitic material. As with the Bushveld crystals, the activation analysis values for Ab content are markedly lower than those obtained from refractive indices. This seems to be due to some factor in the analysis as yet imperfectly understood. On the other hand, it is perhaps worth noting that F. Chayes,[1] discussing recent chemical analyses given by R. C.

[1] Amer. Journ. Sci., 1954, vol. 252, p. 172 [M.A. 12–368].

Emmons and others, suggests that inclusions of quartz, potassium felspar, and mica would tend to raise the refractive index of plagioclase, whereas potassium felspar or excess SiO_2 in solid solution would probably lower it. Where unexplained discrepancies do occur in these American results, the Ab value obtained from the refractive index is usually higher than that given by chemical analysis—although the difference, of course, is much less than that found with the activation analysis.

The third plagioclase examined was an andesine from an olivine-gabbro, Stonehead, Aberdeen. This rock is really too fine-grained and complex to be satisfactorily analysed by this technique; it was included because a number of optical measurements had already been made on the plagioclase.[1] It proved rather difficult to obtain a large enough sample of felspar without including other minerals, and the crystals finally selected proved to be complex and zoned, with poorly defined twinning: the analysis results suggest that they are, in part, perthitic. Earlier optical work on this plagioclase gave an albite composition of about 50 % which agrees fairly well with two out of the three activation analyses. The plagioclase crystals include small apatites; the phosphorus in these is undoubtedly responsible, in part, for the unsatisfactory calcium analyses described later.

Potassium felspars. Only literature analyses of other specimens from the same locality were available for these felspars, and they could not, of course, be checked by optical measurements. However, these analyses provide a general guide to the composition, which is all that is required in this early stage of investigation. Two potassium felspars were examined, and the results are summarized in table II.

The first felspar was an adularia from St. Gotthard, Switzerland. This material is microscopically clear and appears homogeneous, except for a limited amount of parallel intergrowths. The activation analysis gives a consistent and satisfactory value for the potassium content; the sodium values, although more variable, are still not improbable.

Secondly, an amazonite from Mursinsk, Urals, was examined. This microcline is crowded with unidentifiable sub-microscopic inclusions. The samples used are largely single crystal fragments, but it proved difficult to obtain these sufficiently homogeneous. In one case (no. 58) some small plagioclase lamellae are included; in a second (no. 55) a fragment of quartz. The sodium and potassium values for this mineral are variable but agree tolerably well with the recorded analysis. The reason for the high potassium value of no. 58 is not known but when

[1] O. Bradley, loc. cit.

TABLE II. Activation analysis of sodium and potassium in potassium-rich felspars.

Material.	Spec. no.	Wt. in mg.	Activation analysis % K.	% Na.	% Or.	% Ab.
Adularia,* St. Gotthard, Switzerland.	59	3·5	10·9	0·8	77	9
	60	2·6	11·0	1·32	77	15
	61	3·05	10·9	1·08	77	12
Amazonite,† Mursinsk, Urals.	55	1·5	8·4	0·92	70	10
	56	1·3	12·5	0·61	89	7
	57	0·85	11·4	0·57	81	6·5
	58	0·8	16·3	2·2	115	25

* Literature analysis has K 11·6 %, Na 0·75, Ca 0·96 % (Dana, System of mineralogy, 6th edn, 1892, p. 319); this gives orthoclase 82·5 %, albite 8·5 %, anorthite 6 %.

† Literature analysis has K 11·55 %, Na 1·23 %, Ca 0 % (Dana, loc. cit., p. 323); this gives orthoclase 82·0 %, albite 14·2 %.

the weight of the crystal is only 0·8 mg. small errors in weighing can invalidate the whole analysis. Samples weighing 2–3 mg. should be used whenever the nature of the material permits it.

Calcium determinations.

These values are the least reliable part of the analysis; there are a number of elements that may be present as impurities in the crystals, and which are capable of interfering with the relatively weak calcium radiation. It appears likely that accurate determinations can only be made on a nearly pure plagioclase.

Figs. 1 and 2 show a selection of the decay curves obtained. In all cases the filtered and unfiltered decay curves are shown. The difference between these two curves, the residual radiation, should correspond to the 150-day half-life of Ca^{45}—if no interfering radiation is present. Three different samples of calcite (Iceland spar) were used as control material; in each case the hard radiation formed an insignificantly small part of the total, and can be neglected. The blank experiments with Canada balsam showed that some radioactivity can be induced in this material, but that this is not important when only a small amount is used for mounting. The blank experiment used about ten times as much balsam. Moreover, the early activity shown on the graph is due to the aluminium foil which adheres to the balsam but not to the crystals, and can therefore be ignored.

Three of the five felspars investigated had more or less suitable decay curves, but the calcium values, quoted in table III, should be treated

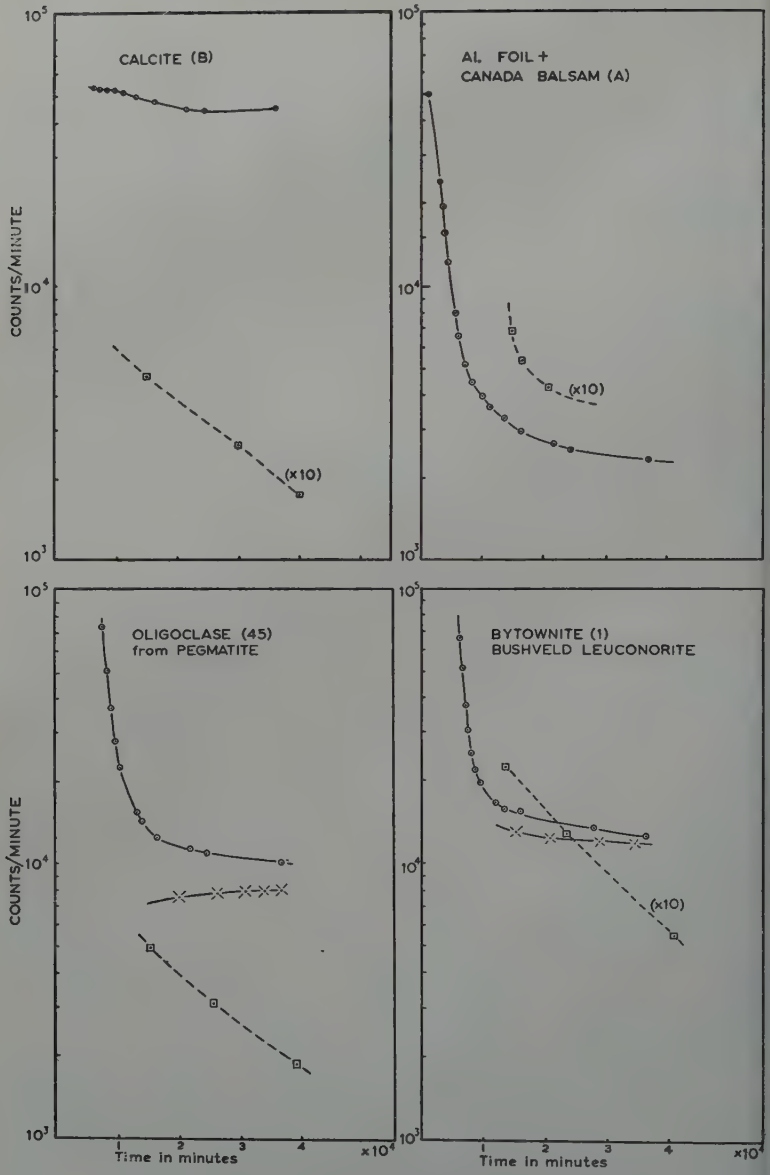

FIG. 1. Decay curves from first activation. —⊙— unfiltered radiation; —⊡— filtered radiation; —×— soft β-component.

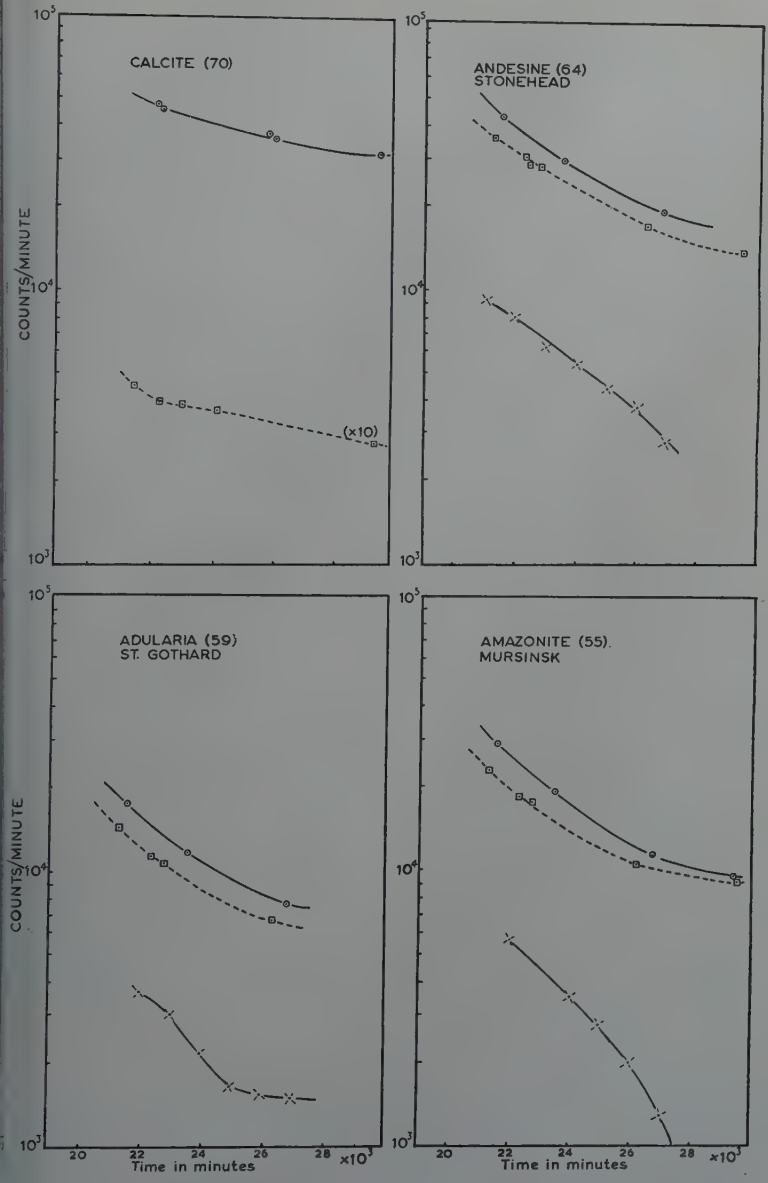

IG. 2. Decay curves from second activation. —⊙— unfiltered radiation; —⊡— filtered radiation; —×— soft β-component.

with some reserve. All values for Ca were taken at 25,000 minutes. The Bushveld bytownite gives satisfactory results, at least in three out of four cases; the St. Gotthard adularia is once again surprisingly homogeneous; and the pegmatitic oligoclase is still very variable. It is perhaps significant in this latter case that high Ca values are linked with high K values, suggesting that the impurity complicating the calcium decay curve is associated with the potassium. The andesines from Stonehead cannot be estimated because the interfering radiations are too complex, while in the example shown of the Mursinsk amazonite (fig. 2) the induced radioactivity is not due to calcium at all.

Finally, as a matter of interest, the sum of all the felspars is given in the last column of table III. It appears that when the Na, K, and

TABLE III. Activation analysis of calcium in suitable felspars.

Material.	Spec. no.	% Ca.	% An.	% Or.*	% Ab.*	'Total felspar' %†
Bytownite in Bushveld leuco-norite.	1	10·8	79	0·5	18	98
	2	11·5	80	0·7	16	97
	3	14·3	99	0·1	15	115
	4	12·1	84	0·9	15	100
Oligoclase from pegmatite. Locality unknown.	45	5·5	39	17	62	118
	46	3·1	22	6	54	82
	47	5·9	41	12	58	111
	48	2·9	20	3·5	61	85
Adularia, St. Gotthard, Switzerland.	59	2·0	14	77	9	100
	60	2·2	15	77	15	107
	61	2·1	14·5	77	12	103·5

* From tables I and II.

† That is, the sum of the An, Or, and Ab calculated from the percentages of Ca, K, and Na found.

Ca present are recalculated in terms of the felspar molecules, there is in most cases excess silica, or alumina, or both (see, for example, R. C. Emmons (loc. cit.), and more particularly E. D. Belyankina).[1] If the two quoted analyses of potassium felspar are recalculated in this way, both have excess silica and alumina; the adularia has 89 % felspar, the amazonite 96 %.

Acknowledgements.—The authors wish to express their thanks to Prof. J. H. Taylor for much advice and encouragement, and for the provision of research facilities. The cost of the activation was met by a grant from the Central Research Fund of the University of London, which is hereby gratefully acknowledged.

[1] Е. Д. Белянкина, Труды Инст. Геол. Наук, Акад. Наук СССР [Trans. Inst. Geol. Sci., Acad. Sci. USSR], 1953, no. 147, Petrogr. Ser. no. 43, p. 185 [M.A. 12–417].

The unit-cell contents of anthophyllite.

By G. H. Francis, M.A., Ph.D., and Max H. Hey, M.A., D.Sc.
Department of Mineralogy, British Museum.

[Read 27 January 1955.]

Summary.—Conclusions concerning the unit-cell contents and chemical formula of a mineral are all too often drawn from a small part of the available data. A procedure is outlined by which any chemical analysis for which a density is available can be utilized, provided X-ray data are available for a reasonable range of analysed specimens. The effects of possible errors in the determination of water, and in the assessment of essential and non-essential water, are discussed both qualitatively and quantitatively.

A survey of all available data for anthophyllite has not disclosed any specimens in which the number of oxygen atoms per unit cell is significantly in excess of 96 with the possible exception of the Glen Urquhart gedrite and the Edwards (New York) material. But it is certain that the number of cations per unit cell is normally well in excess of 60 (partial occupation of the *A* lattice positions), and that, although 'excess' water in some fibrous anthophyllites may be adsorbed impurity, the number of hydroxyl groups in others is well in excess of 8 per unit cell; it is also fairly clear that the number of hydroxyl groups may fall below 8 per unit cell.

IT has generally been assumed that the total number of large anions per unit cell in anthophyllite, and indeed in silicates generally, is always an exact integer (96 in anthophyllite) within the limits of experimental error. It is true that in a number of hydroxyl-bearing minerals partial dehydration without lattice breakdown is possible,[1] a process ($2OH' \rightarrow O'' + H_2O$) that must produce vacancies in the oxygen lattice; that a few examples of oxygen lattice deficiencies are known among oxide minerals;[2] and that interstitial substitution of large anions is not unknown.[3] But the Glen Urquhart gedrite described by one of the authors[4] may be the first example of a non-integral oxygen content in a silicate (apart, of course, from the water of the zeolites). A critical

[1] See, for example, R. E. Grim and W. F. Bradley, Journ. Amer. Ceram. Soc., 1940, vol. 23, p. 242 [M.A. **8**–295]; S. Z. Ali and G. W. Brindley, Proc. Leeds Phil. Soc., 1948, vol. 5, p. 109 [M.A. **11**–104]; G. W. Brindley and S. Z. Ali, Acta Cryst., 1950, vol. 3, p. 25 [M.A. **11**–104]; W. F. Bradley and R. E. Grim, Amer. Min., 1951, vol. 36, p. 182 [M.A. **11**–345]; W. P. Johns, Min. Mag., 1953, vol. 30, p. 186.

[2] L. G. Sillén and B. Aurivillius, Zeits. Krist., 1939, vol. 101, p. 483 [M.A. **7**–491]; L. G. Sillén, Inaug. Diss., Stockholm, 1940 [M.A. **9**–98]; B. Aurivillius, Arkiv Kemi, Min. Geol., 1943, vol. 16A, no. 17 [M.A. **9**–44].

[3] E. Zintl and A. Udgård, Zeits. anorg. Chem., 1939, vol. 240, p. 150 [M.A. **8**–117].

[4] G. H. Francis, Min. Mag., 1955, vol. 30, p. 709.

review of the unit-cell contents of anthophyllite appeared desirable, and is presented here.

We feel that all too often conclusions concerning the unit-cell contents and chemical formula of a mineral are drawn from a small part of the available data, and represent only a portion of the field of variation. Chemical analyses are often rejected for no other reason than their age, whereas there is adequate evidence that the standard of accuracy of analyses of many, though by no means all, classes of minerals has changed very little in the last hundred years,[1] and many of Berzelius's analyses, made 130 years ago, appear to be perfectly satisfactory. Particular analyses are often rejected solely because they fall outside the general field defined by the bulk of analyses of the same species; but it seems to us that, while the unusual analysis may well be in error, it should never be rejected out of hand but examined critically, since it may represent some unusual and unexpected isomorphous substitution, and will at least suggest where useful new data should be sought. For quite a number of minerals, a critical review of existing data is at least as important as the accumulation of additional data.

While true empirical unit-cell contents, based on chemical analyses of specimens for which X-ray and specific-gravity data are available, form the most satisfactory evidence for a suggested chemical formula, it is often possible, as will be shown below, to make good use of any analysis for which the specific gravity is available; when the specific gravity is not known, interpretation is more difficult and uncertain.

A major difficulty in the interpretation of many chemical analyses, including some of minerals generally accepted as anhydrous, is to define the role of water shown in the analysis. Apart from difficulties in the accurate determination of the total water content, there is no known method by which a reliable discrimination between adsorbed and essential water can always be made.[2]

[1] For many elements modern analytical methods are more rapid, more convenient, and more adaptable to microchemical procedures, but do not appear to be inherently more accurate. On the other hand, many old analyses are demonstrably incomplete, and for some elements (e.g. B, Cb, and Ta) satisfactory methods of analysis have only recently been developed.

[2] Even if a complete dehydration curve is prepared, it is often impossible to fix with any certainty the point at which loss of adsorbed water ends and loss of essential water begins; often the two stages overlap inextricably. And, as has been pointed out by G. D. Nicholls and J. Zussman (Min. Mag., 1955, vol. 30, p. 717), the amount of adsorbed water may vary sufficiently with the state of subdivision to call for caution in derivation of empirical unit-cell contents, owing to uncertainties in the correction of the observed density for adsorbed water.

In many cases the only satisfactory procedure is to calculate empirical unit-cell contents on two or more different assumptions concerning the distribution of the water; even then the interpretation of the results may remain in doubt.[1] Fortunately, certain generalizations are possible.

The effect of errors in the determination of water on the empirical unit-cell contents.

If the reported $H_2O(+)$ does not truly represent the hydroxyl or other essential water of the mineral there are four possibilities to consider: either the reported $H_2O(+)$ is too high, in that it includes non-essential adsorbed water, that is, impurity; or it is too low, in that some of the essential water was included in the reported $H_2O(-)$ and incorrectly regarded as an impurity; or it is too low, in that part of the essential water escaped determination altogether; or too high, in that the analysis shows more water than was actually present.

Further, even if the non-essential $H_2O(-)$ is correctly distinguished from the essential $H_2O(+)$, it may be in error by excess or defect, and this error will affect the empirical unit-cell contents. The treatments appropriate to these several possibilities may now be considered (obviously the water determination may be in error in more than one respect in the same analysis, so more than one correction may be needed).

If a mineral, of observed density D_o, gives on analysis a % of an oxide A_mO_n, of molecular weight M, an unknown part of which is present as an impurity of density d; if the conversion factor[2] is $F_o = VD_o/1{\cdot}6603\ S$, calculated on the assumption that the oxide is all essential; and if it may be assumed that the element A fills α lattice positions in the mineral, and that the rest, x %, of the oxide A_mO_n is impurity, then it can be shown that $x = Sd(\alpha - aF_om/M)/(D_o\alpha - SdF_om/M)$. The modifications necessary when the α lattice positions include elements other than A, or when the impurity is a compound including other oxides than A_mO_n, will not now be considered.

This relation is obviously applicable to the first possibility mentioned above, the inclusion of adsorbed water in the $H_2O(+)$, and in the present instance, with $M/m = 9{\cdot}0078$, $d = 1$, and $\alpha = 8$, it simplifies to $x = S(aF_o - 72)/(SF_o - 72D_o)$; but it is also applicable where essential water has been wrongly included with the $H_2O(-)$, and the same equation will then give a negative value of x, indicating the amount of water that

[1] M. H. Hey, Min. Mag., 1954, vol. 30, p. 493.

[2] Here V is the volume of the unit cell in Å.^{3}, and S the summation of the analysis.

must be transferred from '$H_2O(-)$', accounted as impurity, to '$H_2O(+)$', accounted as essential. In either case the density must be corrected for the amount of adsorbed water now found (if any), before the unit-cell contents are recalculated, a recalculation based on the assumption that there are exactly 8(OH) per unit cell. It will be found that a recalculation in which part of the water formerly regarded as essential is now taken as an impurity will almost always increase both the oxygen atoms per unit cell and the total cations.[1]

The position is different if essential water has escaped determination altogether. In this case the density does not need correction, and the factor F_o is only affected by the underestimation of the total analytical sum (excluding impurities), S. If y % of essential water had escaped determination, all the constituents except oxygen, and their sums, will be high in the uncorrected calculation by a factor $(S+y)/S$, that is, by approximately y % of their value, while the oxygen atoms per unit cell will invariably be low; the corrected value of $\sum$(O,OH,F) will be obtained by adding $F_o y/18$ to the uncorrected value and multiplying the sum by $S/(S+y)$, while the corrected value of $\sum$(OH,F) is obtained by adding $F_o y/9$ to the uncorrected value and multiplying by $S/(S+y)$. An overestimation of the essential water is obviously the converse of this.

If the adsorbed water, $H_2O(-)$, is in error by simple underestimation the net sum S will be unaffected, but the corrected density D_{corr} will be low; accordingly, all the empirical unit-cell contents, including oxygen, will be low by the same factor.

The qualitative effects on the observed $\sum$(O,OH,F) and $\sum$(cations) of various possible errors in the water determinations are summarized in table I. Even in their qualitative form these general relations will be found very useful in deciding on the possible interpretation of an analysis; and when combined with a rough estimate of the probable accuracy of the physical data they provide a useful device for the critical appraisal of analyses.

The unit-cell contents of anthophyllite.

The available data. J. C. Rabbitt[2] lists 84 chemical analyses of anthophyllite, together with a further nine that can[3] be rejected on the grounds

[1] G. H. Francis, Min. Mag., 1955, vol. 30, p. 713 (footnote).

[2] J. C. Rabbitt, Amer. Min., 1948, vol. 33, p. 263 [M.A. 10–416].

[3] He actually lists 11 analyses as 'doubtful or discredited'. Of these, nine can certainly be excluded on the grounds he assigns; but no. 88, while indeed very doubtful on many grounds, including the high value for b_{calc}, cannot be unequivocally rejected; and no. 85 is also doubtful, but cannot be definitely excluded.

TABLE I. Summary of the effect of errors in the water determination on the empirical unit-cell contents of a mineral (provided the atomic ratio of oxygen, derived from the percentage composition and molecular weights, is greater than $5{\cdot}51/(D+1)$ where D is the density of the mineral).

If:	$\sum$ (O,OH,F) observed will be:	$\sum$ (cations) observed will be:
Part of the H_2O, taken as essential, is really adsorbed:	Low	Low*
Part of the H_2O, rejected as adsorbed, is really essential:	High	High*
Part of the essential H_2O has escaped determination, but the estimate of adsorbed H_2O is correct:	Low	High
The essential H_2O is overestimated; adsorbed H_2O absent or correctly estimated:	High	Low
Essential H_2O absent or correctly estimated; adsorbed H_2O underestimated:	Low	Low†
Essential H_2O absent or correctly estimated: adsorbed H_2O overestimated:	High	High†

* In these cases the observed $\sum$ (cations) will be low (or high) by a larger factor than is the observed $\sum$ (O,OH,F).

† In these cases the observed $\sum$ (cations) and the observed $\sum$ (O,OH,F) will be low (or high) by the same factor.

of gross incompleteness or inaccuracy, or demonstrable impurity or misidentification of the material analysed; in the following discussion, all analyses included in Rabbitt's review will be referred to by his numbers. To these we add a further seven analyses, distinguished below by the letters *A* to *G*.

This collection of analyses can be divided into three classes, of decreasing value in assessing the unit-cell contents: Analyses for which X-ray measurements and density determinations are available; for these the empirical unit-cell contents can be determined. Analyses for which densities are available but not X-ray data; for such analyses it may be possible in favourable circumstances (and is possible in the case of anthophyllite) to form an estimate of the probable cell dimensions, and using this we can calculate what we may perhaps call semi-empirical unit-cell contents. And analyses for which neither X-ray measurements

nor densities are available; for these, only atomic ratios to an assumed basis can be calculated. We consider each class separately.

Empirical unit-cell contents. There are only 11 analyses for which all the data necessary to calculate the empirical unit-cell contents are available. J. C. Rabbitt (loc. cit.) studied seven gedrites and anthophyllites from Montana and a gedrite ('bidalotite') from Mysore; K. Johansson[1] examined anthophyllite from Falun, Sweden; and B. E. Warren and D. I. Modell[2] obtained X-ray measurements and a density on material from Edwards, New York, for which the chemical data by E. T. Allen and J. K. Clement[3] may reasonably be accepted. The empirical unit-cell contents for these 10 analyses have been calculated on the assumption that the water is all essential, and are included in table II, together with the unit-cell contents for the Glen Urquhart gedrite (G. H. Francis, loc. cit.).

The resulting figures are of considerable interest; analyses 1, 8, 9, 14, 26, 29, and 30 yield values for the sum (O+OH+F) within the probable experimental error[4] of the accepted 96, but all of these, except nos. 26 and perhaps 30, show a distinct excess of cations over the repeat formula $4[(Mg,Fe'',Al)_7(Si,Al)_8O_{22}(OH,F)_2]$, and it is clear that an appreciable proportion of the so-called *A*-positions, commonly assumed to be vacant in anthophyllite, are in fact occupied, probably mainly by (Na+Ca).

For analysis 17, the (O+OH) figure, 97·6, is high, but we note that there is a considerable discrepancy between the density as measured by the pycnometer and by the suspension method (J. C. Rabbitt, loc. cit., p. 298), and that if the latter value is accepted instead of the former, an (O+OH) content much nearer the normal 96 results; clearly the evidence of abnormality in this anthophyllite is not conclusive. For completeness, the (O+OH) contents deduced for the other six Montana specimens using the suspension value for the density instead of the pycnometric have also been included in table II, and it will be seen that for analyses 1, 8, and 14, as well as analysis 17, a value nearer 96 results, while for analyses 9, 29, and 30 the departure from 96 is increased.

[1] K. Johansson, Zeits. Krist., 1930, vol. 73, p. 31 [M.A. **4**–356].

[2] B. E. Warren and D. I. Modell, ibid., 1930, vol. 75, p. 161 [M.A. **4**–463].

[3] E. T. Allen and J. K. Clement, Amer. Journ. Sci., 1908, ser. 4, vol. 26, p. 111.

[4] J. C. Rabbitt did not assess the probable accuracy of his chemical data, but it may probably be assumed that the errors are of the same order as those for the Glen Urquhart gedrite (column *G*, table II). It is possible that some of his water determinations may be a little low, in view of his experience with no. 30; if they are the true values for $\sum$(O,OH,F) would be higher, and those for $\sum$(cations) lower than the values in table II.

TABLE II. Empirical unit-cell contents of anthophyllite occurrences for which full physical and chemical data are available.

	1.	8.	9.	14.	17.	20.	26.	29.	30.	43.	43*a*.	43*b*.	*G*.
Si	24·97	26·10	26·27	27·61	29·47	30·06	31·33	31·40	31·51	30·63	32·02	31·41	23·97±0·25
Al	12·23	10·73	10·05	8·70	5·56	7·02	0·39	0·91	1·26	0·36	0·38	0·37	17·50±0·22
Ti	0·21	0·19	0·23	0·18	0·19	0·48	—	—	—	0·01	0·01	0·01	0·30±0·02
Fe'''	0·45	1·27	0·27	0·55	0·96	1·86	0·61	—	—	0·11	0·12	0·12	0·28±0·06
Fe''	8·94	7·36	8·32	6·95	8·99	8·24	7·20	4·01	5·12	0·03	0·03	0·03	5·44±0·06
Mn	0·07	0·04	0·02	—	—	—	0·23	0·05	0·06	1·20	1·27	1·23	0·06±0·003
Mg	13·51	15·08	15·56	17·45	15·33	8·53	19·23	23·65	22·05	23·86	24·95	24·47	7·96±0·14
Ca	—	0·09	0·04	0·02	0·47	—	0·22	0·88	0·38	0·69	0·73	0·71	0·76±0·04
Na	1·72	0·31	0·52	0·12	0·79	—	0·12	0·70	0·29	0·37	0·39	0·38	0·52±0·10
K	0·02	—	—	—	—	—	0·02	—	0·04	0·12	0·13	0·12	0·15±0·04
OH	7·55	7·05	5·75	5·62	6·60	7·67	8·70	5·84	7·58	13·10	[7·66]	13·42	12·43
F	0·57	—	—	—	—	—	0·80	—	—	0·32	0·34	0·33	—
O	88·71	89·79	89·78	90·95	90·99	87·34	86·36	90·18	88·89	81·40	88·05	83·34	83·57
Σ (cations) ...	62·12	61·17	61·28	61·58	61·76	56·19	59·35	61·60	60·71	57·38	60·03	58·85	56·95 ±0·54
Σ (O,OH,F)	96·83	96·84	95·53	96·57	97·59	95·01	95·86	96·02	96·47	94·82	96·05	97·15†	98·55†±0·81
D_{corr} ...	3·277	3·261	3·245	3·259	3·279	3·22	3·157	3·106	3·102	2·91	3·01	[2·984]	3·150±0·010
D_{susp} ...	3·25	3·25	3·25	3·25	3·23	—	—	3·09	3·04	—	—	—	—
Σ (O,OH,F)*	96·04	96·51	95·09	96·30	96·13	—	—	95·53	94·54	—	—	—	—
b_{obs}	17·96	17·86	17·84	17·70	17·99	18·14	18·08	17·94	18·02	17·94	—	—	17·79
b_{calc}	17·90	17·80	17·82	17·79	18·03	18·17	18·03	18·00	17·98	17·95	—	—	17·95

For the localities, percentage compositions, &c., of analyses 1 to 43, see J. C. Rabbitt, Amer. Min., 1948, vol. 33, p. 263 [M.A. **10**–416], and for analysis *G*, see G. H. Francis, Min. Mag., 1955, vol. 30, p. 709. Analyses 43*a* and 43*b* are analysis 43 recalculated on two different assumptions.

* The density determined pycnometrically was used for all the empirical cell contents except this sum, which was derived using the density as found by the suspension method, D_{susp}.

† Including 1·15 and 2·55 mols. H_2O respectively.

Analysis 20 shows a rather low figure for (O+OH), combined with a very low figure for the total cations (normally 60), and a normal water content; there must be an appreciable proportion of vacancies in the lattice positions normally occupied by Mg, Fe″, with a replacement $3Mg \rightleftharpoons 2Al$. There is no evidence here of the presence of interstitial water molecules, indeed, there is a shortage of (O+OH); but the analysis has a rather low summation (99·68), and the water determination may be too low. The optical data also show some peculiarities, and a new study of this material ('bidalotite') would be of considerable interest; if the water content and density prove to be in error on the low side, we may, indeed, have here an example of interstitial water.

Analysis 26 shows normal values for (O+OH+F) and total cations, but (OH+F) is high, at 9·50 instead of the accepted 8; the excess is not great and could be accounted for by reckoning some of the $H_2O(+)$ as adsorbed water, without bringing $\sum$ (O,OH,F) too high to be explained by the probable error of the physical data; accepting the water as all essential, the analysis can be formally expressed in many ways—for instance, as a substitution of AlOH for SiO.

Analysis 43, from Edwards, New York, is of particular interest in that it is the only hydrous anthophyllite for which complete data are available. Unfortunately, the density was not determined on the analysed material but on the specimen used by B. E. Warren and D. I. Modell for their X-ray work. Accepting this density, and assuming the water is all essential, we derive the low total (O+OH+F) = 94·8, along with a low value of total cations; if it is assumed that the water in excess of 8(OH+F) per unit cell is adsorbed impurity, we calculate, using the formula given above (p. 175), that this impurity amounts to 1·67 %, leaving 2·13 % of essential water, and yielding the corrected density and empirical unit-cell contents shown in table II under 43*a*. Clearly this assumption of adsorbed water is a plausible one so far as the analysis and physical data go, but E. T. Allen and J. K. Clement found that at 600° C. only 0·6 % of water was lost in 60 hours, while at 820° C. 2·05 % of water was lost in 37 hours without any marked change of optical properties.

A third interpretation is to assume that the water is all essential; that the material has an integral total of anions, cations, and water molecules (156), but some water molecules in cation positions; and that the density determined by Warren and Modell is low. If a density of 2·984 is assumed, we derive the cell contents shown in table II

under 43*b*, with 1·2 molecules of water per unit cell in cation positions. This interpretation is supported by the dehydration experiments of Allen and Clement and appears to us the most probable one. The Edwards anthophyllite is practically free from FeO, so that their loss in weight figures can be taken as a true value for the loss of water. The water lost at 600°C. is 0·6 % = 1·2 molecules of H_2O per unit cell; this is almost exactly the amount of interstitial water shown under 43*b* (table II), whilst at 820° C. nearly half the remaining water has been lost. The Edwards anthophyllite was originally described by G. Cesàro as a new species and named valléite; it is particularly low in iron, and higher in manganese than most anthophyllites though its manganese content is only about 3 %. It has been analysed by G. Cesàro (anal. 79*a*) and by W. Kunitz (anal. 41), with results appreciably different from those of Allen and Clement. Kunitz did not give X-ray data, but it will be shown below (table III) that his analysis corresponds to a normal anthophyllite; on the other hand, his refractive indices are noticeably low compared with the values calculated from the regression equations[1] we have obtained. Cesàro found a density of 2·88, even lower than Warren and Modell's figure, and this, taken with his analysis, leads to a very low value for both (O+OH) and total cations; if we assume that the true value for (O+OH) should be 96, the density calculated for Cesàro's analysis, 2·96, agrees reasonably with the value of 3·006 observed by Kunitz (see table III). On the other hand, the dehydration work of Allen and Clement and the distinctly low refractive indices observed by Kunitz suggest some abnormality, and a new study of the Edwards anthophyllite is clearly desirable.

Semi-empirical unit-cell contents. In order to determine the empirical unit-cell contents of any substance it is necessary to know the cell dimensions, density, and chemical composition. If the density is not known, no estimate of the unit-cell contents is possible, but if only the cell dimensions are lacking it may still be possible to determine the cell contents, though not with the same degree of confidence as when density, cell dimensions, and chemical analysis are made on the same materials. For example, it may be known that the cell dimensions do not vary appreciably with composition, or only vary within fairly narrow, known limits; or it may be possible to predict the approximate cell dimensions from the composition, through a regression equation derived from X-ray work on analysed material. Both these possibilities are exemplified by anthophyllite; the variation in the *a*- and *c*-dimensions is small and we

[1] M. H. Hey, Min. Mag., 1956, vol. 31, p. 69.

TABLE III. Semi-empirical unit-cell contents of anthophyllite (summarized), taking $a = 18{\cdot}58$ Å., $c = 5{\cdot}30$ Å., and b values calculated from the composition, using the above regression equation.

	2.	3.	4.	6.	7.	13.	16.	21.	22.	24.	34.
b (Å.)	18·16	17·89	17·62	18·02	18·01	18·29	18·22	17·81	18·10	18·05	17·93
D_{corr}	3·371	3·281	3·178	3·26	3·176	3·23	3·27	3·068	3·241	3·157	3·134
(OH+F)	4·9	7·9	5·4	8·8	10·5	4·3	4·4	7·6	9·0	8·8	8·7
Σ(O,OH,F)	95·9	98·6	96·5	97·2	96·2	93·5	92·8	93·2	97·6	98·7	96·4
Σ(cations)	62·9	62·1	61·7	62·0	60·8	60·8	59·5	58·0	61·0	62·4	61·3

	35.	38.	39.	40.	41.	49.	50.	62*a*.	76.	79*a*.	85.
b (Å.)	17·91	17·84	17·83	17·85	18·04	18·18	17·80	18·14	17·96	18·25	17·77
D_{corr}	3·101	2·98	2·86	2·96	3·006	3·225	2·98	3·26	3·068	2·88	3·100
(OH+F)	6·1	13·2	15·4	5·9	9·9	7·4	10·4	8·9	12·1	10·9	5·0
Σ(O,OH,F)	97·0	95·6	92·5	92·4	96·7	93·3	94·9	83·6	97·4	93·2	96·8
Σ(cations)	62·0	57·9	55·0	58·7	59·9	58·0	59·4	54·2	59·2	57·4	63·3

	88.	*A*.	*B*.	*C*.	*D*.	*E*.	*F*.	38*X*.	39*X*.	76*X*.	79*aX*.
b (Å.)	18·62	17·63	18·27	17·85	17·93	18·02	17·97	17·90	17·89	17·99	18·30
D_{corr}	3·243	3·21	3·15	3·05	3·07	3·06	3·08	3·08	3·00	3·15	[2·96]
(OH+F)	7·8	6·4	7·9	8·4	8·8	8·2	3·0	[8·0]	[8·0]	[8·0]	11·2
Σ(O,OH,F)	94·3	99·2	95·4	100·0	102·6	101·5	95·0	97·7	95·3	99·3	[96·0]
Σ(cations)	59·9	64·0	59·7	62·5	64·9	64·1	61·8	61·0	59·2	60·6	58·7

For the localities, references, and other details of analyses 2 to 88, see J. C. Rabbitt, Amer. Min., 1948, vol. 33, p. 263 [M.A. **10**–416].

A. Fiskernäs, Greenland. –. Lorenzen [Undersøgelse Min. Grønland, Kjøbenhavn, 1884]; quoted in C. F. Rammelsberg, Handb. Mineralchemie, 2nd edn, 1875, p. 398.

B. Greenland. –. Lechartier, in C. F. Rammelsberg, Handb. Mineralchemie, 2nd edn, 1875, p. 398.

C. Val di Bresimo, Italy. R. Pirani, Atti (Rend.) Accad. Naz. Lincei, Cl. fis. mat. nat., 1952, ser. 8, vol. 13, sem. 2, p. 83 [M.A. **12**–30].

D. Alpe di Brez, Italy. R. Pirani, ibid., p. 170 [M.A. **12**–140].

E. Vedretta, Alta-Hochwart, Italy. R. Pirani, ibid., 1953, vol. 15, sem. 2, p. 422 [M.A. **12**–374].

F. Ilmen Mts., Russia. (Kupfferite.) R. Hermann, Bull. Soc. Nat. Moscou, 1862, vol. 35, p. 243.

38*X*, 39*X*, and 76*X*. Analyses 38, 39, and 76 recalculated on the assumption that all water in excess of 8 (OH) per unit cell is impurity. This involves the rejection of 1·59 % of the $H_2O(+)$ in analysis 38, 2·38 % in analysis 39, and 1·25 % in analysis 76.

79*aX*. Analysis 79*a* recalculated on the assumption that the observed density is in error, and that $\Sigma(O,OH) = 96$.

can write $a = 18{\cdot}58$ Å. $\pm 0{\cdot}06$, and $c = 5{\cdot}30$ Å. $\pm 0{\cdot}03$ for any antho-phyllite with fair confidence; and the b-dimension is related to the com-position by the approximate regression equation:[1]

$$b\ (\text{Å.}) = 16{\cdot}44 + 0{\cdot}28\text{Si} - 0{\cdot}13\text{Mg} + 0{\cdot}40(\text{Ca}+\text{Na}+\text{K}) \pm 0{\cdot}04,$$

where the composition is expressed in atoms per 24(O,OH,F). Using the cell dimensions thus derived, a considerable number of analyses for which densities are available yield the results collected in table III. If we take the b-dimensions as liable to an error of $\pm 0{\cdot}09$, not independent of the errors in a and c, and assume an accuracy of $\pm 0{\cdot}02$ in the density, we calculate that the probable error in $\sum$(O,OH,F) should be about 1·6, and in $\sum$(cations) about 1·0. In view of the fact that the regression equation is being used outside the range of composition for which it was established, and that it neglects the effect of variations in OH′,F′, and $\sum$(cations), this error is probably on the low side, and we may reasonably extend it to about 2·0 in $\sum$(O,OH,F) and 1·5 in $\sum$(cations).

Of the 29 analyses included in table III, $\sum$(O,OH,F) for 15 falls within $\pm 2{\cdot}0$ of the normal 96, but only five of these have $\sum$(cations) within 1·0 of 60, while seven have markedly high values for $\sum$(cations); this is in agreement with the result found above for the 11 analyses for which direct cell dimensions are available and it is clear that an appreciable proportion of the A-positions is normally occupied in anthophyllite. Six analyses give high values for both $\sum$(O,OH,F) and $\sum$(cations); these analyses (nos. 3, 24, *A*, *C*, *D*, and *E*) show low or normal water contents and good summations, and it appears probable that the densities are in error, from 2 to 7 % (0·06 to 0·2) too high. The remaining eight analyses (nos. 13, 16, 21, 39, 40, 41, 50, and 79*a*) have low values for $\sum$(O,OH,F) and low or normal values for $\sum$(cations). Of these no. 39 is very high in water, and, as will be shown below, it is possible that much of this water is adsorbed impurity and that the composition is normal; no. 79*a* is an analysis of the Edwards mineral, and is discussed above; the other 6 are probably to be explained by low density determinations, from 2 to 4 % low (0·06 to 0·12).

It will be noted that the high b-dimensions calculated for analyses 13, 3, and *B*, falling well outside the range observed by J. C. Rabbitt, do not lead to high cell contents, while of the analyses yielding low values for $\sum$(O,OH,F), not one has a calculated b-axis outside the range observed by Rabbitt; this tends to support the validity of the proposed regression equation for b.

[1] M. H. Hey, Min. Mag., 1956, vol. 31, p. 69.

Atomic ratios to 96 (O,OH,F). There remain five analyses for which no densities are available, and for these we cannot calculate the cell contents; the best we can do is to calculate atomic ratios to an assumed basis, preferably 96(O,OH,F), since the evidence so far goes to show that this is the normal unit-cell content of anthophyllite (with the possible exceptions of the Glen Urquhart gedrite and the Edwards anthophyllite). As J. C. Rabbitt has already made such a calculation to the basis 24(O,OH,F) new calculations are needless. From Rabbitt's tables it is clear that of these analyses only no. 66, a highly hydrous anthophyllite from the Lizard, Cornwall, analysed by J. J. H. Teall,[1] falls outside the field of compositions defined by the first 40 analyses. This specimen may perhaps contain interstitial water, but it is more likely that an analysis has been made on impure material. In other respects these analyses confirm the conclusions reached on the evidence of the first 40 analyses in that there is a marked tendency for $\sum$ (cations) to be high ($> 15{\cdot}2$ in 21 of the 51 analyses); and more than a third of the analyses, irrespective of date, show water contents differing substantially from 2(OH,F) per 24(O,OH,F).

Other possible interpretations of the anthophyllite analyses notably high or low in water. Before summarizing the results of this survey of the unit-cell contents of anthophyllite, we must consider a number of analyses that appear to be notably high or low in water. Of the 40 available analyses of anthophyllite for which densities, or densities and X-ray data are available (tables III and II respectively), six show a notable excess of water (nos. 38, 39, 43, 76, 79*a*, and the Glen Urquhart gedrite, *G*) and 10 show less than three-quarters of the usually accepted figure of 8(OH) per unit cell (nos. 2, 4, 9, 13, 14, 16, 29, 40, 85, and *F*); and there are 18 analyses showing substantially abnormal water contents (nine low, nine high) among the group for which density data are not available.

Some of these apparently abnormal water contents may be explicable as adsorbed water, or by errors in the water determination. To test this possibility, we must consider the effect of assuming that an apparent excess of hydroxyl groups is due to adsorbed water, or that an apparent deficit of hydroxyl groups is due to analytical error; if in either case the effect is to increase the departure of $\sum$ (O,OH,F) from the normal 96, we can reasonably reject the assumption.[2] If the qualitative effect (see

[1] J. J. H. Teall, Min. Mag., 1888, vol. 8, p. 116.

[2] To prove that Σ (O,OH,F) for any particular analysis really differs from the normal, it is essential to show that the departure from normality exceeds the probable experimental error, however we assess the distribution of the water.

table I) favours a proposed explanation of any apparently abnormal analysis, we can then consider it quantitatively. Clearly such tests are not possible for those analyses for which density data are not available; such analyses can only serve as secondary confirmation to conclusions based on empirical and semi-empirical unit-cell contents, or as pointers to occurrences for which new data would be of particular interest.

If it is assumed that an amount of water sufficient to bring the hydroxyl groups to 8 per unit cell has escaped determination in analyses 2, 4, 9, 13, 14, 16, 29, 40, and 85, the amount involved will be from 0·6 to 0·7 % and this will involve a decrease of $\sum$(cations) by about 0·4 to 0·5, and an increase in $\sum$(O,OH,F) by about 0·5 to 0·7; for analysis *F*, 1·4 % H_2O would have to have escaped determination, reducing $\sum$(cations) by 0·9 and increasing $\sum$(O,OH,F) by 1·2. This improves the approach of $\sum$(cations) to 60 in every case except nos. 16 and 40, and improves the approach of $\sum$(O,OH,F) to 96 in analyses 9, 13, 16, 40, and *F*, but makes it less satisfactory in the other five. Clearly we have a strong suggestion, though no definite proof, that the hydroxyl content may fall quite appreciably below 8 per unit cell.[1]

Turning to the hydrous anthophyllites, analyses 38, 39, 43, 76, and 79*a*, the oxygen content is low[2] (39, 43, 79*a*) or normal (38, 76). Of the five analyses, no. 43 (Edwards, New York), for which unit-cell measurements are available, has already been discussed above, together with no. 79*a*, also from Edwards; of the other three, nos. 38 and 39 are asbestiform minerals from Paakila, Finland, in which much of the excess water might well be adsorbed; calculations made by the above methods[3] on the assumption that all water in excess of 8(OH) per unit cell is adsorbed yield the results included in table III under 38*X* and 39*X*, and it will be seen that this interpretation is quite possible. Similar calculations for analysis no. 76, a coarsely crystallized anthophyllite from Mainland, Shetland (table III, 76*X*), indicate that the water in this specimen was probably all essential; this analysis was rejected by J. C. Rabbitt (loc. cit.) on the grounds of date (1879) and a high summation (100·68), but it would have to be very badly in error to conform

[1] Another possible explanation of some of these low water contents is that the mineral might contain fluorine, which passed undetermined; this would have very nearly the same effect as an underestimation of the water.

[2] The additional evidence of a dehydration curve suggests that the observed densities for nos. 43 and 79*a* may be in error, and that this material may have $\sum$(O,OH,F) a little in excess of 96 (see above).

[3] Since the *b*-dimension of the unit cell was calculated from the composition by means of the above regression equation, a revision of this dimension was also made.

to the 'normal' 8(OH) per unit cell, and it appears probable that we have here another truly hydrous anthophyllite, with a low cation total and high hydroxyl content; a new and complete study of this material is clearly desirable.

Conclusions. The results of our survey of all available data for the unit-cell contents of anthophyllite are: The total anions per unit cell, $\sum$ (O,OH,F), cannot be shown to depart significantly from 96 except possibly in the Glen Urquhart gedrite and the anthophyllite from Edwards, New York. The total cations per unit cell are normally significantly in excess of 60. And the hydroxyl (+fluorine) content may depart considerably from 8 per unit cell, either by excess or by defect.

Addendum. Since this paper was submitted doubt has been cast on the purity of the powdered gedrite from Glen Urquhart, owing to the presence of un-indexed lines in the X-ray powder pattern. The traces of impurity mentioned in the original study (Min. Mag., 1955, vol. 30, p. 710) are colourless and may have been underestimated owing to their parallel growth on the gedrite prisms. A re-investigation of the mineral is being undertaken.

G. H. F.

Subsolidus data for the join Ca_2SiO_4—$CaMgSiO_4$ and the stability of merwinite.[1]

By Della M. Roy, B.S., M.S., Ph.D.

College of Mineral Industries, The Pennsylvania State University, University Park, Pennsylvania, U.S.A.

[Communicated by Dr. M. H. Hey; taken as read 26 January 1956.]

Summary.—A study of phase equilibria among the orthosilicates on the a_2SiO_4—$CaMgSiO_4$ join was undertaken with the use of hydrothermal techniques ı the temperature range 600-900° C. at water pressures from 1000 to 15000 psi.[2] [onticellite, merwinite, and Ca_2SiO_4 crystallize as pure phases throughout this ›mperature range, and intermediate compositions contain mixtures of the end ıembers. Powder X-ray diffraction data obtained on the mixtures indicate no ıange in lattice dimensions from the end members. Hence, very little or no solid ›lution is indicated at these temperatures. Ca_2SiO_4 was crystallized as the γ-form ɛlow 675° C. (at 2000 psi) and the β-form above this temperature (presumably ıving inverted from the α'-form on cooling to room temperature). Infra-red ›sorption spectra obtained on the compounds γ–Ca_2SiO_4, β–Ca_2SiO_4, merwinite, ıd monticellite show characteristic differences in the pattern within the 9–13 .icron region. All the data thus appear to confirm merwinite as a unique compound ıable in the temperature range studied.

ONE of the most elusive problems within the complex system CaO—MgO—SiO_2 has been the determination of the equilibria ı the orthosilicate join Ca_2SiO_4—Mg_2SiO_4. On the basis of similarity ı crystal structure, partial or complete solid solution might be expected ɛtween forsterite and monticellite, and similarly between monticellite ıd γ–Ca_2SiO_4, all of which possess the olivine structure. When O'Daniel 942) assigned the olivine structure to γ–Ca_2SiO_4 he predicted that ɛtensive solid solution should exist between γ–Ca_2SiO_4 and monticel-ɛe; and Bredig (1950) later suggested that this solid solution should be ›ntinuous. Recent work of Ricker and Osborn (1954) on the subsolidus gion of the join $CaMgSiO_4$—Mg_2SiO_4 has shown that a solid solution ries extends to a maximum of about 30 weight % from each compound ; solidus temperatures, but the amount of solid solution decreases ›pidly with decrease in temperature.

The presence of the intermediate compound merwinite ($Ca_3MgSi_2O_8$)

[1] Contribution no. 54–66, College of Mineral Industries.

[2] Pounds per square inch; this contraction is used throughout this paper.

must be explained, however, for it is a naturally occurring mineral (Larsen and Foshag, 1921), and has been shown by Phemister *et al.* (1942) and by Osborn (1943) to be a unique (incongruently melting) compound having a stability field in the system CaO—MgO—SiO_2. The presence of merwinite on the join Ca_2SiO_4—$CaMgSiO_4$ was explained by Bredig (1950) as a composition in the α' solid solution series, i.e. he considered merwinite to be merely an end point in a solid solution series extending from α'-Ca_2SiO_4[1] to the composition $Ca_3MgSi_2O_8$. Complete solid solution was presumed by Bredig to exist between the lower temperature polymorph (γ-Ca_2SiO_4) and monticellite. However, the possibility of a complete solid solution series between γ-Ca_2SiO_4 and monticellite, as well as the proposed α'-Ca_2SiO_4—merwinite solid solution series, was considered unlikely by Ricker and Osborn (1954) on the basis of theoretical considerations. A recent summary of the current knowledge on the chemistry and polymorphism of Ca_2SiO_4 is that of Nurse (1954), who believed that single-crystal X-ray data and powder X-ray data obtained at elevated temperatures favour the designation of monoclinic merwinite as a distinct compound, not a solid solution of orthorhombic α'-Ca_2SiO_4. Bredig (1954, see Nurse, 1954), in discussion of the above paper, suggested that merwinite (monoclinic, pseudo-orthorhombic) may be considered to be a 'fifth polymorphous form of calcium orthosilicate, related to α', and stabilized by large amounts of Mg_2SiO_4', presumably formed on cooling from high temperatures.

The present study was undertaken with the application of hydrothermal techniques in order to aid crystallization and in the hope of attaining equilibrium at subsolidus temperatures. It was hoped to establish more positively the character of merwinite and its equilibrium relations with the other orthosilicates, as well as to obtain new information on the polymorphism of Ca_2SiO_4.

Experimental procedure

Briefly, the experimental procedure was as follows: One or more samples contained in individual gold envelopes in a bomb were quickly brought up to the desired temperature. Water was pumped into the

[1] The complexity of the relations among polymorphic forms of Ca_2SiO_4 is, of course, involved in the equilibria; recent papers of Newman and Wells (1946), Van Valkenburg and McMurdie (1947), Trömel (1949), Trömel and Möller (1949), and Bredig (1950) give evidence of four polymorphic forms, from the highest to lowest temperature, respectively, hexagonal α, orthorhombic α', monoclinic β, and the olivine γ. Bredig (1950) has further suggested that the β-modification is only metastable.

bomb through pressure tubing to reach the desired water pressure. The bomb was then heated at this regulated pressure and temperature for a period varying from a few hours to several days. Most runs were made at low pressures, about 2000 psi, in an attempt to avoid entering an area of hydrate stability in the Ca_2SiO_4-rich mixtures. After completion of the run the water pressure was released to zero and after $\frac{1}{2}$ to 1 minute the bomb was quenched in water. The samples were examined by X-ray diffraction and the petrographic microscope, and in a few cases infrared absorption spectra were obtained.

The hydrothermal equipment used was similar to that described by Roy, Roy, and Osborn (1950), and Roy and Osborn (1952). Stellite 'test-tube' bombs were used almost exclusively, and the water pressure was released just before quenching, as described above, in order to prevent hydrate formation during heating or cooling. A few 'dry' runs were made in a Pt-wound quenching furnace.

Starting materials used included mixed $CaCO_3$, $MgCO_3$, and silicic acid reacted at high temperatures, but most frequently a type of mixture which is much more intimate and almost 'amorphous to X-rays', prepared in the following manner: weighed amounts of $CaCO_3$ and MgO (or $MgCO_3$) were dissolved in dilute HNO_3 and added to an excess of absolute alcohol. Ethyl orthosilicate was measured out with a burette and dissolved in alcohol and the two solutions mixed, evaporated at 10° C., then heated to about 400° C. for a few hours, then to 700° to 900° C. overnight. Chemical analyses of the final products were not made, but compounds formed from stoichiometric ratios were found to be quite free from other phases when studied microscopically or by X-ray diffraction.[1]

Results and discussion.

A summary of pertinent hydrothermal quenching data is given in table I, indicating phases present as detected by a combination of X-ray diffraction and optical data. The results are represented diagrammatically in fig. 1, which shows the phases present at the various temperatures in equilibrium with H_2O at a constant pressure of 2000 psi. The three orthosilicate compounds Ca_2SiO_4, $Ca_3Mg(SiO_4)_2$, and $CaMgSiO_4$ crystallize as unique phases in the temperature range studied, 600–1000° C., and intermediate compositions show a mixture of monticellite and merwinite in the one case, and in the other a mixture of merwinite and Ca_2SiO_4 (the γ-form below 675° C. and β above).[2] Runs made at temperatures as low

[1] Mixtures of CaO or $CaCO_3$ and silica gel were found to be less satisfactory with respect to attainment of equilibrium.

[2] New information obtained on the polymorphism of Ca_2SiO_4 is the subject of a separate paper to be published soon. Briefly, the data obtained using 'amorphous' starting materials inbicate that γ–Ca_2SiO_4 crystallizes below 675° C. (at 2000 psi) and that β forms above this temperature. The β–Ca_2SiO_4, however, is probably

TABLE I.

Summary of hydrothermal quenching data for the join Ca_2SiO_4—$CaMgSiO_4$.

The pressure was 2000 psi except for the runs at 475° C., for which it was 15 000 psi, and at 1472° and 1455°, for which it was atmospheric.

Abbreviations used: X = Ca_2SiO_4-hydrate, not completely identified. C_2S = Ca_2SiO_4; tr. = trace; Mer. = Merwinite; Mont. = Monticellite.

Mol. % Ca_2SiO_4.	Temp. ° C.	Time hrs.	Phases present.
100	640	24	γ–C_2S+tr. X
100	662	48	γ–C_2S+some X
100	670	96	γ–C_2S+β–C_2S+some X
100	685	48	β–C_2S+X
100	705	24	Mostly β–C_2S
100	870	24	β–C_2S
100	1472	20	γ–C_2S on quench
75	655	96	Mer.+γ–C_2S+X
75	665	72	Mer.+γ–C_2S+tr. X
75	685	48	Mer.+γ–C_2S+β–C_2S
75	743	24	Mer.+β–C_2S
75	885	96	Mer.+β–C_2S
50	475	168	Mont.+hydrate
50	625	96	Mer.+tr. Mont.?
50	645	24	Mer.
50	650	96	Mer.
50	744	120	Mer.
50	870	20	Mer.
50	1472	20	Mer.
25	655	96	Mont.+Mer.
25	750	24	Mont.+Mer.
25	850	72	Mont.+Mer.
0	475	168	Mont.
0	610	72	Mont.
0	705	24	Mont.
0	860	24	Mont.
0	1455	2	Mont.

as 475° C. at 15 000 psi indicated that monticellite is stable under these conditions. Merwinite was not formed at 475° C. and 15 000 psi from an 'amorphous' mixture of the merwinite composition, which gave a mixture of monticellite and a dicalcium silicate hydrate. This is not positive evidence, however, that merwinite is no longer stable under these conditions.

formed only metastably, through a fairly rapid inversion on cooling, from α'–Ca_2SiO_4. A further complication is the formation of a small amount of a lime-silica hydrate below about 700° C., both in pure Ca_2SiO_4 mixtures and the 75 mol. % Ca_2SiO_4 mixture.

Within the experimental error, the transition temperature from γ to α' Ca_2SiO_4 is unchanged in the 75 mol. % Ca_2SiO_4 mixtures from that for pure Ca_2SiO_4, i.e. 675±10° C. at 2000 psi. The *d*-spacings of phases present in the intermediate mixture show no change (within the experimental error of ±0·02° in 2θ) from those of the pure components Ca_2SiO_4 and merwinite. There is similarly no change in the spacings of merwinite and monticellite found in the 25 mol. % Ca_2SiO_4 mixture from those of the pure end-members.

Measurements from typical X-ray diffraction patterns of the end member compounds and intermediate compositions are given in table II. Most of these data were obtained with less than maximum precision in recording, but they demonstrate clearly that the intermediate compositions contain mixtures of the end-members, not an intermediate solid solution. More precise measurements obtained with slower speed of recording of a few selected reflections, which are diagnostic,[1] and in which there is no shift due to overlapping of peaks, demonstrate that very little, if any, solid solution exists among the various compounds and polymorphs.

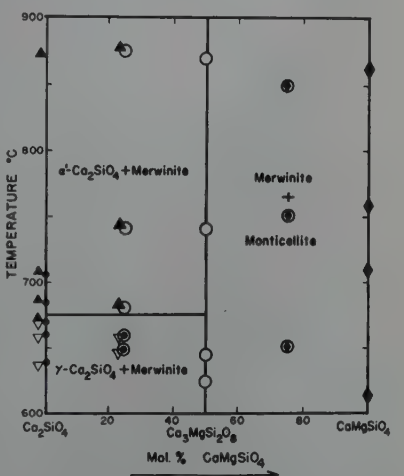

FIG. 1. Subsolidus phase equilibrium diagram for the join Ca_2SiO_4—$CaMgSiO_4$ at a water pressure of 2000 psi. Symbols used: ○ = merwinite, ♦ = monticellite, ▽ = γ–Ca_2SiO_4, ▲ = α'–Ca_2SiO_4 (inverted to β at room temperature), ● = hydrate.

Although the crystals formed, especially at low temperatures, are too small for accurate determination of optical properties, the differences in index of refraction are distinctive. The low index (*c.* 1·644) crystals of monticellite stand out clearly against the higher index (*c.* 1·700) merwinite crystals in the mixture with 25 mol. % Ca_2SiO_4, and the low index (*c.* 1·650) γ–Ca_2SiO_4

[1] Peaks at 2θ values (Cu-$K\alpha$) of 50·10° and 30·405° for monticellite, at 34·35°, 32·60°, 32·02°, and 32·16° for β–Ca_2SiO_4, at 32·86° and 29·715° for γ–Ca_2SiO_4, and at 38·445°, 33·78°, and 33·43° for merwinite were unchanged within the experimental error of ±0·03° in 2θ in intermediate compositions showing mixtures of merwinite plus one of the other phases.

TABLE II. X-ray diffraction data for phases on the Ca_2SiO_4—$CaMgSiO_4$ join. Spacings measured on Norelco High-angle diffractometer using filtered Cu radiation.

β Ca_2SiO_4.		γ Ca_2SiO_4.		γ Ca_2SiO_4 + Merwinite.		β-Ca_2SiO_4 + Merwinite.		Merwinite.		Merwinite + Monticellite.		Monticellite.	
d (Å.)	I/I_0	d (Å.)	I/I_0	d (Å.)	I/I_0	d (Å.)	I/I_0	d (Å.)	I/I_0	d (Å.)	I/I_0	d (Å.)	I/I_0
3·807	0·05	5·62	0·2	5·62	0·05	3·818	0·02	3·883	0·05	5·55	0·05	5·56	0·1
3·381	0·05	4·33	0·4	4·33	0·1	2·876	0·3	3·633	0·05	5·12	0·02	4·19	0·3
3·243	0·1	4·058	0·3	3·824	0·3	2·790	0·7	3·340	0·1	4·20	0·1	3·640	0·8
3·048	0·05	3·821	0·5	3·345	0·2	2·782	0·7	3·173	0·1	3·898	0·05	3·192	0·4
2·876	0·1	3·014	1·0	3·043	0·3	2·744	0·8	2·868	0·1	3·645	0·4	2·939	0·4
2·791	1·0	2·898	0·1	3·010	0·35	2·730	0·5	2·749	0·2	3·326	0·05	2·771	0·05
2·783	0·9	2·840	0·2	2·990	0·1	2·722	0·5	2·682	1·0	3·199	0·1	2·676	1·0
2·746	0·9	2·780	0·1	2·780	0·1	2·681	1·0	2·675	0·9	3·169	0·05	2·598	0·6
2·726	0·4	2·750	0·9	2·750	0·4	2·671	0·9	2·652	0·3	3·052	0·05	2·546	0·15
2·607	0·4	2·728	1·0	2·726	0·3	2·655	0·2	2·618	0·02	2·997	0·05	2·404	0·3
2·545	0·1	2·686	0·1	2·685	1·0	2·609	0·3	2·589	0·05	2·940	0·25	2·359	0·05
2·449	0·05	2·589	0·1	2·660	0·1	2·547	0·1	2·398	0·05	2·873	0·1	2·213	0·1
2·406	0·2	2·536	0·1	2·522	0·05	2·283	0·2	2·318	0·1	2·755	0·2	1·920	0·02
2·283	0·2	2·519	0·2	2·321	0·1	2·214	0·2	2·306	0·1	2·714	0·1	1·819	0·3
2·189	0·4	2·475	0·1	2·212	0·1	2·189	0·3	2·214	0·1	2·686	1·0	1·777	0·02
2·164	0·1	2·327	0·1	2·032	0·05	2·166	0·1	2·171	0·1	2·679	0·9	1·749	0·02
2·047	0·05	2·249	0·05	1·911	0·4	2·027	0·05	2·060	0·05	2·656	0·4	1·725	0·1
2·022	0·1	2·189	0·1	1·879	0·2	1·983	0·1	2·030	0·1	2·592	0·3	1·689	0·02
1·985	0·2	2·026	0·15	1·809	0·1	1·910	0·25	1·909	0·3	2·549	0·1	1·600	0·2
1·895	0·05	1·910	0·8	1·757	0·1	1·878	0·1	1·877	0·2	2·517	0·05	1·508	0·05
1·804	0·02	1·806	0·3	1·689	0·1	1·630	0·1	1·722	0·02	2·465	0·05	1·390	0·05
1·708	0·05	1·755	0·05	1·535	0·15	1·610	0·1	1·705	0·02	2·405	0·1	—	—
1·631	0·05	1·689	0·2	—	—	1·535	0·1	1·579	0·05	2·317	0·05	—	—
1·608	0·1	1·637	0·2	—	—	1·414	0·05	1·549	0·05	2·216	0·1	—	—
1·526	0·02	—	—	—	—	—	—	1·535	0·1	2·173	0·05	—	—
1·486	0·02	—	—	—	—	—	—	—	—	2·029	0·05	—	—
—	—	—	—	—	—	—	—	—	—	1·912	0·3	—	—
—	—	—	—	—	—	—	—	—	—	1·882	0·2	—	—
—	—	—	—	—	—	—	—	—	—	1·781	0·05	—	—
—	—	—	—	—	—	—	—	—	—	1·752	0·05	—	—
—	—	—	—	—	—	—	—	—	—	1·724	0·05	—	—
—	—	—	—	—	—	—	—	—	—	1·602	0·05	—	—
—	—	—	—	—	—	—	—	—	—	1·535	0·05	—	—

crystals are distinct from those of merwinite in the 75 mol. % Ca_2SiO_4 mixture treated below 675° C. The higher index β–Ca_2SiO_4 crystals, formed in the latter mixture just above 675° C., are not easily distinguished optically from those of merwinite, but the X-ray diffraction

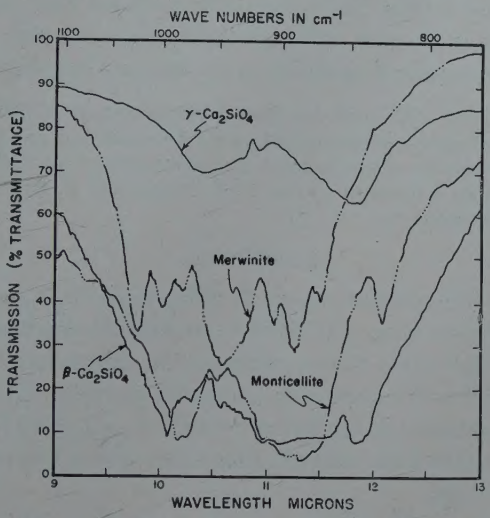

FIG. 2. Infra-red absorption spectra. Monticellite and β–Ca_2SiO_4 obtained using 0·4 % concentration in KBr pellet, merwinite 0·2 % in KBr; γ–Ca_2SiO_4 obtained from 'Nujol' mull on NaCl plates.

patterns of the two phases are readily identified in mixtures, as has been demonstrated above.

Another diagnostic property of these phases was the infra-red absorption spectrum. Spectra were obtained on the Perkin–Elmer model 21 double-beam instrument, using both the 'Nujol' mull technique and pressed KBr pellets.[1] Typical spectra of γ–Ca_2SiO_4, β–Ca_2SiO_4, merwinite and monticellite are shown in fig. 2. The diagnostic portion is mainly within the 9·5–12·5 micron range, although spectra were obtained from 2 to 15 microns. The four phases are seen to be quite distinct in their infra-red absorption spectra, and even structurally similar monticellite and γ–Ca_2SiO_4 exhibit differences.

[1] Standard techniques of sample preparation for crystalline materials include the suspension of a few milligrams of the sample in a mull with a high-boiling paraffin oil such as 'Nujol', smeared between polished flat NaCl plates. The paraffin oil has a few sharp characteristic absorption bands, but an alternative method employs KBr, which is completely infra-red transparent, as a suspending medium. A small concentration of sample (0·2–2 %) is mixed with finely ground KBr and pressed under a hydrostatic load of about 100 000 psi into a flat disk.

Although the KBr method generally gives better and more easily reproducible spectra, the pattern shown for γ–Ca_2SiO_4 is that obtained by the 'Nujol' method. The pattern obtained from the KBr pellet in this case was diffuse, which may be the result of a pressure-inversion. The spectra obtained by the 'Nujol' and KBr methods were comparable in the other three substances, although the KBr spectra were more sharp, more easily reproducible, and had no interfering absorption maxima.

Acknowledgements.—This work was done as part of a study of phase equilibria in steelplant refractories systems sponsored by the American Iron and Steel Institute, on the recommendation of the Research Sub-committee of the Refractories Committee. The author is indebted to Drs. E. F. Osborn and R. Roy for advice and discussion of the manuscript.

Conclusions.

Studies of phase relations among Ca_2SiO_4, $Ca_3MgSi_2O_8$, and $CaMgSiO_4$ in the temperature range 600°–900° C. confirm the existence of each of these compositions as a unique compound in the system CaO—MgO—SiO_2. X-ray diffraction, optical and infra-red absorption data on crystalline material obtained in the hydrothermal runs all point to the conclusion that no appreciable solid solution exists among the phases in this temperature range.

References.

Bredig (M. A.), 1950. Journ. Amer. Ceram. Soc., vol. 33, p. 188.

Larsen (E. S.) and Foshag (W. F.), 1921. Amer. Min., vol. 6, p. 143 [M.A. **1**–254].

Newman (E. L.) and Wells (L. S.), 1946. Journ. Res. Nat. Bur. Stand., vol. 36, p. 137.

Nurse (R. W.), 1954. 'The Dicalcium Silicate Phase', Paper No. 3, pp. 56–90, Proceedings of the Third International Symposium on the Chemistry of Cement, 1952. Cement and Concrete Association, 52 Grosvenor Gardens, London, S.W. 1.

O'Daniel (H.) and Tscheischwili (L.), 1942. Zeits. Krist., vol. 104, p. 124 [M.A. **8**–290].

Osborn (E. F.), 1943. Journ. Amer. Ceram. Soc., vol. 26, p. 321 [M.A. **10**–108].

Phemister (James), Nurse (R. W.), and Bannister (F. A.), 1942. Min. Mag., vol. 26, p. 225.

Ricker (R. W.) and Osborn (E. F.), 1954. Journ. Amer. Ceram. Soc., vol. 37, p. 133.

Roy (D. M.), Roy (R.), and Osborn (E. F.), 1950. Ibid., vol. 33, p. 153.

Roy (R.) and Osborn (E. F.), 1952. Econ. Geol., vol. 47, p. 717.

Trömel (G.), 1949. Naturwiss., vol. 36, p. 88.

—— and Möller (H.), 1949. Fortschr. Min. Krist. Petr., vol. 28, p. 80 [M.A. **11**–470].

Van Valkenburg (A.) and McMurdie (H. F.), 1947. Journ. Res. Nat. Bur. Stand., vol. 38, p. 415.

Frederick Noel Ashcroft